THE THERMAL INSULATION OF MINE AIRWAYS

Paul Bottomley

A dissertation submitted to the Faculty of Engineering, University of the Witwatersrand, Johannesburg, for the degree of Master of Science in Engineering.

Johannesburg, 198?

DECLARATION

I declare that this dissertation is my own, unaided work. It is being submitted for the Degree of Master of Science in Engineering in the University of the Witwatersrand, Johannesburg. It has not been submitted before for any degree or examination in any other University.

P.B.

(Signature of Candidate)

this 1st day of September 1987

ABSTRACT

The application of insulation material to the surfaces of airways has the potential of reducing the heat load on the ventilation air of deep mines. This study aims at assessing the viability of this technique.

Previous investigations on heat transfer from insulated airways are reviewed and are found to be flawed or out of date. A more reliable thermal analysis is presented. This shows that reductions in heat load of 50 to 70 per cent can be achieved in fully insulated tunnels, 20 to 40 per cent with partial insulation (footwall uninsulated) and less than 20 per cent with the footwall both uninsulated and wet. Nomograms are presented which predict the reduction in heat load for a wide range of conditions.

An experimental study on tunnel insulation in a deep gold mine is reported. The reductions in heat load were 57 per cent with full insulation, and 30 per cent with partial insulation. These values are lower than those predicted, namely 71 and 50 per cent respectively, largely because of the uneven thickness of the insulation layer.

Guidelines are provided for the selection of insulation systems. Estimates of the financial benefits accruing from the insulation of airways are presented.

ACKNOWLEDGEMENTS

This dissertation arises from work carried out as part of the research programme of the Environmental Engineering Laboratory of the Research Organization of the Chamber of Mines of South Africa.

I would like to express my thanks to Professor A.M. Starfield and Dr. H.H. Jawurek of the University of the Witwatersrand.

The assistance of the management and ventilation department of the Western Deep Levels Gold Mine is appreciatively acknowleged.

I am most grateful to the members of the Administration and Professional Services Branch of the Chamber of Mines Research Organization for the typing of the manuscript, preparation of the figures and editing.

CONTENTS Page

LIST OF FIGURES

LIST OF TABLES

NOMENCLATURE

A	surface area	m^2
AF	radiation exchange area	m^2
a	airway radius	m
a_i	quadratic coefficients	
b	dimension of a square cross-sectional tunnel	m
c	specific heat	J/kgK
D	diameter of a circular cross-sectional tunnel	m
F	fraction of total heat flow that passes through the hangingwall and sidewalls	
F_{ev}	Combined emissivity and view factor	
F_{ij}	geometric view factor between surface i and surface j	
f	wetness factor, varying from 0 for a perfectly dry surface to 1 for a thoroughly wet surface	
G	irradiation, or the total radiation incident upon a surface area, per unit time, per unit area	W/m^2
h	surface convection heat transfer coefficient	W/m^2K
h_e	equivalent heat transfer coefficient for an insulated surface	W/m^2K
h_r	radiative heat transfer coefficient	W/m^2K
I	functional (a function of a function)	
J_o	Bessel function of the first kind of order 0	
J_i	radiosity or the total radiation leaving surface i per unit time per unit area	W/m^2
K	coefficient for radiation from the insulated to the uninsulated portion of a rock surface, or rock thermal conductivity matrix in Chapter 3	
K'	coefficient for radiation from the uninsulated to the insulated portion of a surface	
k	thermal conductivity	W/m^2K

NOMENCLATURE (contd)

L	unit of length	m
L_e	mean beam length	m
N	interpolation matrix for finite element method	
Nu	Nusselt number (hD/K)	
P	barometric pressure	N/m^2
Pr	Prandtl number ($\mu c/k$)	
Psat(T)	saturated vapour pressure at temperature T	N/m^2
P'sat(T)	differential of the saturated vapour pressure at temperature T	
Q	heat flux	W/m^2
q_{ij}	net radiation exchange between two ces	W/m^2
R	Radius to the outer boundary whe ng to the quasi-steady method, the rock can d to be at the virgin rock temperature	m
R_e	Reynolds number ($\rho vD/\mu$)	
ΣR	total thermal resistance	mK/W
r	radial dimensions	
T	absolute temperature	K
Ta	absolute air temperature	K
T'	Tunnel heat flow function	
t	temperature	°C
t_{DB}	dry-bulb temperature	°C
t_{ins}	temperature of insulated surface	°C
t_s	rock surface temperature	°C
t_{unins}	temperature of uninsulated surface	°C
Δt	temperature difference	°C
U	overall heat transfer coefficient	W/m^2K

NOMENCLATURE (contd)

V	volume	m^3
VRT	virgin rock temperature	°C
v	velocity	m/s
x	cartesion co-ordinate	
Yo	Bessel function of second kind of order 0	
y	cartesion co-ordinate	
z	parameter of integration	

GREEK SYMBOLS

α	thermal diffusivity	m^2/s
β	half the angle subtended at the centre by the uninsulated portion	
λ	latent heat of evaporation	kJ/kg
ϵ	emissivity	
σ	Stefan-Boltzman constant ($5,699 \times 10^{-8}$)	W/m^2K^4
ρ	density	kg/m^3
θ	angle in radial co-ordinate system	
τ_a	transmissivity	
μ	viscosity	Ns/m^2

1 AIMS AND OUTLINE OF STUDY

1.1 Introduction

Deep-level mines are characterised by high virgin rock temperatures. Traditional mining practice treats the associated high heat loads on the ventilation air as inevitable and makes use of large refrigeration plants to achieve acceptable working environments. This study aims at assessing a method of reducing the heat load at source, namely by means of insulating the main intake airways. Working depths in South African gold mines at present extend to approximately 3 600 m below surface, with virgin rock temperatures of up to 60 °C, and serious consideration is being given to extending operations to depths of 5 000 m, into rock temperatures of approximately 70 °C. Since 1976 the increase in heat load on mine ventilation systems has resulted in the rapid growth of installed refrigeration capacity and, as shown in Figure 1.1, is expected to continue. A similar trend is evident in the cost of owning and operating refrigeration plant which at present amounts to a present value of R2 000 per kW cooling. It is therefore desirable to develop cost effective methods for combatting the underground heat load problem, and reduce the flow of heat to underground workings. Other methods of reducing the heat flow include the backfilling of worked out areas, the design of mine layouts and the design of mine cooling systems.

There are several sources of heat underground (for example rock, machinery, men and explosives), the most significant being that of the rock mass surrounding the workings (Bluhm et al, 1986). In particular the many kilometres of intake airway contribute a significant proportion to the overall mine heat load. This proportion grows with the life of the mine as the airways have to extend to service the workings further from the shaft. Surface or station bulk air cooling also results in an increase of the heat load contribution by the airways, owing to an increased temperature driving force between the air and rock. One possible method of reducing the heat flow from the rock mass consists of insulating the rock surfaces.

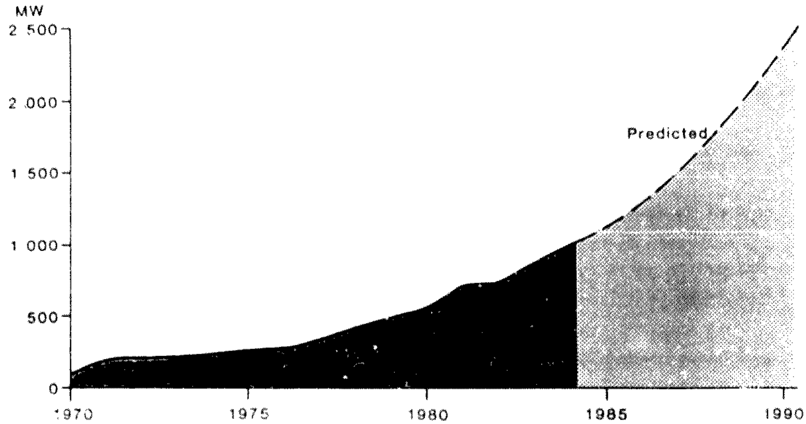

Figure 1.1 The installed refrigeration capacity on South African gold mines

1.2 Aims of Study

The aims of this study are to:

(i) Conduct a theoretical analysis of the reduction in heat flow that can be achieved with both full and partial insulation of tunnel rock surfaces.

(ii) Provide for the mining industry a straightforward means of predicting the reduction in heat flow due to full and partial insulation under a wide variety of mining conditions.

(iii) Test the theoretical predictions by experiment at an underground tunnel.

(iv) Obtain experience in the practical problems of applying insulation to tunnel surfaces in deep level mines.

1.3 Outline of Study

The major sections of this dissertation are devoted to a theoretical study of the heat flow reductions that can be gained by insulating rock surfaces, and to the results of actual heat flow reductions achieved at an experimental test site. However other important aspects of the analysis of the thermal insulation of mine airways have been examined.

Initially a literature search was conducted of previous work on insulating mine airways. The findings of this are presented in Chapter 2. Among the several authors who have examined the possibility of insulating mine airways as a means of reducing heat gain, most have concluded that although insulation should, theoretically, reduce the heat flow into an airway, there are no materials available which are practical for use in mines. Unfortunately the mathematical analyses were in general over-simplified, leading to errors in the estimation of the final effectiveness of the insulation. This was so mainly because neither the effect of the [illegible] of the airway on the heat flow from the rock, nor the temperature history of the rock prior to the application of the insulation were taken into account. From this review, a more thorough analysis than any previously published appears to be warranted.

Also in Chapter 2 a review of the techniques and problems associated with evaluating heat flow into mine tunnels is presented. A knowledge of this information is essential for conducting an analysis of the heat flow reduction that can be achieved by insulating mine airways.

To mathematically assess the effect of insulation on heat flow into a tunnel, the heat diffusion equation must be solved subject to complex boundary and initial conditions.

The complex boundary and initial conditions are due to:

(i) an irregular, non-circular, tunnel cross-section;

(ii) a rock body extending to infinity;

(iii) irregular boundary conditions on the rock surface, e.g. possible partial insulation of the perimeter; and

(iv) the application of the insulation some time after the rock surface was exposed.

The difficulties in solving the two-dimensional heat flow equation subject to these conditions were overcome by using finite element analysis or, where possible, simplified analytical approaches such as the quasi-steady method (Starfield and Bleloch, 1983). The quasi-steady method was modified to allow for an insulated rock surface, and both this algorithm and the application of finite element analysis to underground heat flow problems were tested in Chapter 3. A computer program based on the modified quasi-steady method is presented in Appendix A.

On establishing suitable methods of predicting heat flow into insulated tunnels a theoretical study was conducted in Chapter 4. Initially each of the many parameters that effect the heat flow were examined to identify which could be assumed to be constant in the analysis. Those parameters which could not be assumed to be constant were examined further over a range applicable to the South African mining industry.

With this information a preliminary study was conducted of the effects of insulation on heat flow at a single tunnel cross-section. Although the results of assessing the heat flow into a single cross-section can not be applied to a mine-wide case, the mathematical procedure is simple and provides a quick and easy assessment of the effects of insulation thickness, insulation thermal conductivity, the percentage covering of the rock surface and the insulation effect of the footwall ballast.

This work was then extended to allow for the effects of a finite length of tunnel. The results of a large number of computer runs for varying conditions are presented in the form of nomograms.

To discover the practical implications of insulating mine airways and to obtain an indication of the accuracy of the theoretical analysis a section of airway at Western Deep Level gold mine was insulated. The test site was divided into three 30 m sections, which were treated as follows:

(i) Section A - An uninsulated control section.

(ii) Section B - The sidewalls, hangingwall and footwall were insulated with approximately 50 mm thick insulation foam.

(iii) Section C - The sidewall and hangingwall were insulated with approximately 50 mm thick insulation foam. The footwall was left untreated.

Data was collected over 24 weeks and the heat flowing into the tunnel cross-sections was determined from a knowledge of the rock body temperatures and thermal properties. The reductions in heat flow due to the insulation were established by comparison of the insulated section with the uninsulated control sections. These results are presented in Chapter 5.

The theoretical and experimental work is compared in Chapter 6. The theoretical results were derived using finite elements which modelled the experimental test site as closely as possible. In addition a comparison was made with simple techniques of heat flow analysis and the accuracy of both methods is commented on.

Whilst the main body of work presented in this thesis is concerned with the assessment of the heat flow reduction due to the insulation, it is also appropriate to comment upon suitable materials for widescale use in underground workings. In Chapter 7 a breakdown of desired properties for an airway insulation is presented.

Another aspect to consider when assessing the implications of insulation is the financial savings when compared with the cost of supplying an equivalent amount of refrigeration. For this reason a financial comparison was conducted for a typical airway both with and without an insulated footwall. The results are presented in Chapter 8. It is unfortunate that this important aspect can only be covered by a typical example, but the large number of site specific variables involved in the analysis prevent any global analysis.

In conclusion a set of recommendations have been presented as a guide to the selection and implementation of airway insulation.

1.4 Mining Terms

In this dissertation the term 'footwall' can be considered to be the floor of a rectangular cross-sectional tunnel. Similarly the '*hanging-wall*' corresponds to the ceiling and the 'sidewalls' to the walls of the tunnel.

The 'ballast' is a layer of rubble, typically 300 mm thick, placed on the footwall for laying rail tracks on.

The terms 'intake airway', 'airway', 'ventilation airway', and 'tunnel' have been used synonymously throughout this dissertation.

This dissertation reports on work carried out as part of the research programme of the Chamber of Mines of South Africa.

2 LITERATURE REVIEW

2.1 Introduction

The aim of this chapter is to review previous theoretical and experimental studies on the effect of insulating mine airways. Since the study of heat transfer to insulated airways has as a prerequisite the understanding of heat transfer to uninsulated airways, studies on the latter are of necessity included in the review. Chapter 3 deals in detail with the techniques of computing heat transfer to mine airways. The present chapter thus treats computational studies in outline only, with emphasis on the limitations and on the results that have been achieved, rather than on the techniques.

2.2 Heat Flow into Insulated Tunnels

In simplified form the heat flow into a tunnel can be assessed by making the following assumptions:

(i) The rock is homogeneous.
(ii) There is negligible axial heat transfer.
(iii) The initial temperature distribution is uniform throughout the rock.
(iv) The tunnel has a circular cross-section.
(v) The rock surface temperature is equal to the ambient temperature (i.e. there is no surface resistance to heat transfer).

Assumption (i), (ii), and (iii) are not questioned in the literature, which from the experimental work of Hemp (1966, 1969, 1970a, 1970b) appears to be justified. In the work presented in this dissertation assumptions (i) and (ii) have been accepted, but the assumption of a uniform initial temperature distribution throughout the rock can not be made when considering events (such as the application of insulation) which occur some time after the holing through of the tunnel excavation.

It is convenient to assume a circular cross-section as this facilitates an analytical solution for the rate of heat transfer to be found. By also making assumption (v), of no surface heat transfer resistance, a solution in the form of an intractable integral is available (Nicholson, 1921). This integral was numerically tabulated by Goch and Patterson (1940), and enables a good estimate of tunnel heat flow to be simply evaluated.

An improvement on this solution was achieved when a similar integral, which made allowance for uniform surface convection, was formulated (Goldstein 1932). This integral was comprehensively tabulated (Jaeger and Chamalaun, 1966) for different Biot and Fourier numbers and similarly provides a quick and easy solution.

These two solutions are important because they have been used not only for these simple cases but as the basis of more complex problems. The solution by Goch and Patterson forms the basis of the quasi-steady method of Starfield and Bleloch (1983), which is capable of dealing with non-uniform boundary conditions, and the solution by Jaeger and Chamalaum can be used to allow for cases of uniform wetness or uniform insulation around the tunnel perimeter (Hemp, 1982).

Thus, for example the effect of a layer of insulation can be accounted for by ignoring its heat storage capacity, and calculating an effective surface heat transfer coefficient. Neglecting the very small area change due to the thickness of insulation x, the effective surface heat transfer coefficient h_e, is given by:

$$h_e = 1/(x/k + 1/h)$$

where k is the insulation thermal conductivity and h is the surface convective heat transfer coefficient.

Most airways in mines are approximately square or rectangular in cross-section. It is therefore desirable to derive some equivalent radius so that these simple methods may be applied. A method was devised (Wiles and Graves, 1954) from the results of an experiment making use of an electrolytic tank to study the heat flux around a square cross-section with a wet footwall. Two relationships for equivalent radii were derived:

$$a = b/2 \exp(-1{,}765+2{,}473F) \tag{2.1}$$

$$a = b/2 \exp(0{,}795-0{,}940F), \tag{2.2}$$

where a is the equivalent radius, b is the side of the square tunnel and F the fraction of total heat flow through the hangingwall and sidewalls. Equation 2.1 applies to the heat flux through the footwall and Equation 2.2 to the hanging and sidewalls. It should be noted that when the footwall is totally dry (that is $F = 0{,}75$) Equations 2.1 and 2.2 are the same, resulting in $a = 0{,}547b$.

This work unfortunately has been misinterpreted, with most authors assuming an equal cross-sectional area relationship, resulting in $a = 0{,}564$ and applying this also to situations other than totally dry. This is acceptable for the totally dry case since this relationship is close to the $a = 0{,}547b$ of Wiles and Graves, but erroneous for wet or partially insulated cases.

The heat flow into a tunnel of square cross-section and partially wet surfaces has been solved numerically by Starfield and Dickson, (1967). The results of many computer runs were assembled into a data base. The wet and dry bulb temperature increase along a length of airway is calculated by accessing the data base through an interpolation program, known as 'rapid method' (Starfield, 1969).

Many other simplified models have been proposed to allow for wet airways. Most of them rely on the fundamental methods previously mentioned and they have been adequately reviewed (Vost, 1983). Perhaps the most useful method which allows irregular boundary conditions on the tunnel circumference is the quasi-steady method of Bleloch and Starfield (1983). The basis of this method considers a thick walled, hollow cylinder with steady state heat flow conditions. The diameter of the outer wall of the cylinder varies with time so that the heat flow at the tunnel surface at any instant is equal to that of the real transient problem. In this present work much use is made of this technique in extended form so as to accommodate partial insulation, and more detail is given in Chapter 3 and Appendix A.

Only two authors have published heat transfer data from actual measurements taken in mine tunnels (Lambrechts, 1967 and Hemp, 1966, 1967, 1970). The work of Lambrechts was based on 305 sets of observations in mine airways, from which empirical equations for calculating wet-bulb temperature gradients as a function of air velocity and VRT were derived. His results have no direct bearing on the work in this dissertation as the equations cannot be adapted to account for the effects of insulation.

Hemp (1966, 1967, 1970) produced a series of reports based on practical measurements of air and rock temperatures. The work consisted of measuring air temperatures along an airway and measuring rock temperatures to various depths at a test site. The most salient objectives of the work were to correlate observed values of heat flow with those calculated from theory, to establish values of heat transfer coefficients, and to investigate heat and mass transfer processes from a wet footwall. His results showed that it is more accurate to assess tunnel heat flow by measuring rock temperatures rather than through measuring increases in air temperature.

Hemp stated:

> 'Perhaps the most significant finding has been that the theory of heat flow into an airway surrounded by homogeneous isotropic rock provides values of the heat flow rate which agree closely with those observed by means of rock temperature measurements,' (Hemp, 1970).

He is in fact referring to the work of Starfield (1966), with which he compared his experimental observations and obtained close agreement.

2.3 Insulation of Mine Airways

The first work on the insulation of mine airways was conducted during the period 1962 to 1964 when an insulation field trial was conducted at Loraine Gold Mines Limited. This project utilized two types of insulation, namely polyurethane foam and slag wool. The heat flow was measured by drilling holes to a depth of about 3 m into the rock mass and measuring temperatures at 300 m intervals. Although a number of measurements were made over a period of more than two years and it was found that the heat flux into the airway was reduced, the results were never published and the wide scale insulation of airways never implemented. Presumably either the results were not conclusive or the benefits not sufficiently attractive at that time.

The first documented work was concerned with the simulation of the effects of total insulation by reducing the surface heat transfer coefficient on the tunnel surface (Scott, 1959). A graph was produced showing the reduction in air temperature of an insulated tunnel when compared to that of an uninsulated tunnel.

Unpublished, internal work of the Chamber of Mines of South Africa Research Organization attempted, by means of a resistance paper analogue, to quantify the reduction in heat flow experienced when the hanging and sidewalls are insulated. Although the method was analogous to steady state heat transfer, it was shown how this method could be applied to the transient problem of heat flow into a tunnel. Using the steady state analogue the radius was found at which the temperature was halfway between the virgin rock temperature and the rock surface temperature. By using the solution given by Carslaw and Jaeger (1946) for heat flow from an infinite mass to a circular tunnel it was possible to calculate the age of the corresponding airway. The justification for this method was that the dimensionless temperature around a circular hole varies linearly for the most part with the logarithm of the radius for different values of age, and the corresponding plot for a steady state field shows the same linear relationship. This approach is the same as that applied computationally in the later quasi-steady method (Starfield and Bleloch, 1983).

Whilst the method of analysis was noteworthy, the conducting sheet procedure was doubtful. In order to account for the layer of insulation, an equivalent thickness of rock with the same thermal resistance as the layer of insulation was evaluated. For example, a 50 mm thickness of insulation with a thermal conductivity of 0,03 W/mK is equivalent to 1,98 m of rock with a thermal conductivity of 5,6 W/mK. For a typical mine airway the effective tunnel radius was reduced to one percent of the actual and the results are thus open to doubt.

It is possible to use the above analytical technique to calculate heat flow into a simple uninsulated tunnel without using the electrical analogue. When comparing the results of such an exercise with the results obtained using the Goch and Patterson tables, accuracies within five per cent are obtained. It is unfortunate that the results of the paper analogue were not subjected to a similar check. This would have established the validity or otherwise of the technique.

In view of this uncertainty the analogue results should be treated with some scepticism. The main conclusion was:

> 'It is considered that these benefits (reduced cooling costs) are small compared with the expense and complexity of installing and maintaining efficient insulation, and in view of this it is concluded that insulation of mines airway tunnels is not a justifiable proposition.'

It is worth noting that the authors examined the decreased benefits of insulation with a finite length of tunnel. The benefit decreases because insulation, by reducing heat pick-up, promotes a smaller air temperature gradient along the airway, thereby maintaining the temperature driving force at a higher level than in the uninsulated case. This means that estimates of heat flow reduction in an airway cannot be based on estimates referring to a single locality.

Other work conducted at the Chamber of Mines of South Africa in 1967 used an electrical analogue to study the insulation of development ends. The insulation had a conductivity of 0,52 W/m °C, which is high compared with values as low as 0,02 W/mK available for modern materials. The insulation was applied six hours after exposure of the rock surface. The model assumed linear heat transfer rather than radial, and was only concerned with the heat flow during the first 20 hours from the time of exposure. The effect of cyclical wetting down of the insulation and rock surface was also incorporated. While this work is not strictly relevant to long term insulation of a mine airway under dry conditions, the results show considerably lower surface temperatures as a result of insulation.

A numerical method, based on the Goch-Patterson approach, was used to compare the temperature rise of air through 600 m of tunnel (Gould, 1968) when either completely insulated or uninsulated (with varying degrees of wetness for the uninsulated case). The results show a significant decrease in the outlet air temperature as a result of insulation, typically 1,5 °C wet-bulb. The overall conclusion was that there are many practical problems which require attention before insulation becomes feasible, and that the higher the virgin rock temperatures, the more justifiable the expense of insulating. However, at the virgin rock temperatures being encountered at the time (1968) there was no merit in its application.

In more recent research some advantages of insulating airways were highlighted (Hughes, 1978). The economic benefits due to the reduction in heat flow and reduction in resistance to air flow were quantified and break-even cost figures for the insulation were evaluated. A positive case for the use of insulation was presented. Unfortunately the economic justification is erroneous due to, amongst other things, the assumption of steady state rather than transient heat flow, as well as the consideration of only one cross-section of tunnel rather than a finite length.

The past work on mine insulation has generally resulted in negative conclusions with regard to its wide spread implementation. However, most of this work was either flawed or done some 20 years ago. Since then the environmental control practices in South African gold mines have changed radically. Significantly higher virgin rock temperatures are being encountered and the widespread use of chilled service water and its natural partner - the bulk cooling of air - are well established. The available insulation materials have also changed radically over these two decades. Furthermore, the increased depths and higher rock stresses have increased the possible benefits with regard to rock support. All these factors indicate the need for a careful consideration of the insulation of mine airways.

3 COMPUTATIONAL METHODS

3.1 Introduction

In this chapter the computational methods used in evaluating magnitude of heat flow from insulated airways are presented.

Initially the *finite element* method and the commercial computer program 'ADINA T' (Automatic Dynamic Incremental Nonlinear Analysis of Temperature), which was used extensively are introduced. The accuracy and suitability of the package were tested and the results are fully presented. The test cases described were used to derive a suitable finite element mesh configuration and time step scheme for the solution of heat flow from an infinite medium into a tunnel. A simple test of the effect of variable insulation thickness was also conducted and the results are presented.

The quasi-steady method of analysis is then described together with details of *modifications which were* made to accommodate the effects of partial insulation. The algorithm is then compared with the finite element method in order to assess its accuracy for a typical test case.

Finally a method for predicting heat flow into fully insulated or uninsulated tunnels is shown. The method is based on the published tables of Jaeger and Chamalaum.

3.2 Finite Element Method

3.2.1 Introduction

The *finite element method* is a *numerical* analysis technique for obtaining approximate solutions to differential equations which occur in many engineering problems. The method was originally developed to study the stresses in airframe structures (Huebner, 1975) but has been applied to other fields such as hydraulics, dynamics and heat transfer (Desai and Abel, 1972). The attractiveness of the method lies in its ability to handle problems having complex geometries, and boundary conditions which are seldom amenable to classical solutions (Owen and Hinton, 1980).

The basis of the finite element method is the division of the region of interest into discrete elements over which the temperatures are interpolated. The ability to specify different element sizes and shapes is one of the most powerful features of the method. It enables the boundaries of the domain of interest to be modelled accurately and is capable of solving irregular meshes, which may typically have a greater density of elements at regions of greater temperature gradient. The selection of element size, shape, and distribution is largely governed by experience. Unfortunately the accuracy of the results are often limited by the availability of computer running time or funds. A greater number of elements will tend to produce higher accuracy but will increase the use of computer resources. Typical element shapes used in commercial packages are shown in Figure 3.1. The nodal points are the positions at which temperatures are interpolated. The governing equation for transient heat conduction in two dimensions is given by:

$$k \frac{\partial^2 T}{\partial x^2} + k \frac{\partial^2 T}{\partial y^2} = \rho c \frac{\partial T}{\partial \theta} \qquad (3.1)$$

In order to solve Equation 3.1 by the finite element method, use is made of the calculus of variations (Spiegel, 1971). This variational approach leads to a functional (function of a function) which when minimised provides the solution to Equation 3.1. The functional, I, for this problem is of the form (Heubner, 1975):

$$I = \tfrac{1}{2} \int_{Area} [k \frac{\partial T^2}{\partial x} + k \frac{\partial T^2}{\partial y} + \rho c \frac{\partial T^2}{\partial \theta}] \, dy \, dx \qquad (3.2)$$

The temperature distribution is then approximated by assuming:

$$T = [N] [T] \qquad (3.3)$$

[T] is a column matrix of the unknown nodal temperatures and [N] are the interpolating or shape functions which approximate the temperature behaviour throughout an element.

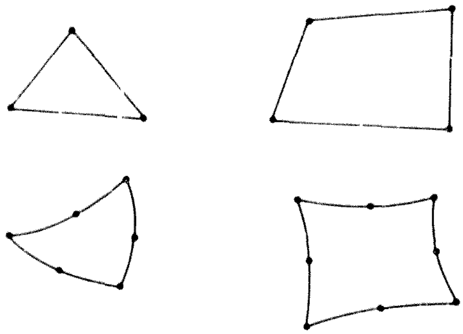

Figure 3.1 Typical two-dimensional element shapes

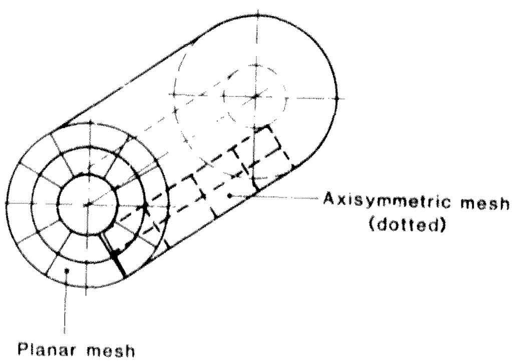

Figure 3.2 Planar and axi-symmetric meshes

Substituting Equation 3.3 into Equation 3.2 and performing the relevant mathematics (Myers, 1971) to minimise Equation 3.2 produces:

$$[C]\,[\dot{T}] + [T]\,([K] + [H]) = 0 \qquad (3.4)$$

where the elements of the matrices [C], [K] and [H] are given by:

$$K_{ij} = k[\frac{\partial N_i}{\partial x}\frac{\partial N_j}{\partial x} + \frac{\partial N_i}{\partial y}\frac{\partial N_j}{\partial y}]\,dy\,dx$$

$$C_{ij} = \rho c[N_i\,N_j]\,dy\,dx$$

$$H_{ij} = h[N_i\,N_j]\,dy\,dx$$

Equation 3.4 shows the relationship between the nodal temperatures and their time derivatives which must be satisfied at each point in time to minimise I in Equation 3.2. This system of equations is usually solved by one of the classical Crank-Nicolson, or Euler (Myers, 1971) numerical difference techniques.

The computer program 'ADINA T' has been developed to solve Equation 3.4 for various boundary conditions. Comprehensive use of this program was made in assessing the heat flow from rock into a tunnel.

3.2.2 The 'ADINA T' finite element program

The following tests were carried out in order to gain experience with the 'ADINA T' program, as well as to assess its accuracy, and to help arrive at a suitable mesh for a partially insulated tunnel in an infinite medium.

TEST 1

The steady state temperature distribution in an infinitely long, thick walled pipe, subject to the following boundary conditions, as determined.

Inside radius $r_1 = 1{,}0$ m
Outside radius $r_2 = 2{,}0$ m
Inside temperature $T_1 = 100$ °C
Outside temperature $T_2 = 0$ °C

The solution to this simple problem, given in many texts (Bayley et al., 1972, McAdams, 1954), serves as a useful assessment of the 'ADINA T' package.

This problem is governed by the Laplace equation, which for cylindrical co-ordinates in one dimension is given by:

$$\frac{d^2T}{dr^2} + \frac{1}{r}\frac{dT}{dr} = 0$$

or

$$\frac{d}{dr}\left(\frac{r dT}{dr}\right) = 0$$

Successive integration leads to the general solution

$$T = A \ln r + B$$

By subsitution of the boundary conditions

$T = T_1$ at $r = r_1$
$T = T_2$ at $r = r_2$

into the general solution, constants A and B are obtained:

$$A = \frac{T_2 - T_1}{\ln (r_2/r_1)} \qquad B = T_1 - \frac{\ln (T_2 - T_1)}{\ln (r_2/r_1)}$$

The temperature distribution through the cylinder wall is then given by:

$$T = T_1 + \ln (r/r_1) \left[(T_2 - T_1)/\ln (r_2/r_1)\right] \qquad (3.5)$$

Inside radius	$r_1 = 1{,}0$ m
Outside radius	$r_2 = 2{,}0$ m
Inside temperature	$T_1 = 100$ °C
Outside temperature	$T_2 = 0$ °C

The solution to this simple problem, given in many texts (Bayley <u>et al</u>., 1972, McAdams, 1954), serves as a useful assessment of the 'ADINA T' package.

This problem is governed by the Laplace equation, which for cylindrical co-ordinates in [illegible] dimension is given by:

$$\frac{d^2T}{dr^2} + \frac{1}{r}\frac{dT}{dr} = 0$$

or

$$\frac{d}{dr}\left(\frac{r\,dT}{dr}\right) = 0$$

Successive integration leads to the general solution

$$T = A \ln r + B$$

By subsitution of the boundary conditions

$$T = T_1 \quad \text{at } r = r_1$$
$$T = T_2 \quad \text{at } r = r_2$$

into the general solution, constants A and B are obtained:

$$A = \frac{T_2 - T_1}{\ln (r_2/r_1)} \qquad B = T_1 - \frac{\ln (T_2 - T_1)}{\ln (r_2/r_1)}$$

The temperature distribution through the cylinder wall is then given by:

$$T = T_1 + \ln (r/r_1) \left[(T_2 - T_1)/\ln (r_2/r_1)\right] \qquad (3.5)$$

Owing to the axisymmetric condition of the problem only one dimension need be considered when using the finite element method. However, to explore the two dimensional features of the 'ADINA T' package, a quarter of a planar section was analysed. The difference between an axisymmetric mesh and a planar mesh is shown in Figure 3.2, the finite element mesh used is shown in Figure 3.3.

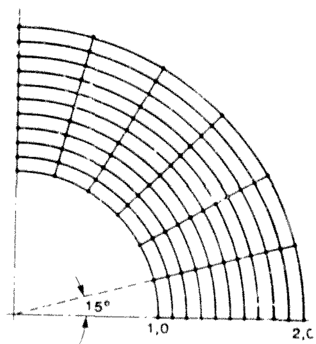

Figure 3.3 Planar Finite element mesh layout for test 1.

The results from the finite element method were compared with the analytical solution given by Equation 3.5. As expected they were identical and axisymmetrical. They are not, therefore, reproduced here.

TEST 2

In order to test a convective boundary condition, a similar problem to Test 1 was set up, but with the following changes in conditions.

Inside fluid bulk temperature T_1 = 30,0 °C
Outside temperature T_2 = 45,0 °C
Inside surface convection

heat transfer coefficient	h	= 10,0 W/m²K
Thermal conductivity	k	= 1,0 W/mK

With boundary conditions:

$$k \frac{dT}{dr} = h\,(T_{r_1} - T_f) \quad \text{at} \quad r=r_1$$

By differentiating Equation 3.5 :

$$\frac{\partial T}{\partial r} = (T_2 - T_{r_1})/\ln(r_2/r_1)$$

and equating it to the boundary conditions at r_1, the inside wall surface temperature, Tr_1 can be obtained. Substituting this value into Equation 3.5 the temperature distribution throughout the cylinder is derived.

For the finite element solution of the problem the same mesh as that in Test 1 was used. Although the results were axisymmetric, the temperatures were greater than those from the analytical solution by approximately 0,1 °C at each nodal point. This is somewhat surprising in view of the exact results obtained in Test 1, and indicates that the accuracy of the results depends on the boundary conditions for the same mesh configuration.

TEST 3

In order to assess the transient behaviour of the package the following problem was devised. A composite hollow cylinder, initially at steady state (Figure 3.4), was subject to the following conditions:

Radius	r_1	= 50 mm
Radius	r_2	= 55 mm
Radius	r_3	= 80 mm
Thermal conductivity	k_{12}	= 45 W/mK
Thermal conductivity	k_{23}	= 0,09 W/mK
Inside surface heat transfer coefficient	h_1	= 5000 W/m²K

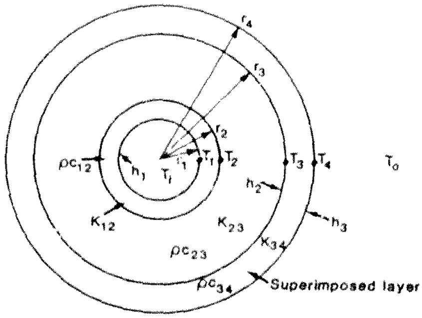

Figure 3.4 Physical configuration for test 3

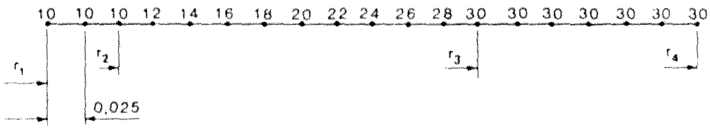

Figure 3.5 One-dimensional finite element mesh layout for test 3 showing initial nodal point temperatures

Outside surface heat transfer coefficient	h_2	=	25 W/m²K
Density x specific heat	$\varrho_1 c_1$	=	$3,9 \times 10^6$ J/m³K
Density x specific heat	$\varrho_2 c_2$	=	$7,2 \times 10^4$ J/m³K
Inside temperature		=	10 °C
Outside temperature		=	30 °C

At time zero a further layer was superimposed on the outer surface. The heat transfer through the compounded cylinder decayed to a new steady state solution, which was obtained analytically and served as an evaluation on the transient 'ADINA T' solution.

In the finite element analysis, 18 equal length, one- dimensional elements were used (see Figure 3.5). The initial temperature distribution throughout the composite was derived analytically from the conditions given above. The overall heat transfer coefficient before superimposition is given by:

$$UA_1 = 2\pi/\Sigma R$$

wher

$$\Sigma R = 1/h_1 r_1 + \ln(r_2/r_1)/K_{12} + \ln(r_2/r_3))/K_{23} + 1/h_2 r_3$$

The heat flux per metre length is then given by:

$$Q/L = UA\ (T_O - T_i) \quad W/m$$

Once Q/L is known the intermediate temperatures can be calculated.

The conditions specified for the superimposed layer were:

Thickness		=	15 mm
Thermal conductivity	k_{34}	=	0,035 W/mK
Outside surface heat transfer coefficient	h_3	=	25 W/m²K
Density x specific heat	$\varrho_3 c_3$	=	$3,63 \times 10^4$ J/m³K

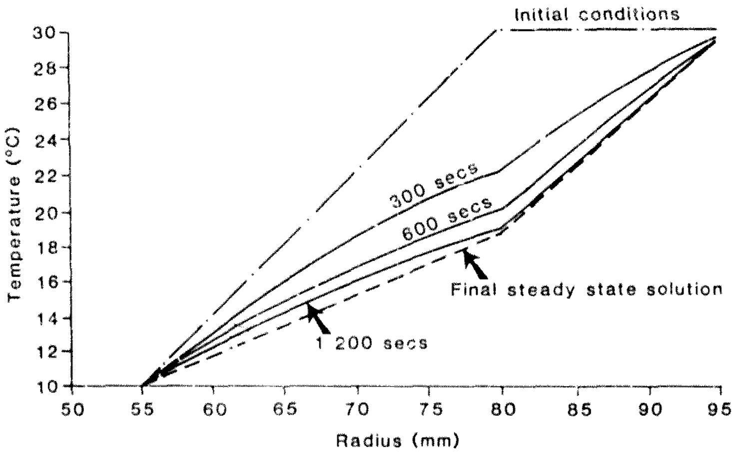

Figure 3.6 Analytical and finite element solutions for test 3

The new overall heat transfer coefficient then becomes:

$UA_2 = 1/(UA_1 + \ln(r_3/r_4)/(2\pi k_{34}))$

Using the same process as before, the steady state heat flux can be calculated and hence the temperature distribution within the solid. These results were then used to assess the finite element solution.

Figure 3.6 shows the steady state analytical solution before and after superimposition and the finite element solutions for various time intervals after superimposition. The finite element solutions show how rapidly the transient behaviour is damped. After 10 minutes the finite element results modelled exactly the final steady state solution.

TEST 4

An infinitely long cylinder was surrounded by an infinite mass at a uniform initial temperature. The surface of the cylinder was suddenly reduced to a temperature T_1 and maintained at that value. Obtaining the solution to the heat flow at the cylinder surface is extremely important, as it ideally represents the heat flow from rock into a tunnel.

The form of the heat conduction equation expressed in cylindrical co-ordinates which is appropriate to the problem is:

$$k \frac{\partial^2 T}{\partial r^2} + \frac{k}{r} \frac{\partial T}{\partial r} = \rho c \frac{\partial T}{\partial \theta}$$

with initial and boundary conditions given by:

when	$\theta = 0$	$T = VRT$	for $r > r_1$
and	$r = r_1$	$T = T_1$	for $\theta > 0$

The solution to this problem is given by (Nicholson, 1921):

$$\dot{Q}/A = \frac{k}{r_1} (VRT - T_1)\ T' \ \mathrm{W/m^2}$$

$$\text{where } T' = \frac{4}{\pi^2} \int_0^\infty \frac{e^{r_1 z^2}}{J_o^2(z) + Y_o^2(z)} \frac{dz}{z}$$

The evaluation of T' presents considerable difficulties, but has been presented in the literature in the form of tables (Goch and Patterson, 1940).

If it is assumed that:

VRT = 45 °C
T_1 = 30 °C
k = 6,0 W/mK
pc = 2,45 x 10^6 J/m^3K
r_1 = 1,91 m

the heat flux over a two year period, calculated using the Goch and Patterson tables, is that given in Fig 3.7.

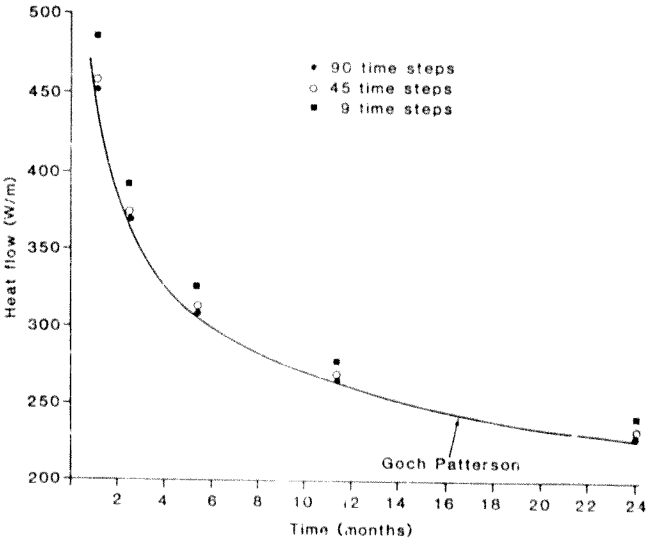

Figure 3.7 Heat flow into a circular tunnel from the Goch Patterson solution and from finite element analysis using different time steps.

The 'ADINA T' package cannot incorporate an infinite element; thus the first step in solving the problem is to decide on an outer boundary at which the temperature does not fall below VRT in the two year period. The relationship between rock temperature and radius at a specific time is given by (Carslaw and Jaeger, 1959):

$$\frac{VRT-T}{VRT-T_1} = (r_1/r)^{0,5}\, X + \frac{(\alpha\theta)^{0,5}(r-r_1)iX}{4\, r_1^{0,5}\, r^{1,5}}$$

$$+ \frac{\alpha\,\theta\,(9r_1^2 - 2r_1 r - 7r^2)\, i^2\, X}{32 r_1^{1,5}\, r^{2,5}} + \ldots\ldots$$

where

$$X = \operatorname{erfc}\,[(r-r_1)/(2\sqrt{\alpha\theta})].$$

From this expression and using the above conditions, it is found that the rock has been cooled below VRT, to a depth of 48 m.

Again this is an axisymmetric problem and a one-dimensional, 19 element, finite element mesh was used as input in the 'ADINA T' program. The first element was 0,1 m long and subsequent elements progressed geometrically by 30 per cent, the nineteenth element being 11,25 m long. This arrangement was arrived at by trial and error, and represents a compromise between the use of computer resources and desired accuracy. The total time was split into nine intervals, each interval being progressively greater than the previous. Each interval was further split into an even number of time integration steps. The computer run was repeated for an increasing number of time integration steps.

The results from the finite element solution are compared with those of Goch and Patterson in Figure 3.7. The 90-time-step solution was accurate to within 1,5 percent over the two year period and the 45-time-step solution was accurate to within 2,5 percent. The 9 time-step solution was unacceptable, differing by 7,5 percent from the Goch and Patterson solution.

As a further test, the number of elements were varied for the 45-time-step solution. The results for 19,9 and 5 elements are shown in Figure 3.8. It can be seen that while 5 elements gave a very inaccurate result, 9 elements provided a quite acceptable solution. The latter was accurate to approximately 4 per cent over the two year time period.

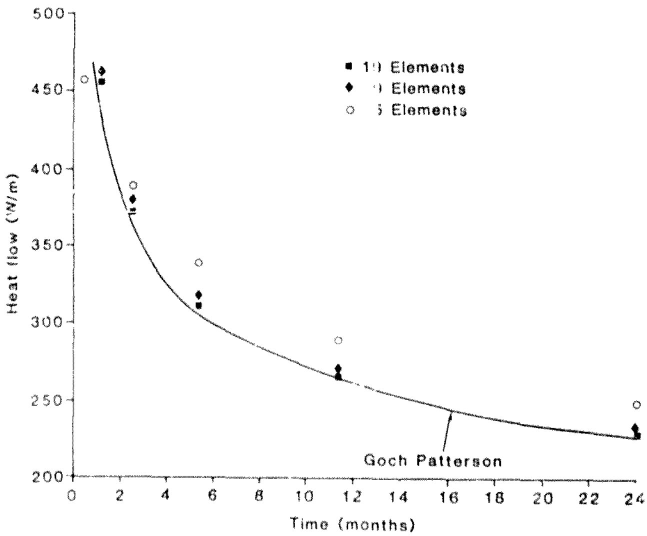

Figure 3.8 Heat flow into a circular tunnel from the Goch Patterson solution and from finite element analysis, using different numbers of elements.

TEST 5

The final test was to investigate the effect of linearly varying the thickness of a layer of insulation on a rock slab. Although this example is not a test of the features of the 'Adina T' program, the results are particularly important and are used in Chapter 6.

The assumed properties of the rock and insulation were as follows:

Height of Slab	=	1,0 m
Width of Slab	=	1,0 m
Rock Thermal Conductivity	=	5,5 W/mK
Insulation Thermal Conductivity	=	0,042 W/mK
Minimum Insulation Thickness	=	10 mm
Maximum Insulation Thickness	=	80 mm

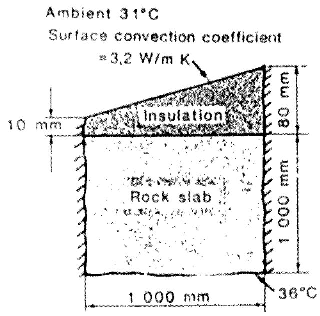

Figure 3.9 Physical layout for test 5 showing the varying insulation thickness on a rock surface.

One side of the rock slab was maintained at 36 °C and the ambient temperature on the side of the insulation was 31 °C. The surface of the insulation was assumed to be subject to a convective heat transfer coefficient of 3,2 W/m²k. A diagram depicting the test case is shown in Figure 3.9.

Using steady state analysis and a 200 element mesh it was found that there was an average heat flux of 3,8 W/m² from the insulated surface.

This is 20 per cent higher than if the same quantity of insulation was distributed evenly over the rock surface with a thickness of 45 mm.

3.3 Quasi-steady method

3.3.1 Introduction

In order to solve the problem of heat flow from rock into a partially wet airway a quasi-steady method was formulated (Starfield and Bleloch, 1983). The basis of the method is that instead of attempting to solve the transient heat diffusion equation, the variation of temperature with time is neglected and the much simpler Laplace equation is solved. A hollow cylinder is assumed, with the internal radius being that of the tunnel, and the external radius receding with time. The selection of the outer radius is such that the thermal gradient at the internal surface matches that given by the Goch and Patterson tables. The mathematical formulation of the method is as follows.

The solution tabulated by Goch and Patterson was for an infinitely long cylinder, surrounded by an infinite mass at a uniform initial temperature. The surface of the cylinder was suddenly reduced to a temperature T_1 and maintained at this value. The form of the heat conduction equation expressed in cylindrical co-ordinates, which is appropriate to the problem, is:

$$k \frac{\partial^2 T}{\partial r^2} + \frac{k}{r} \frac{\partial T}{\partial r} = \rho c \frac{\partial T}{\partial \theta}$$

with initial and boundary conditions given by:

$$\theta = 0 \qquad T = VRT \qquad \text{for } r > r_1$$
$$r = r_1 \qquad T = T_1 \qquad \text{for } \theta > 0$$

and

$$T \to VRT \quad \text{as } r \to \infty.$$

The thermal gradient at the surface, $G(t)$, for this problem has been tabulated by Goch and Patterson. If we further assume unit thermal conductivity, unit diffusivity, initially zero temperature throughout, and ignore the temperat·· time dependence, the problem can be expressed in dimensionless form as:

$$\frac{d^2T}{dr^2} + \frac{1}{r}\frac{dT}{dr} = 0$$

with b· ry conditions

T=

and

T=0 at r=R (some far boundary).

The solution is given by:

$$T(r) = [\ln(R) - \ln(r)]/\ln(R)$$

for which the thermal gradient at r = 1 is:

$$\frac{dT}{dr} = -1/\ln(R)$$

If we now choose R so that the thermal gradient matches the true thermal gradient, G(t), we obtain

$$R = \exp\,[1/G(t)]$$

The authors then assumed that, for typical mining conditions, the position of the far boundary is insensitive to the precise form of the boundary conditions at the tunnel surface. By using finite difference methods as a comparison this was shown to be the case, except for small time periods where the errors became excessive. It is therefore possible to use he quasi-steady approach to solve more complex problems by choosing an outer radius using the expression above, and solving Laplace's equation with the appropriate surface boundary conditions.

3.3.2 Quasi-steady algorithm for a partially insulated airway

The quasi-steady algorithm presented by Starfield and Bleloch was for a partly wet airway and needs some modification to accommodate partial insulation. The mathematical details are given in Appendix A, with the method closely following that given by Starfield and Bleloch. Details of a computer program which calculates heat flux along a length of airway with a partially insulated surface are given in Appendix B.

3.3.3 Accuracy of quasi-steady algorithm

A test case was solved and compared with the results from a finite element analysis in order to assess the accuracy of the quasi-steady algorithm.

The heat flow in a circular tunnel was evaluated as the tunnel aged from 0 to 2 years. The following conditions were assumed:

Rock conductivity	=	6 W/mK
Rock diffusivity	=	$2,4\times10^{-6}$ m²/s
Insulation conductivity	=	0,03 W/mK
Insulation thickness	=	50 mm
Air dry-bulb temperature	=	30 °C
Virgin rock temperature	=	45 °C
Tunnel radius	=	1,5 m
Proportion of surface which is insulated	=	0,667

The results of heat flow (watts per metre of tunnel length) are plotted against time for both the quasi-steady method and the finite element analysis in Figure 3.10. The results from the quasi-steady method compare favourably with those produced using finite elements, the difference being approximately 4 per cent.

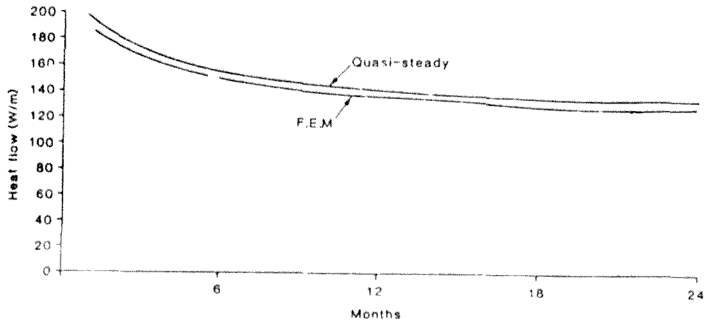

Figure 3.10 Heat flow into a partially insulated tunnel from finite element analysis and the quasi-steady method.

3.4 Simple method

The tables presented by Jaeger and Chamalaum are sufficient for analysing many of the problems of heat flow into circular mine tunnels without insulation, or with full insulation applied immediately after excavation. A computer program is listed in Appendix B which makes use of an approximation to the published tables (Gibson, 1972).

3.5 Conclusion

A commercial finite element program was tested with a number of heat conduction problems which are pertinent to heat flow in tunnels. The program was shown to perform well and is used in Chapter 6 to predict the heat flow at the experimental test site.

The quasi-steady algorithm was described and modified to accommodate partial insulation. A computer program which incorporates the algorithm is presented in Appendix B. The results of using the algorithm compare favourably with the results obtained using the finite element method. The modified quasi-steady algorithm is used comprehensively in this work to assess the heat flow into partially insulated tunnels.

A computer program incorporating an approximation of the Jaeger and Chamalaum tables was presented for calculating heat flow into uninsulated and fully insulated tunnels. The program is used extensively in this dissertation.

4 THEORETICAL ANALYSES OF THE EFFECTS OF INSULATION ON HEAT FLOW

4.1 *Introduction*

In this chapter a theoretical analysis of the effects of insulation on tunnel heat flow is presented. The various parameters which influence heat flow are listed below and each of these was considered.

Condition of ventilation air
Virgin rock temperature
Tunnel age
Rock specific heat
Rock density
Rock conductivity
Tunnel radius
Tunnel length
Surface heat transfer coefficient
Ventilation air flow rate
Heat transfer due to radiation
Dampness of the rock surface
Insulation thickness
Insulation conductivity
Equivalent conductivity of footwall ballast
Percentage covering of insulation
Time of surface exposure of rock prior to application of insulation.

Each of the above parameters was examined to assess its importance on heat flow.

The presentation comprises three major parts. Initially the heat flow parameters were examined to identify those which varied but had little influence upon the heat flow into the tunnel. These parameters were then assumed to be constants. Parameters which could not be treated as constants were also identified and methods of analysis were formulated.

The effects of insulation on heat flow at a single cross-section were then examined. The results of varying the insulation thickness, thermal conductivity and the percentage covering of the rock surface are described. In addition the thermal resistance of the footwall ballast was analysed.

Finally the effects of a finite tunnel length are presented. The effect of insulation is to reduce the heat flow and therefore maintain a higher temperature driving force than would be experienced in an uninsulated tunnel. The results from a single cross-section of a tunnel therefore overestimate the heat flow reduction which would be achieved in practice. Results in the form of nomograms are presented for various conditions and tunnel lengths.

4.2 Analysis of heat flow variables

4.2.1 Tunnel age

The importance of tunnel age on heat flow can be seen by examining the tabulated values of Goch and Patterson (See Section 2.2). The tabulated values, T', are directly proportional to heat flow, and T' is dependent upon the Fourier number, (Figure 4.1). It is clear that heat flow into a tunnel varies markedly with Fourier number (and hence time) for the normal lifespan of a mine tunnel. Therefore, in further analysis the effect of tunnel age was considered but limited to period of up to 10 years.

When considering a long length of tunnel the age may vary considerably from the inlet to the outlet due to the time taken for excavations. It is necessary when calculating the heat flow from a length of tunnel to discretise the total length into short segments, as described in Section 4.2.9. Therefore, for the most accurate results the age of the tunnel should be replaced by the age at each segment.

Two further possibilities are to assume the average age, or to make use of the logarithmic means of the ages at the start and end of the tunnel. In Table 4.1 the heat pickup from different lengths of tunnel with different development face advances is shown. It is assumed that the tunnel excavation is just complete, and that the time span between the start and finish of the tunnel can be found from the development face advance. The three proposed methods of calculating the age were used, namely an arithmetic mean, a logarithmic mean and an incremental increase stepwise along the tunnel. It can be seen that the variation in results is insignificant and the simple option of an arithmetic mean is used throughout the dissertation.

4.2.2 Rock Properties

The average values and ranges of specific heat, density, thermal conductivity and diffusivity found for quartzite in South African gold mines are shown in Table 4.2 (Jones and Bottomley, 1986).

The variation in rock diffusivity found in South African gold mines results in a significant variation in heat flow (Figure 4.2). Shown in Figures 4.3 and 4.4 are the variations in heat flow with changes in rock density and rock specific heat respectively. It is clear that for the range of rock densities and specific heats found in South African gold mines the effect on the heat flow is negligible, and the effect of changes in diffusivity are governed by changes in rock thermal conductivity only (Figure 4.5). Further analysis assumed constant rock specific heat and density, at their average values of 777 J/kgK and 2694 kg/m^3 respectively. The effect of variation in rock thermal conductivity was examined further, with the average of 5,14 W/mK used as a standard (see Chapter 5).

Table 4.1 Variation in calculated heat pickup from tunnels using different assumptions to calculate age

TUNNEL LENGTH M	DFA M/MTH	HEAT PICKUP kW		
		LOG	AVE.	INC.
480	20	125	113	118
	40	138	127	132
	80	151	143	147
1000	20	214	191	201
	40	232	211	222
	80	252	234	243
2000	20	330	298	312
	40	353	322	337
	80	377	350	364

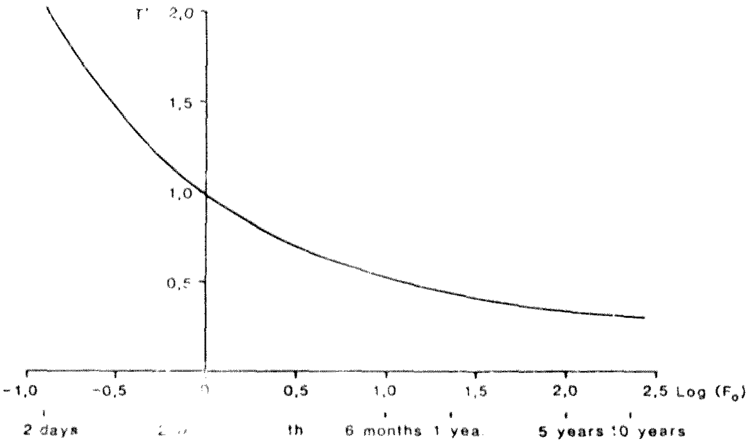

Figure 4.1 Decay with age of heat flow into a circular tunnel

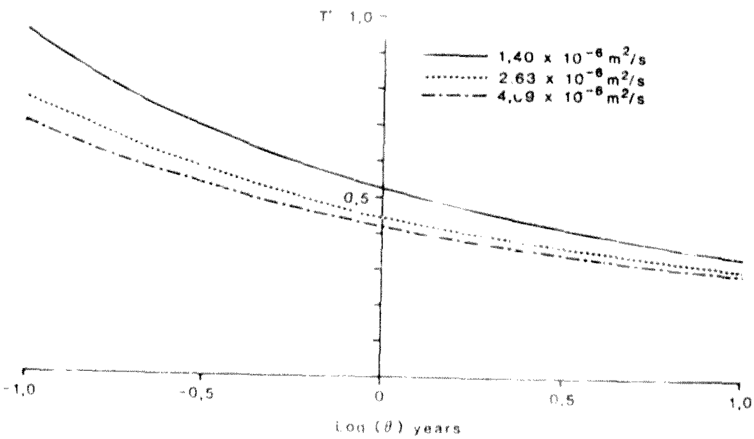

Figure 4.2 Variation of T' with time for different rock diffusivities

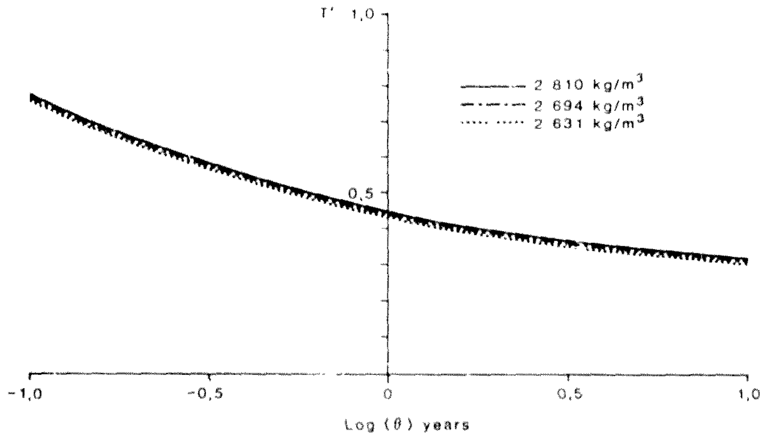

Figure 4.3 Variation of T' with time for different rock densities

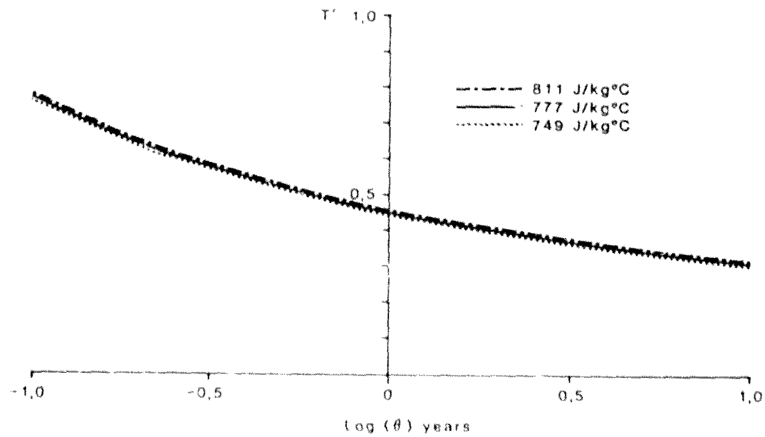

Figure 4 4 Variation of T' with time for different rock specific heats

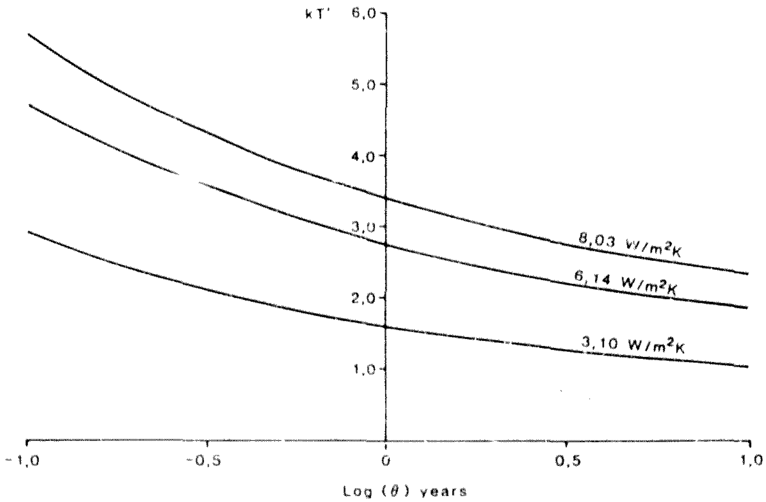

Figure 4.5 Variation of T' with time for different rock thermal conductivities

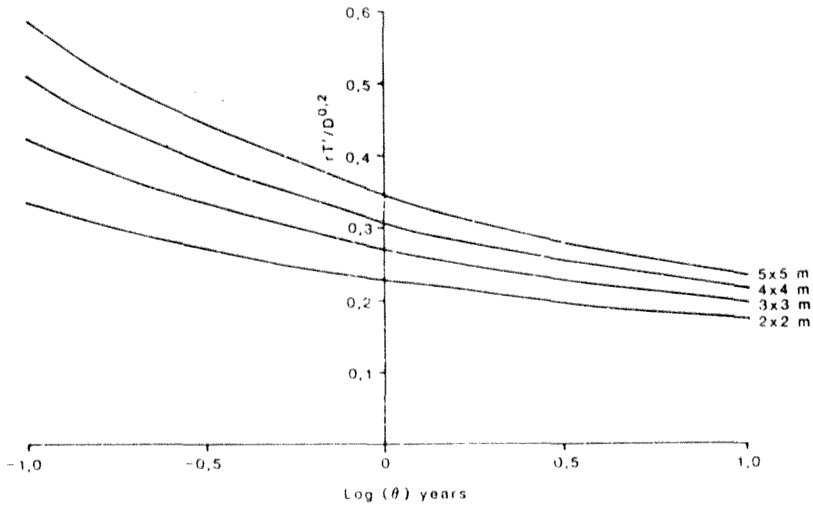

Figure 4.6 Variation of $rT'/D^{0,2}$ with time for different tunnel dimensions

Table 4.2 Typical values of quartzite properties found in South African gold mines

ROCK PROPERTY	AVERAGE	MAXIMUM	MINIMUM	UNITS
Conductivity	6,14	8,03	3,10	W/mK
Density	2694	2810	2631	kg/m^3
Specific heat	777	811	749	J/kgK
Diffusivity	$2,63x10^{-6}$	$4,09x10^{-6}$	$1,40x10^{-6}$	m^2/s

4.2.3 Tunnel size

Mine intake airways are typically rectangular or square in cross-section. An estimate for an equivalent radius needs to be made to make use of solutions, such as that by Goch and Patterson, for heat flow into a circular cylinder. From experiments conducted in an electrolytic tank two relationships were derived for equivalent radii for square cross-sections with wet footwalls (Wiles and Grave 1954). They were

$$a = b/2 \text{ Exp } (-1,765 + 2,473 \text{ F}) \tag{4.1}$$

$$a = b/2 \text{ Exp } (0,795 - 0,940 \text{ F}) \tag{4.2}$$

where a is the equivalent radius, b is the side of the square and F the fraction of total heat flow that flows through the hanging and side-walls. Equation 4.1 applies to the heat flux through the footwall and the significantly different Equation 2 holds for the hanging and side walls. When conditions are uniform around the perimeter, Equations 4.1 and 4.2 become identical, resulting in

$$a = 0,547 \text{ b.}$$

This is very close to assuming an equal area relationship (See Section 2.2) which results in

$$a = 0,564 \text{ b.}$$

When considering the effects on heat flow due to a change in radius, it is important also to consider the change in the surface heat transfer coefficient.

The following relationship has been derived for airflow inside pipes (Dittus and Boelter, 1947):

$$hD/k = 0{,}02\ R_e^{0{,}8} \tag{4.3}$$

or

$$h = 0{,}02\ k(\rho v/\mu)^{0{,}8}/D^{0{,}2}$$

where D is the hydraulic diameter given by the ratio of the cross-sectional area to the perimeter. Values of equal area radius and hydraulic diameter for varying tunnel sizes are provided in Table 4.3.

Table 4.3 Equivalent area radius and hydraulic diameter for different tunnel sizes

TUNNEL SIZE	r	D
2 x 2	1,13	0,5
3 x 3	1 69	0,75
4 x 4	2,26	1,0
5 x 5	2,82	1,25

Substituting values for thermal conductivity **k**, density ρ, and viscosity μ of air at 20 °C and atmospheric pressure results in:

$$h = 3{,}63\ v^{0{,}8}/D^{0{,}2}$$

The size of intake airways are generally governed by a limiting ventilation air velocity and it is prudent to consider that, for a change in radius, it is the air quantity that varies and not its air velocity. Considering, therefore, a typical design air velocity of 4 m/s the surface heat transfer coefficient is given by:

$$h = 11{,}0/D^{0{,}2} \tag{4.4}$$

Introducing a surface heat transfer coefficient into the calculation of heat flux requires reference to the tables by Jaeger and Chamalaun (1966), rather than those by Goch and Patterson (1940) which assume n infinite heat transfer coefficient. In this case the heat flow rate per unit length of tunnel is given by:

$$Q/L = 2\pi hr\, \Delta T\, T' \ W/m \qquad (4.5)$$

where T' is a function of both the Biot and Fourier numbers. By substituting Equation 4.4 in Equation 4.5 it can be seen that:

$$Q/L \propto rT'/D^{0,2}$$

In Figure 4.6 the variation of $rT'/D^{0,2}$ with time for different tunnel sizes is shown (the *rock thermal conductivity* was assumed to be 6,14 W/m°C). It is evident that tunnel size has a significant effect on heat flow and a range of sizes (Table 4.3) were examined.

4.2.4 Surface heat transfer coefficient

In the previous section the *expression for surface* heat transfer coefficient given by Equation 4.3 was simplified to give Equation 4.4. This was necessary for the evaluation of the effects of varying tunnel sizes. In practice the air velocity, density and hydraulic diameter vary considerably, and it is impractical to impose limitations on the range of surface heat transfer coefficients. The surface heat transfer coefficient was evaluated for the range of conditions prevailing in practice, by means of Equation 4.3.

4.2.5 Ventilation air flow rate

The design parameters for the ventilation air quantity are the tunnel size and the air velocity. A typical range of air velocities from 2 to 6 m/s was considered, 3 m/s being the standard value.

4.2.6 Dampness of the rock surface

The only surface considered to be damp was that of the uninsulated rock as it is assumed that the insulation prevents moisture transfer between the surface and the ventilation air. tness fractions' of 0,2, 0,5 and 1,0 were considered as being typi... .or damp tunnels, where the *wetness fraction is defined as varying from zero for a perfectly dry* footwall, to unity for a totally wet footwall. A wetness fraction of 0,2 describes a fairly dry tunnel, whereas a wetness fraction of 0,5 is indicative of a damp tunnel.

4.2.7 Condition of ventilation air

For dry conditions the rate of heat flow from the rock mass to the ventil tion a r is directly proportional to the difference between the virgin rock temperature and the ventilation bulk air temperature The inlet air temperature was assumed to be constant at 30 °C dry-bulb, and heat flows for other inlet temperature are easily deduced.

Heat transfer from damp surfaces was determined for relative humidities of 50 and 75 per cent at the standard dry-bulb temperature.

The influence of barometric air pressure on heat flow from the rock is negligible and a standard value of 110 kPa was assumed.

4.2.8 Tunnel length

Many of the effects of insulation can be evaluated by considering a single cross-section of tunnel. In dealing with longer tunnels, lengths of up to 2 000 m were considered.

In calculating heat fl... into a finite tunnel it is necessary to dis-cretise the t .al length into shorter segments. Heat flow into the first segment was used to compute the air environmental conditions in the secondsegment. This process was repeated until the final segment was reached. The shorter the segment length the greater is the accuracy of the results, but with the penalty of greater computational effort. In Table 4.4 the effect of using various step lengths on calculating the heat pickup from 100 m and 2 000 m lengths of tunnel are shown. Typical mining parameters were used in the calculation, with the assumption of dry heat transfer and a tunnel age of one year.

A step length of 100 m gives adequate results, differing by less than 2,5 per cent from these obtained for a step length of 1 m. This value was used for all further work.

Table 4.4a Change in calculated heat pickup due to varying step length for a tunnel length of 100 m

STEP LENGTH m	HEAT LOAD kW	DIFFERENCE PER CENT
1	25,8	-
10	25,9	0,39
100	26,4	2,33

Table 4.4b Change in calculated heat pickup due to varying step length for a tunnel length of 2 000 m

STEP LENGTH m	HEAT LOAD kW	DIFFERENCE PER CENT
1	354,6	-
10	355,0	0,11
100	359,6	1,41
1 000	415,9	17,29
2 000	527,4	48,73

4.2.9 Heat transfer due to radiation

In a ventilation airway heat transfer due to radiation takes place between the rock surfaces and the ventilation air, and also between the rock surfaces which are at different temperatures. The latter occurs with partial wetness or partial insulation. The overall process is shown schematically in Figure 4.7. A satisfactory analysis of the radiation heat transfer process in mine airways does not appear in the literature and is presented in detail in Appendix C. The radiation equivalent network method (Holman, 1981) was followed in the analysis.

In Appendix C it is shown that although the net heat transfer between the two surfaces in a partially insulated tunnel is relatively large, the resulting heat transfer to the ventilation air due to radiation is quite small. Nonetheless, in general the heat transfer due to radiation has been accounted for.

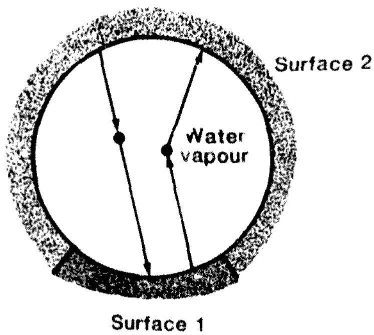

Figure 4.7 Paths of radiation heat exhange in a ventilated tunnel.

4.2.10 Virgin rock temperature

For dry conditions the rate of heat flow is directly proportional to the temperature difference between the ventilation air and the virgin rock temperature.

In Figure 4.8 the heat flow into a typical mine tunnel cross-section for varying temperature driving forces is shown. For the same set of conditions the heat flow into fully insulated and partially insulated tunnel cross-sections are provided in Figures 4.9 and 4.10. The results are expressed as percentage reductions in heat flow (Figure 4.11) and are independent of virgin rock temperature. Unless otherwise stated the virgin rock temperature was assumed to be 50 °C.

4.2.11 Age of rock surface prior to application of insulation

In practice it is likely that some time will elapse from breaking new ground to the application of the insulation. It is also necessary to

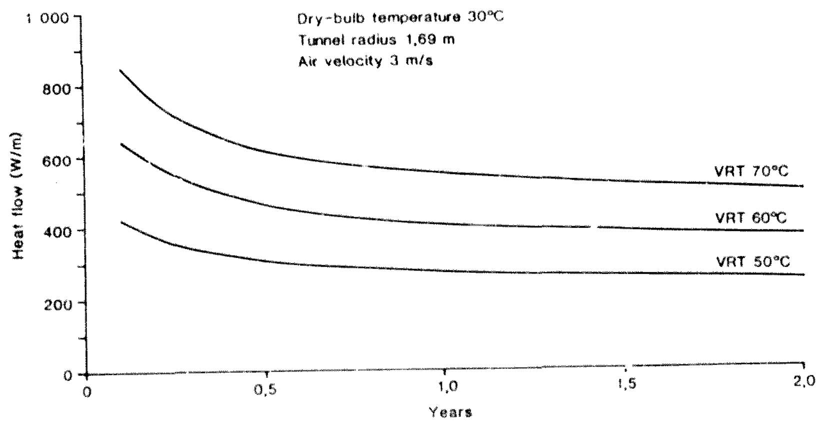

Figure 4.8 Variation in tunnel heat flow with time for different virgin rock temperatures

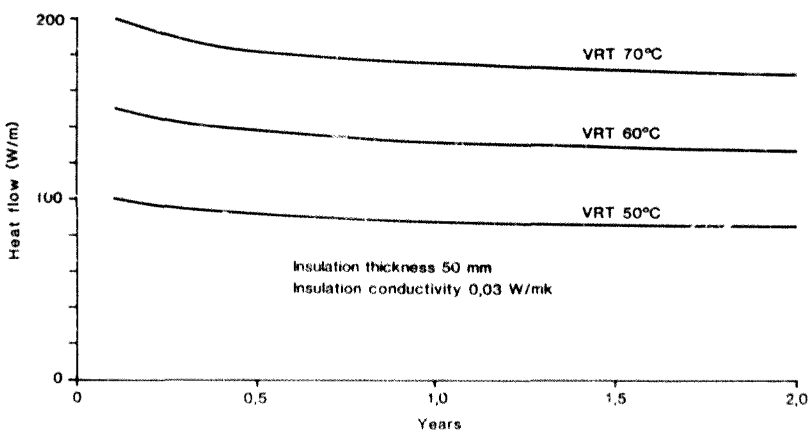

Figure 4.9 Variation in tunnel heat flow with time for different virgin rock temperatures (Fully insulated tunnel)

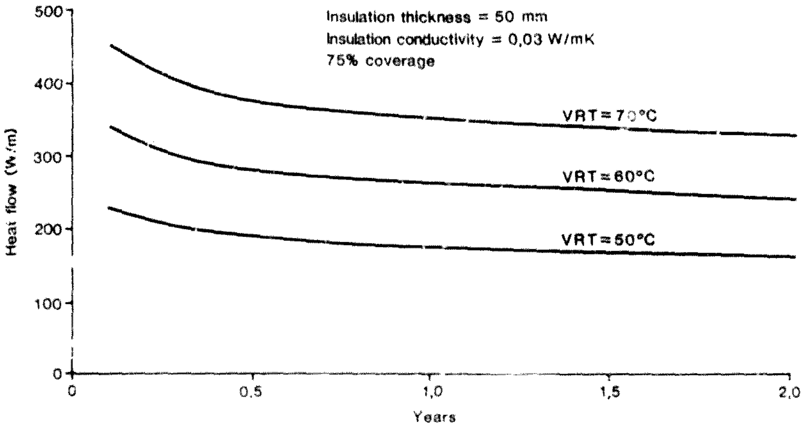

Figure 4.10 Variation in tunnel heat flow with time for different virgin rock temperatures (Partially insulated tunnel)

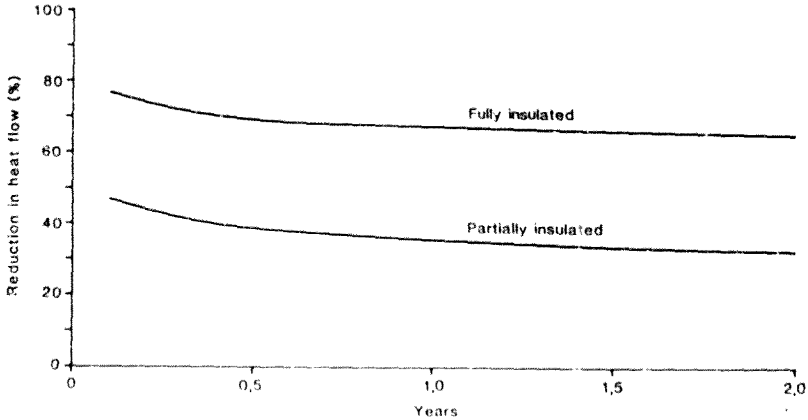

Figure 4.11 Reduction in heat flow for a partially and fully insulated tunnel

consider the importance of insulating established airways. In both these cases the rock has cooled to a certain extent prior to the insulation being applied, and the rock mass has a temperature history. This type of problem poses many difficulties and can be solved only by numerical methods. The effect will be examined closely in Chapter 6 for the conditions prevailing at the experimental test site.

4.2.12 'Standard' or average values

It may be assumed that the standards or average values have been used where all of the parameters used in an analysis have not been presented. The standard or average values are summarised in Table 4.5 along with the ranges which were examined.

Table 4.5 Parameter standards or ranges for theoretical analyses

PARAMETER	STANDARD	RANGE	UNITS
Age	-	0-10	years
Rock Density	2694	-	kg/m^3
Rock Specific Heat	777	-	J/kgK
Rock Thermal Conductivity	6,14	3,0-8,0	W/mK
Tunnel Radius	1,69	1,13-2,82	m
Air Velocity	3,0	3,0-6,0	m/s
Tunnel Length	1,0	1-2000	m
Insulation Thermal Resistance	1,67	0-5,0	m^2K/W
Virgin Rock Temperature	50,0	-	°C
Temperature Driving Force	20,0	-	°C

4.3 Insulation at a single cross-section

4.3.1 Introduction

The evaluation of the heat reduction due to insulation at a single cross-section does not permit the assessment of the exact magnitude of heat flow over practical lengths of tunnel. It does, however, allow the effect of insulation thickness, insulation percentage covering and presence of the footwall ballast to be investigated.

4.3.2 Insulation thickness and thermal conductivity

The most simple method of determining the effects of insulation thickness and insulation conductivity is to combine the two parameters to form the thermal resistance, given by the ratio of thickness to conductivity. A good quality insulation has a thermal conductivity as low as 0,03 W/mK, and thicknesses from zero to 150 mm gives a range of thermal resistance from zero to 5 m^2K/W.

An 'equivalent' surface heat transfer coefficient h_e, which includes the thermal resistance of the insulation and the surface convective heat transfer coefficient h, is given by:

$$h_e = 1/[\frac{\text{Insulation thickness}}{\text{insulation conductivity}} + 1/h]$$

The reduction in heat flow into a tunnel cross-section with varying insulation thermal resistance, compared to the uninsulated case derived from Figure 4.8, is shown in Figure 4.12. There is a clear diminishing return on increasing the thermal resistance, and obviously the optimum thickness of applied insulation is directed by financial considerations. This aspect is examined further in Chapter 8.

4.3.3 Percentage covering of insulation

In practice it is difficult to insulate the footwall effectively. Although the ballast on the footwall should have some insulating effect (see Section 4.3.4), this has been ignored for the moment and the effect of partially insulating the rock surfaces has been examined. The estimation of heat flow into a cylindrical tunnel with non-uniform boundary conditions was calculated using the quasi-steady method.

Figure 4.13 shows the effect of varying the percentage covering of insulation. The thermal resistance of the insulation used in these calculations was 1,67 m^2 K/W. Insulating 75 per cent of the perimeter is equivalent to an uninsulated footwall. The case of 95 per cent covering may be considered as damaged insulation. It is clearly evident that it is important to have as complete a covering of insulation as possible. The effect of not insulating the footwall is

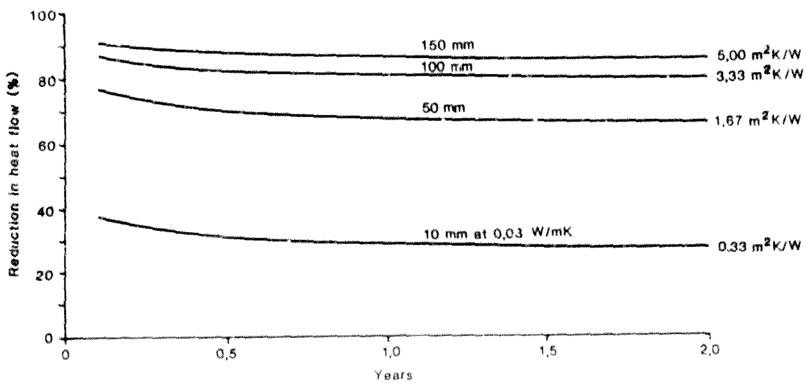

Figure 4.12 Reduction in heat flow for a fully insulated tunnel with different insulation thermal resistances

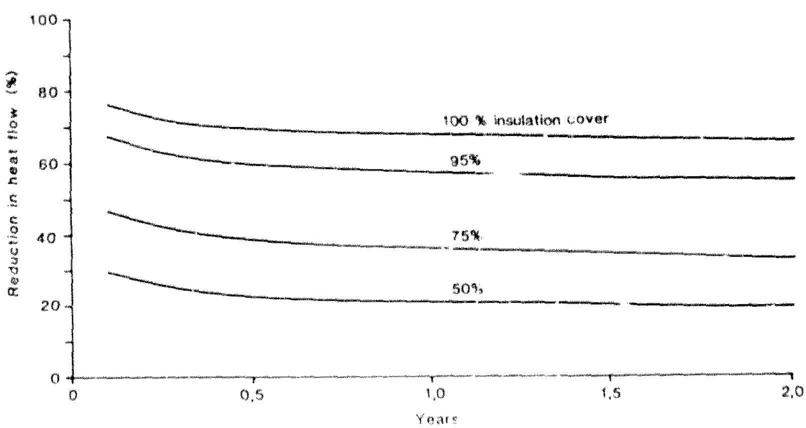

Figure 4.13 Reduction in heat flow for a tunnel with different insulation coverage

severe, reducing the benefits of insulation from approximately 70 per cent to below 40 per cent. It is also important to maintain the covering of insulation, and repair wear and tear.

4.3.4 Thermal conductivity of footwall ballast

In Section 4.3.3 the importance of insulating the footwall was highlighted. However in practice the ballast in the footwall may provide a thermal barrier. The effective conductivity of the footwall ballast ranges from one sixth, to one half of that of the solid quartzite rock (Wiles and Maxwell, 1959).

In Figures 4.14 and 4.15 the effect of the thermal resistance of the footwall ballast on heat flow is shown. It was assumed that the ballast was 300 mm thick. It can be seen that for an uninsulated tunnel the ballast has little effect on heat flow, but when the tunnel is partially insulated the effect becomes more significant. The reduction in heat flow for a partially insulated tunnel is approximately 35 per cent when the effect of the ballast is ignored. The reduction in heat flow rises to approximately 50 per cent if the ballast is assumed to be one sixth the thermal conductivity of the solid rock.

The effect of the footwall ballast is examined further at the experimental test site and the results are described in Chapter 5.

4.4 Effect of tunnel length

4.4.1 Introduction

The examination of a single cross-section of a tunnel overestimates the overall heat reduction which can be gained by insulating a finite length of tunnel. It is necessary when evaluating the heat flow over a length of tunnel to use a stepping procedure by calculating the air temperatures leaving a segment of tunnel which becomes input temperatures into the next segment. This procedure is easily implemented on a micro-computer.

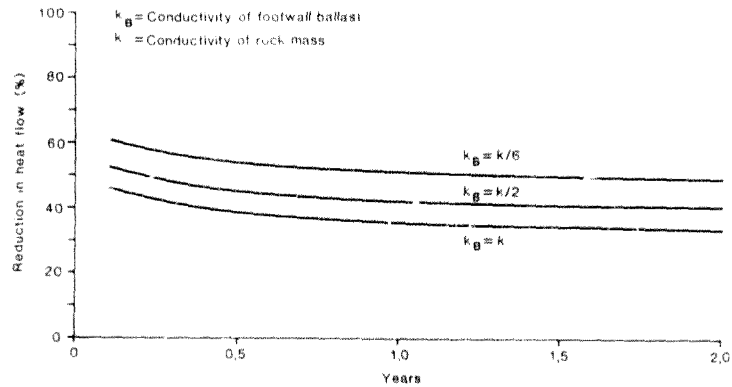

Figure 4.14 Heat flow into uninsulated and partially insulated tunnels with different footwall ballast thermal conductivities

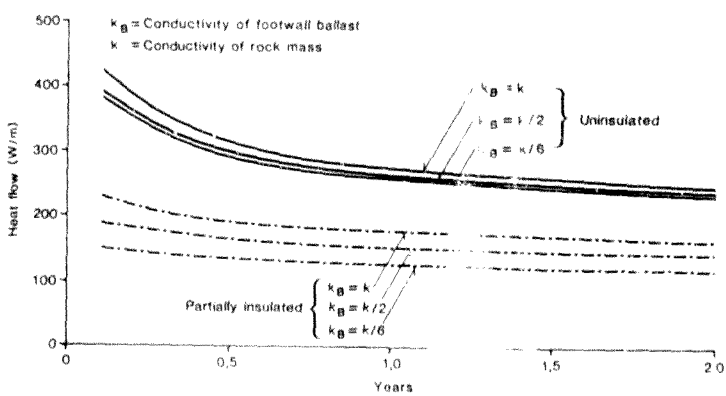

Figure 4.15 Reduction in heat flow for a partially insulated tunnel with different footwall ballast thermal conductivities

Results of using such a procedure for fully insulated, partially insulated, and partially insulated with a damp footwall have been presented in the form of nomograms. By adopting this method of presentation it was possible to incorporate the variation in air velocity, tunnel length and tunnel age in a single diagram. The effect of the insulation is expressed as a percentage reduction in heat flow when compared to an uninsulated tunnel.

4.4.2 Finite length of tunnel with the entire perimeter uniformly insulated from the time of excavation

The results of fully insulating a tunnel are shown in the nomogram in Figure 4.16. The assumed thermal resistance of the insulation is equivalent to 50 mm thick insulation with a thermal conductivity of 0,03 W/mk. The conditions described in Section 4.2.12 were assumed to apply. The nomogram may be used to estimate the heat reduction for varying lengths of tunnel and varying ages.

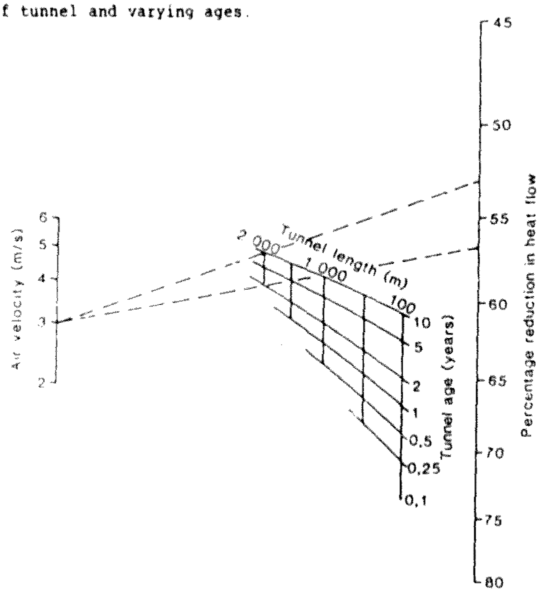

Figure 4.16 Reduction in heat flow for tunnels with a complete covering of 50 mm thick insulation.

As an example, consider an air velocity of 3 m/s for a tunnel length of 2 000 m; the heat flow reduction would vary from 57 to 53 per cent as the age varies from two to ten years. Note that this heat flow reduction is not as high as indicated by investigating a single cross-section; see Figure 4.12 where the corresponding value for the age of two years is 65 per cent.

Similar nomograms are presented in Appendix D for varying insulation thermal resistance, rock conductivity and tunnel equivalent radius.

4.4.3 Finite length of tunnel insulated from time of exposure, with the footwall uninsulated

As in Section 4.4.2 the percentage reduction in heat flow for varying tunnel lengths, and differing air flows are set out as a nomogram (Figure 4.17).

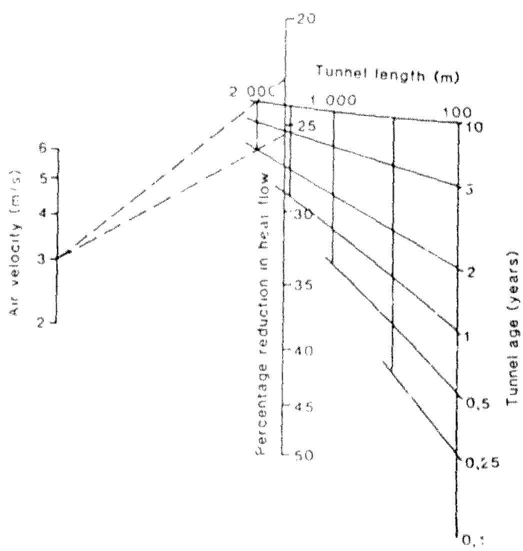

Figure 4.17 Reduction in heat flow for tunnels with a partial covering of 50 mm thick insulation.

For the same example as before, that is an air velocity of 3 m/s and a tunnel length of 2 000 m, the heat flow reduction varies from 26 to 23 per cent as the tunnel ages from two to ten years. These values are approximately half those computed for a totally insulated airway, and significantly different from those values evaluated at a single cross-section.

Further results are presented in Appendix E for varying insulation thermal resistance, rock conductivity and tunnel equivalent radius.

4.4.4 Finite length of tunnel insulated from time of exposure, with the footwall uninsulated and damp

The results for a partially insulated tunnel with a damp footwall are shown in Figure 4.18. The same procedure was followed, while addition-

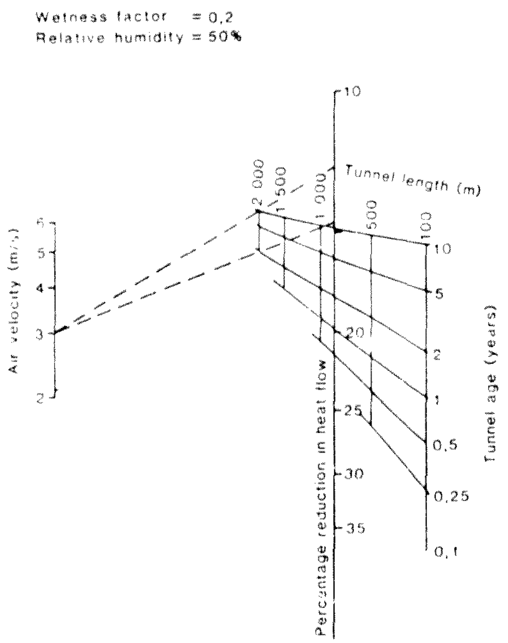

Figure 4.18 Reduction in heat flow for damp tunnels with a partial covering of 50 mm thick insulation.

ully allowing for heat transfer from a wet surface. The wetness factor was assumed to be 0,2 (equivalent to a damp footwall, that is 20 per cent wet) and the ventilation air at the inlet to the tunnel was assumed to have a relative humidity of 50 per cent.

Again for the same example as before, with 2 000 m of tunnel with an air velocity at inlet of 3 m/s, the reduction in heat flow lies between 12 and 15 per cent. Further nomograms are presented in Appendix F for wetness factors of 0,5 and 1,0 and for inlet air relative humidities of 75 per cent. It is clear, however, that should the footwall be at all wet, then the application of insulation to the hanging and sidewalls is of little benefit.

4.5 Summary

From an analysis of a single cross-section of tunnel it was shown that there is a clear diminishing return on increasing the thickness of applied insulation. An optimum thickness can be found from a financial analysis.

For a fully insulated finite length of tunnel it is evident that substantial savings in heat flow can be realized. A reduction in the region of 50 per cent can typically be expected.

For a partially insulated tunnel the savings are not as marked, dropping to approximately 25 per cent. This value is improved by the insulating effect of the footwall ballast.

If a tunnel is only partially insulated and allowed to be damp, the benefits derived are quite small, with a reduction in heat flow of the order of 15 per cent.

The reductions in heat flow due to full and partial insulation can be estimated by reference to a set of nomograms presented in Appendix D. The nomograms cover the range of conditions found in South African gold mines and thus eliminate the need to use computer programs.

5 EXPERIMENTAL INVESTIGATION

5.1 Introduction

Analysis of the magnitude of heat flow into insulated tunnels is extremely complex owing to the large number of variables involved. Any theoretical attempt at quantifying the flow of heat, such as that presented in Chapter 4, must incorporate many approximations. An experiment was conducted at Western Deep Levels gold mine where insulation was applied to the rock surfaces of a tunnel to check the accuracy of the theoretical results.

The specific objectives of the experiment were to:

(i) confirm theoretical predictions of reduction in heat flow due to insulation,

(ii) assess the effect of leaving the footwall uninsulated, and

(iii) gain an understanding of the practicalities involved in applying insulation to mine airways.

Conditions at the site were monitored for 24 weeks and the heat flow was assessed using a knowledge of the rock body temperatures and thermal properties.

5.2 Description of test

A length of airway at 91 level, 2 Shaft, Western Deep Levels Gold Mine was utilized as the experimental test site. The plan view of the test site is shown in Figure 5.1. The nominal details of the site were:

air dry-bulb temperature	= 30 °C
air wet-bulb temperature	= 25 °C
virgin rock temperature	= 44 °C
depth below surface	= 2 600 m
square cross-section	= 3,5 x 3,5 m^2

air velocity = 0,5 m/s
rock thermal diffusivity = $2,4 \times 10^{-6}$ m²/s
rock thermal conductivity = 5,5 W/mK
date of excavation = August 1983
dry rock surface
no fissure water or drain water
quiet site with no through traffic
no meshing or lacing on rock walls.

The total length of the test tunnel was approximately 130 m, of which 90 m were used in the experiment. The site was gated and locked at both ends to prevent interference and through traffic. The test site was divided into three 30 m sections, as detailed below:

Section A - uninsulated control section.
Section B - sidewalls, hangingwall and footwall were insulated with approximately 50 mm thick foam.
Section C - sidewalls and hangingwall were insulated with approximately 50 mm thick foam. The footwall was left uninsulated.

This is shown schematically in Figure 5.2. Before insulating, a comprehensive set of resistance temperature measuring devices was installed in the rock mass at the centre of each section for monitoring heat flow from the rock. Readings from these devices were then used to evaluate the magnitude of heat flow for each section. By comparing the results from each section the effect of insulation was assessed. Only single cross-sections of tunnel were assessed during the experiment to compute the magnitude of heat flow reduction due to insulation because

(i) the capital cost for insulation materials was kept low,

(ii) the experiment was simple, leading to more accurate results than if a long length of tunnel was analysed,

(iii) it was only necessary to locate a short length of underground tunnel which was suitable for the experiment,

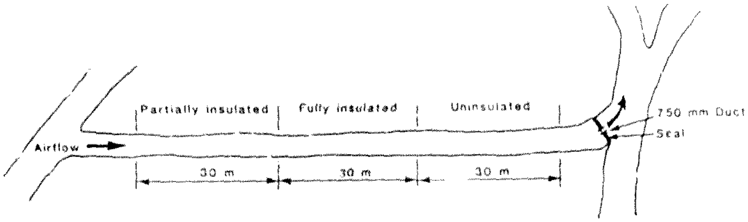

Figure 5.1 Plan view of test site

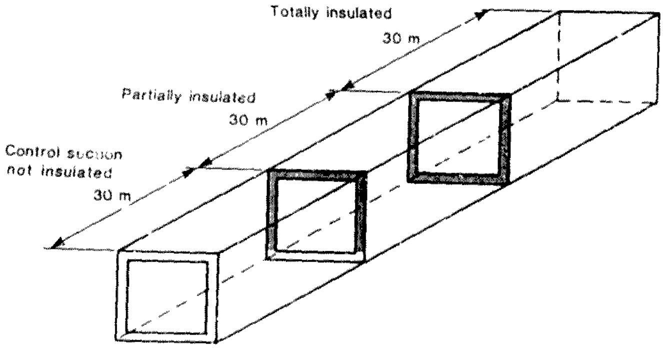

Figure 5.2 Schematic of insulation test site

(iv) the effect of a finite length of tunnel is easily assessed theoretically by psychrometric analysis of the changing air condition.

5.3 Details of Insulation

A nominal 50 mm insulation thickness was selected for the experiment. The choice was based on the theoretical analysis of the effect of varying insulation thickness (Figure 4.12). It can be seen that an insulation thickness of 50 mm results in a reduction in heat flow of the order of 70 per cent, whereas there is a diminishing return on increasing the thickness much beyond 50 mm. Blocks of 50 mm thick polystyrene foam were first bonded to the rock to serve as a guide to the required thickness of insulation foam when being applied. No other preparations were made to the rock surface (Figure 5.3). A photograph of the completed section is shown in Figure 5.4.

Samples of the insulation were submitted to the South African Bureau of Standards for independent thermal conductivity tests. It was found that the thermal conductivity was somewhat higher than expected, namely 0,041 W/mK (density 35,7 kg/m^3).

The average thickness of the insulation at the test site was computed from a total of 834 measurements. The measurements for each individual section, and those for the whole site are summarised in the frequency plots (Figure 5.5). The difficulty in applying the insulation to the specified thickness is reflected both by the large scatter in the results, and in the average thickness, 76,9 ± 31,0 mm (the standard deviation), which is much greater than the specified 50 mm. However, the average thicknesses of 74,9 ± 27,1 mm and 79,6 ± 35,4 mm for the fully and partially insulated sections were similar, and permitted simple comparisons to be made.

5.4 Virgin rock temperature

Knowledge of the virgin rock temperature is necessary only for purposes of comparison with the theoretical heat flow predictions. Recorded rock temperatures suffice for assessing the heat flow into the test sections.

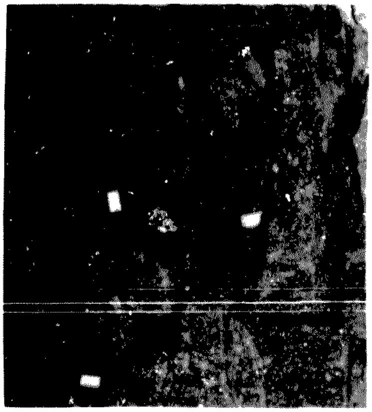

Figure 5.3 Rock surface showing 50 mm high polystyrene blocks

Figure 5.4 Section completely insulated

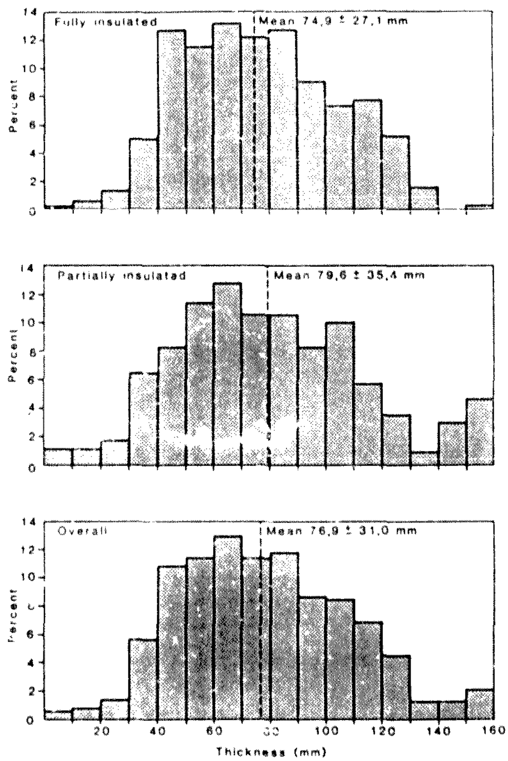

Figure 5.5 Frequency distribution of insulation thickness

The test site was 2 [illegible] m below sea level and correspondingly the virgin rock temperature was found from Figure 5.6 (Jones, 1985) to be 42,7 °C.

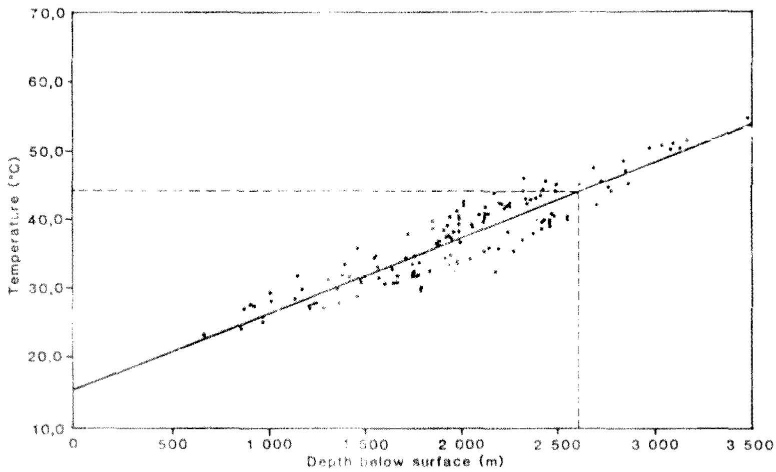

Figure 5.6 **Virgin rock temperature versus depth for the Western Deep Levels Gold Mine.**

5.5 Thermal Properties of Rock from the Test Site

The thermal conductivity of the rock needs to be known before heat flow can be calculated. For this purpose rock samples were collected at the experimental site and analysed. A total of 35 samples from horizontal and vertical directions were taken from the airway. The values of conductivity varied from 4,56 W/mK to 6,68 W/mK with an average of 5,48 W/mK. The rock density varied from 2 670 kg/m³ to 3 000 kg/m³ with an average of 2 790 kg/m³, and the average specific heat was 812 J/kgK with maximum and minimum values of 899 J/kgK and of 765 J/kgK respectively.

Table 5.1 Rock Thermal Properties

SECTION	OBS	DENSITY kg/m³	SPECIFIC HEAT J/kgK	CONDUCTIVITY W/mK	DIFFUSIVITY m²/s x 10⁻⁶
UNINSULATED	1	2980	840	4,72	1,89
	2	3000	890	4,76	1,78
	3	2960	832	5,60	2,27
	4	2720	808	5,45	2,48
	5	2700	787	6,06	2,85
	6	2770	797	4,75	2,19
	7	2700	805	6,05	2,78
	8	2700	806	5,86	2,69
	9	2710	810	5,95	2,71
	10	2680	801	5,75	2,68
	11	2750	807	6,40	2,88
	12	2750	783	6,32	2,94
MEAN	12	2781 ± 122	813 ± 29	5,64 ± 0,60	2,51 ± 0,39
FULLY INSULATED	1	2700	797	6,07	2,82
	2	2720	807	5,81	2,65
	3	3000	834	4,55	1,82
	4	2680	765	5,83	2,84
	5	2720	799	4,59	2,11
	6	2720	811	5,05	2,29
	7	2680	786	6,68	3,17
	8	2670	766	6,57	3,21
	9	2700	790	6,47	3,03
	10	2720	792	4,33	2,01
	11	2710	792	5,47	2,55
	12	2730	807	5,59	2,54
MEAN	12	2729 ± 87	796 ± 19	5,58 ± 0,81	2,59 ± 0,46
PARTIALLY INSULATED	1	2920	857	5,63	2,25
	2	2700	802	5,92	2,73
	3	2930	899	4,68	1,78
	4	2920	823	4,28	1,78
	5	2910	808	4,53	1,93
	6	2930	863	5,40	2,14
	7	2690	796	5,98	2,79
	8	2740	795	6,33	2,91
	9	2930	808	4,56	1,93
	10	2930	838	4,64	1,89
	11	2970	832	4,88	1,97
MEAN	11	2870 ± 104	829 ± 33	5,17 ± 0,71	2,19 ± 0,42
OVERALL MEAN	35	2791± 118	812 ± 30	5,47 ± 0,72	2,43 ± 0,45

When calculating the heat flux from each section the average thermal properties for that section were used and <u>not</u> the overall average values given above. The complete set of measured values is shown in Table 5.1.

5.6 Cross-sectional Dimensions

The dimensions of the tunnel cross-sections at each of the measuring stations were measured for each of the four rock faces. The results are shown in Table 5.2. The texture of the rock faces varied from smooth to fragmented. The cross sectional shape was approximately rectangular.

Table 5.2 Cross-Sectional Dimensions of Test Sections (m)

	SIDEWALL	HANGINGWALL	SIDEWALL	FOOTWALL
Uninsulated	3,5	3,5	3,5	3,5
Fully Insulated	3,3	3,5	3,3	3,5
Partially Insulated	3,2	3,3	3,2	3,3

5.7 Air temperature Measurements

The heat flow into each section was evaluated from the measured rock temperatures, a knowledge of the rock thermal conductivity and the mechanics of two dimensional heat flow. The change in energy content of the air passing through the section was not used to determine heat flow from the rock because air temperatures and airflow cannot be measured with sufficient accuracy.

The heat flow into a typical dry mine haulage is 150 W/m, so that over 30 m of airway the total heat flow is 4,5 kW. For an air mass flow rate of 20 kg/s the temperature increase over the section would be 0,2 °C, with temperature change in the insulated sections being much less. Measuring changes in temperature of this magnitude to a suitable degree of accuracy, at an underground site, is almost impossible.

However, the wet- and dry-bulb air temperatures were monitored continuously at the test section exit. A chart recorder which was calibrated weekly against an accurate thermometer measurement was used for this purpose. The dry-bulb temperature was found to be constant at approximately 31 °C, varying by only ± 1 °C during the experiment. The wet-bulb temperature varied from 22 °C to 26 °C, but was not considered important as the airway was completely dry.

5.3 Air Velocity

The air velocity at the outlet of the test section was recorded on a weekly basis using a hand-held anemometer. The results were computed from an average of five readings taken at different points within the duct cross-section. It was found that the air volume varied greatly over the period of the experiment (Figure 5.7). This resulted in significant variations in the magnitude of the measured heat flow.

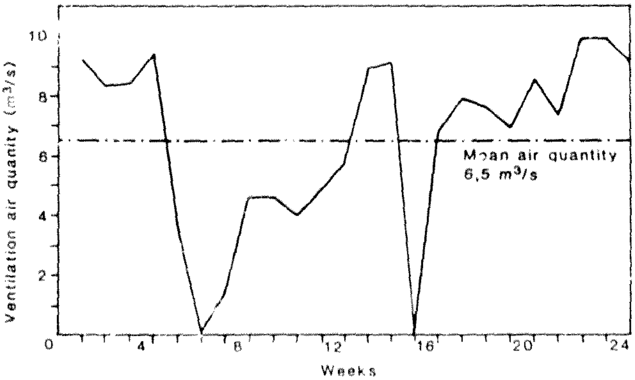

Figure 5.7 Variation in ventilation air flow.

The accuracy of the air velocity measurement was not high, with an expected error of between five and ten per cent. This level of accuracy was however adequate since an energy balance technique was not used to evaluate the heat flows, and the results of air flow measurement were used only to indicate the effect on heat flow, and to evaluate a surface heat transfer coefficient for theoretical comparison purposes.

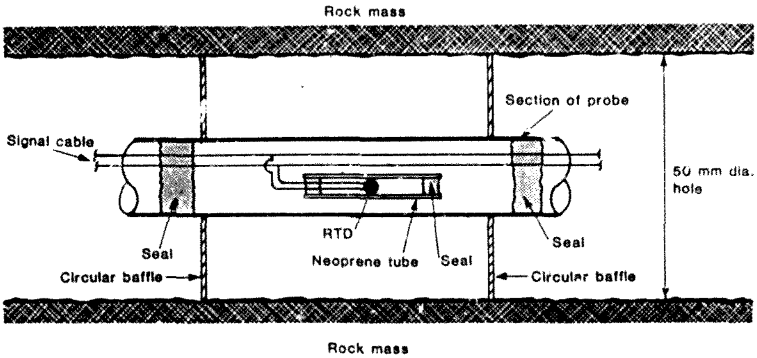

Figure 5.8 Temperature probe schematic

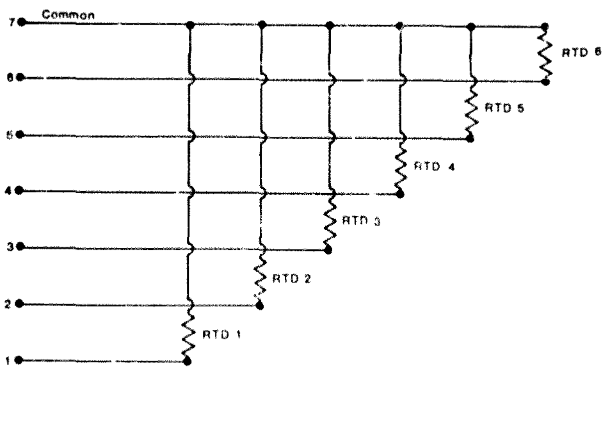

Figure 5.9 Temperature probe wiring diagram

5.9 Rock Temperature Measurements

The sensors used to measure rock temperature were resistance devices (R.T.D's). Great care was taken to protect the sensors from damage by the environment. Each device was sealed in neoprene and then, to make up a probe, inserted into a plastic tube. The probe assembly was completed by positioning flexible plastic baffles at short intervals along the length of the outer plastic sheath. The diameter of the baffles was slightly larger than the holes in the rock, the purpose being to form an interference seal and thus prevent convection currents within the hole. A schematic of the temperature probe is shown in Figure 5.8 and the electrical circuit diagram is shown in Figure 5.9. Prior to inserting the probes into the holes in the rock the holes were cleaned of all drilling water by blasting with compressed air.

Each sensor was calibrated after assembling, so that the resistances of leads and connections were included in the calibration. The expected error in temperatures recorded was less than ± 0,2 °C.

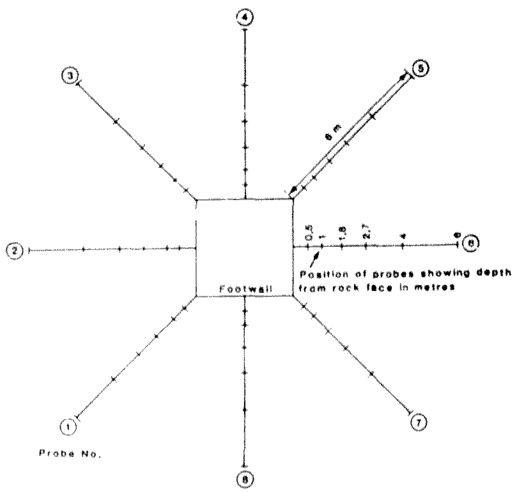

Figure 5.10 Distribution and pattern of temperature measuring points.

The probes were installed at the centre of each section (A,B,C) in holes drilled to a depth of 6 m (Figure 5.10). Also shown are the positions of each sensor. *It should be noted that the sensors were* placed closer together near the surface than deep in the rock, to enable detailed information to be gained for the localities where the temperature gradients were largest. The entrances to the holes were filled with putty to further prevent convection currents. The sensors were tested immediately after installation, and then left for one week before regular weekly measurements commenced.

Some typical rock temperature profiles recorded at the start of the experiment and 24 weeks later are shown in Figures 5.11 to 5.16. Results from every second temperature probe are shown and several points of importance should be noted.

(a) At the uninsulated section the gradients close to the surface were steeper than for those of the insulated section; this indicates a higher heat flux at the uninsulated section than at the insulated sections.

(b) The temperature profiles for the uninsulated section changed little over the 27 week period, particularly deep in the rock where the temperature remained essentially constant at 37 °C.

(c) At the insulated rock faces the temperature profiles were relatively flat with a low thermal gradient at the surface and a correspondingly low heat flux. There was a general increase in temperatures over the 24 week period due to the reduced heat flow across the rock and air interface.

(d) The temperature profile at the uninsulated rock face in the partially insulated section showed characteristics found in the uninsulated section; namely that of a high thermal gradient which is indicative of a high heat flow.

The low scatter of the data points lying on the temperature profiles suggests that random errors were low.

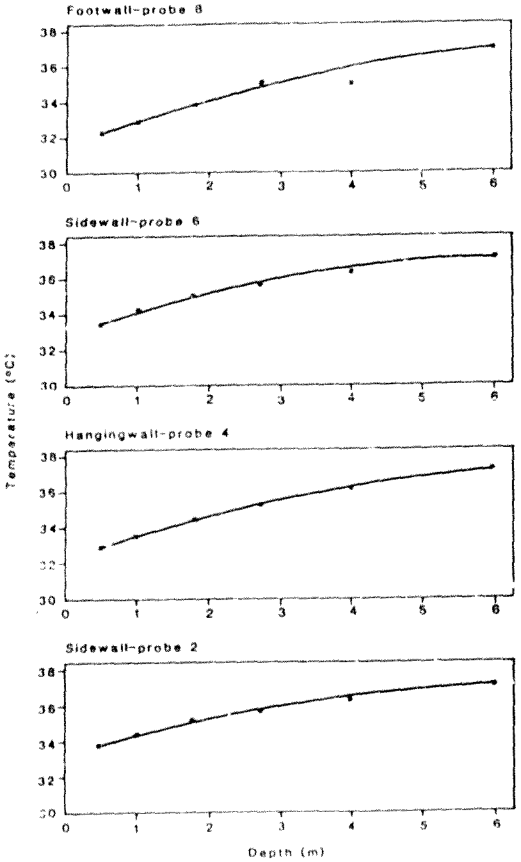

Figure 5.1 Rock temperatures in the uninsulated section during Week 1

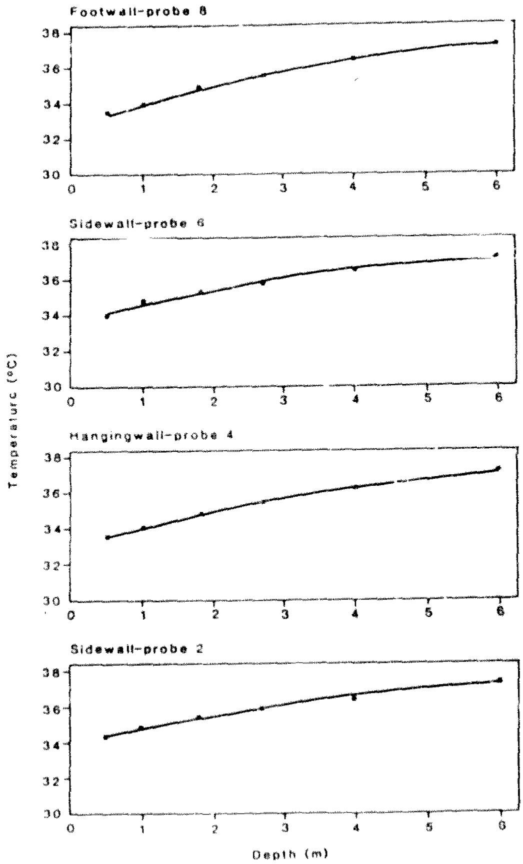

Figure 5.12 Rock temperatures in the uninsulated section during Week 24.

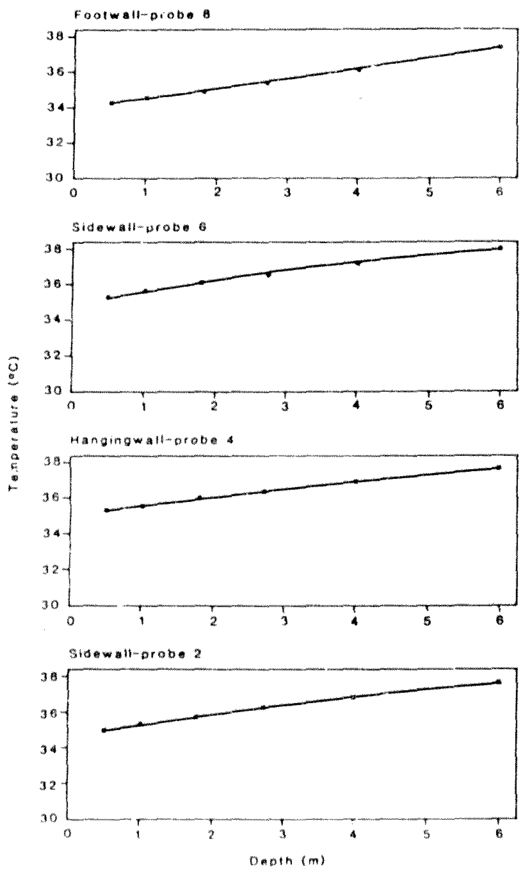

Figure 5.13 Rock temperatures in the fully insulated section during Week 1

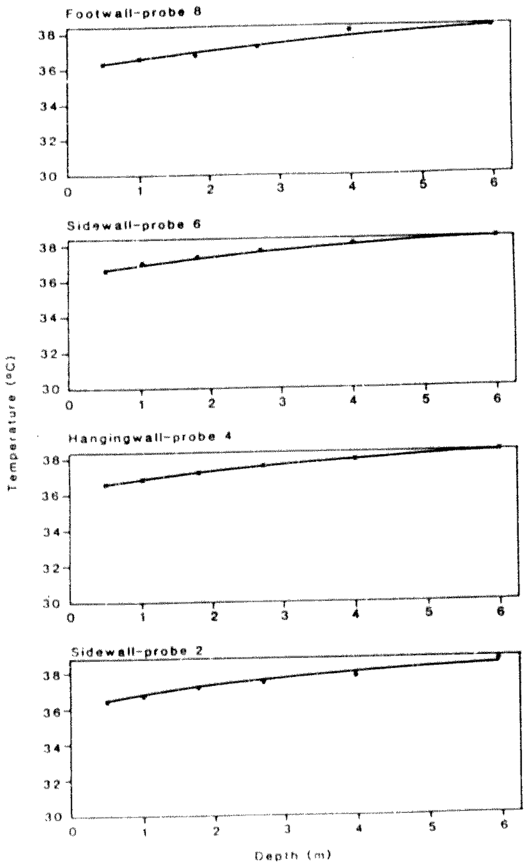

Figure 5.14 Rock temperatures in the fully insulated section during Week 24

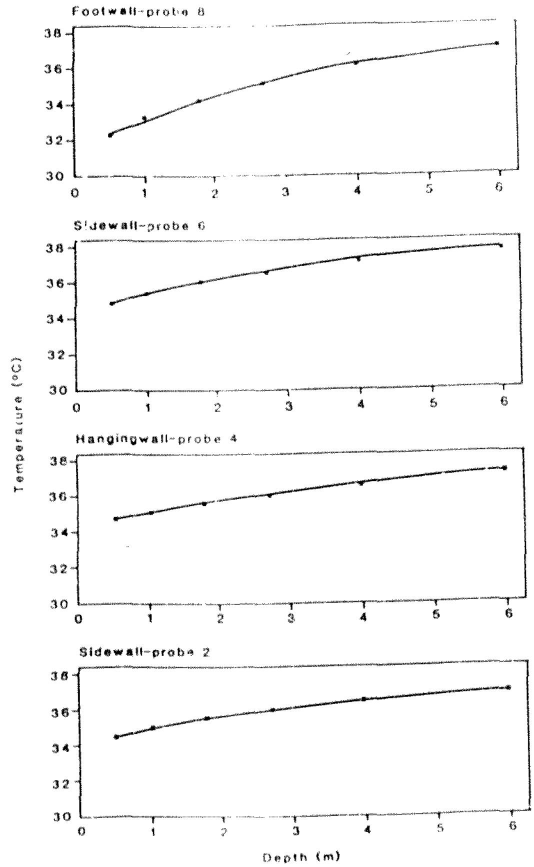

Figure 5.15 Rock temperatures in the partially insulated section during Week 1

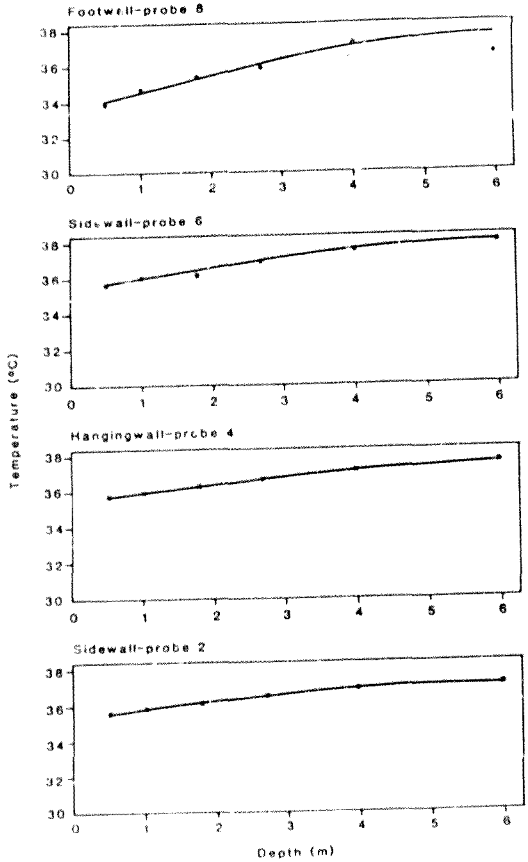

Figure 5.16 Rock temperatures in the partially insulated section during Week 24.

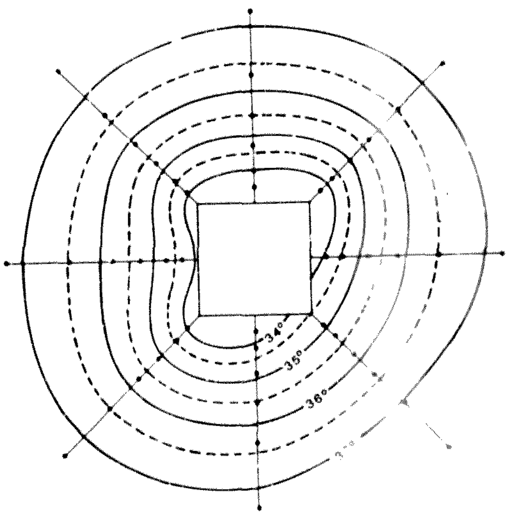

Figure 5.17 Temperature contours at the uninsulated section

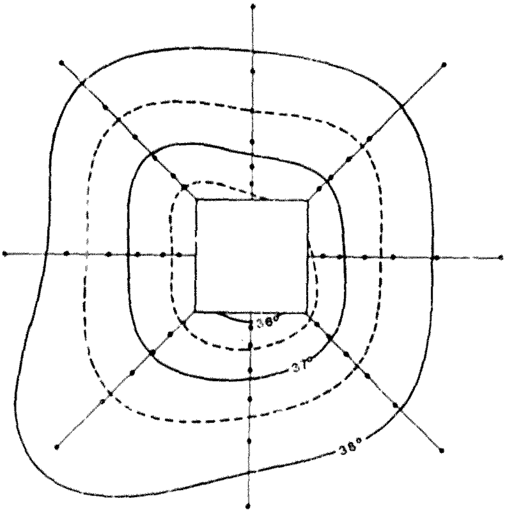

Figure 5.18 Temperature contours at the fully insulated section

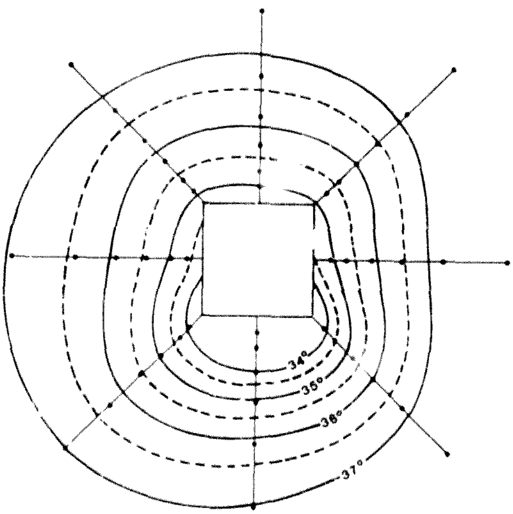

Figure 5.19 Temperature contours at the partially insulated section

Typical temperature contours around the tunnel sections are shown in Figures 5.17, 5.18, and 5.19. Again several points should be noted.

(a) The uninsulated and fully insulated sections having uniform boundary conditions show almost symmetrical and concentrical temperature contours.

(b) The rock temperatures around the fully insulated section are higher than those around the uninsulated and partially insulated sections.

(c) The high rate of heat transfer through the footwall of the partially insulated section is indicated by the divergence of the temperature contours away from the footwall.

5.10 Heat Flux

5.10.1 Method of calculation

The heat flux was found by determining the temperature gradient at the rock surface from a curve fit (both the radial and circumferential dimensions were considered). By using this approach only the rock temperatures and thermal conductivity are necessary to obtain the surface heat flux.

It was not possible to fit one equation to all 48 temperature measurements taken at a section due to the discontinuity of the hole formed by the tunnel in the rock mass. The method used was to fit four curves over segments around the tunnel perimeter. Each segment included temperature recordings from three probes, giving a total of eighteen temperature measurements (Figure 5.20). For example, a curve was fitted within the boundary, outlined by segment 1, from temperature recordings from probes 1,2 and 3. The curve fit for segment 2 was from temperature recordings from probes 3,4 and 5. A quadratic of the form

$$T=a_1+a_2x+a_3x^2+a_4y+a_5y^2+a_6xy+a_7x^2y+a_8xy^2+a_9x^2y^2 \qquad (5.1)$$

was fitted to the temperature data in each segment using a modified least squares method (Hurlburt, 1980).

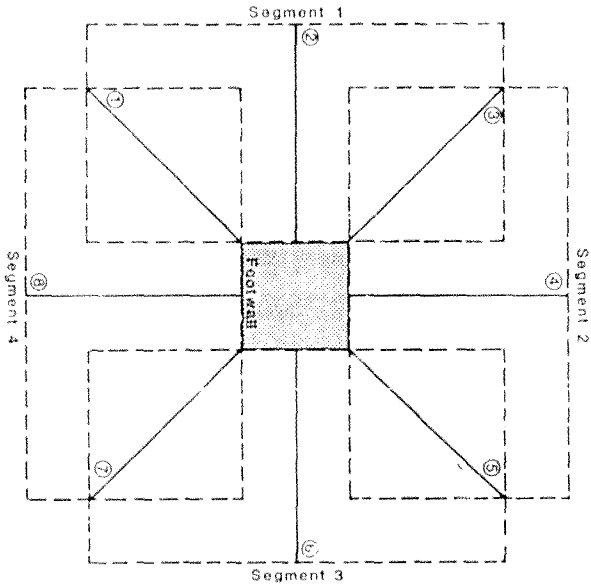

Figure 5.20 Position of four segments over which curve fitting was performed

The dimensional co-ordinates are given by x (parallel to the rock face) and y, (normal to the rock face) and the temperature in the rock body by T. The error at the measuring points using the quadratic fit was less than one per cent in all cases.

The heat flux normal to the surface was then obtained from

$$k \left.\frac{\partial T}{\partial y}\right|_{y=o} = k(a_4 + a_6\, x + a_7\, x^2) \tag{5.2}$$

After determining the variation in heat flux around the perimeter the total heat flow at each section was found by integrating Equation 5.2 for each section, that is

$$\text{Heat flux} = \frac{k}{L} \int_{o}^{\ell} (a_4 + a_6\, x + a_7\, x^2)\, dx \tag{5.3}$$

where L is the length of the side.

5.10.2 Heat flow from each section and percentage heat flow reduction

The total heat flow from the three test sections for the duration of the experiment are given in Table 5.3, and presented graphically in Figure 5.21. Also shown in Table 5.3, and plotted in Figure 5.22, are the percentage reductions in heat flow for the fully insulated and partially insulated cases. The raw data were then smoothed using a cubic spline fit and plots of the heat flow and percentage heat reduction are shown in Figures 5.23 and 5.24.

The average heat flow from the uninsulated section was 80,6 ± 11,1 W/m, whereas for the partially and fully insulated sections the average results were 34,6 ± 4,5 W/m and 56,0 ± 6,1 W/m respectively.

The average reduction in heat flow as compared with the control section, was 56,7 per cent in the totally insulated section and 29,7 per cent in the partially insulated section.

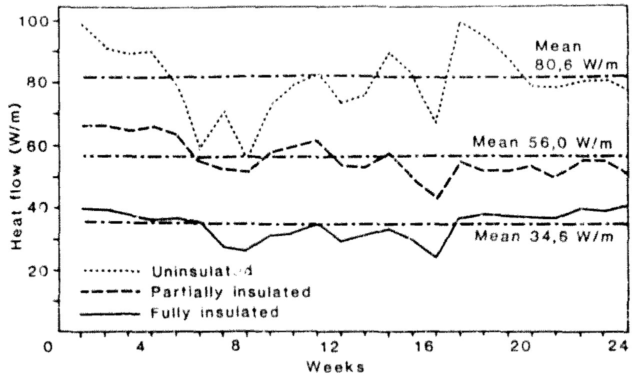

Figure 5.21 Variation in heat flow for insulated, partially insulated, and fully insulated sections

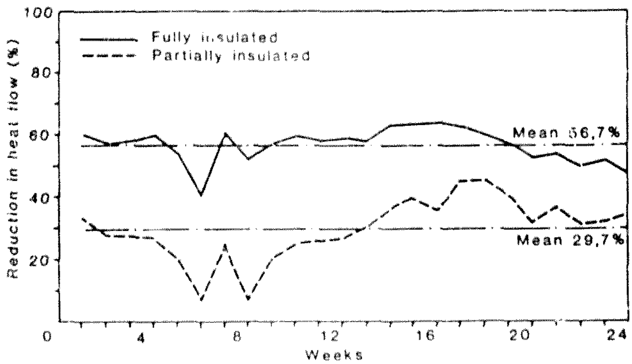

Figure 5.22 Percentage reduction in heat flow due to full and partial insulation

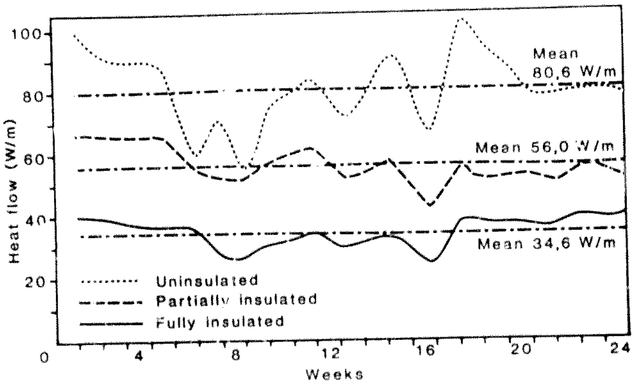

Figure 5.23 Variation in heat flow for insulated, partially insulated, and fully insulated sections (smoothed)

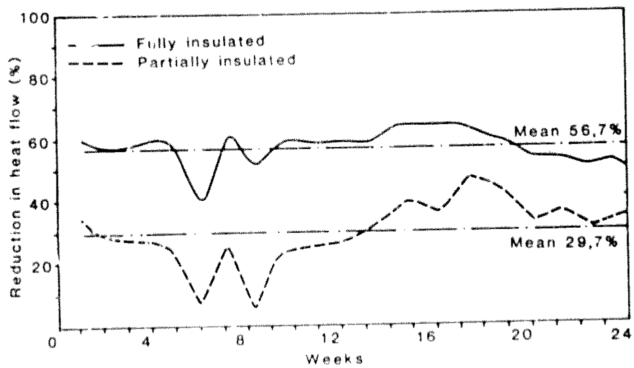

Figure 5.24 Percentage reduction in heat flow due to full and partial insulation (smoothed)

5.10.3 Heat flux variation around section perimeters and the effect of variations in air flow

Typical results for the variations in heat flux around the perimeters of each section are shown in Figure 5.25. In the uninsulated section the heat flux around the rock perimeter varied from 3 to 7 W/m^2. This variation was greater than that in the fully insulated section which only varied from 2 to 3,5 W/m^2. The heat flux in the partially insulated section increased from 2,5 W/m^2 at the insulated hangingwall, to 7,5 W/m^2 at the centre of the uninsulated footwall. The sidewalls in the partially insulated section showed a steadily increasing heat flux from low at the corners adjacent to the insulated hangingwall, to high at the corners next to the uninsulated footwall.

Table 5.3 Heat Flows for the Uninsulated, Fully Insulated and Partially Insulated Sections

WEEK	UNINSULATED	FULLY INSULATED		PART INSULATED	
NO	W/m	W/m	% REDUCTION	W/m	% REDUCTION
1	99,4	40,1	59,7	66,2	33,4
2	91,7	39,6	56,8	66,3	27,7
3	89,5	37,8	57,8	65,1	27,3
4	90,3	36,5	59,6	66,2	26,7
5	79,4	36,6	53,3	63,5	20,0
6	59,9	35,6	40,6	55,0	8,2
7	70,3	27,9	60,3	52,6	25,2
8	55,7	26,6	52,2	51,8	7,0
9	72,1	31,1	56,9	57,5	20,2
10	79,0	32,2	59,2	59,3	24,9
11	82,7	34,5	58,3	61,5	25,6
12	73,3	30,0	59,1	53,7	26,7
13	76,1	31,5	58,6	52,9	30,5
14	89,6	33,1	63,1	57,3	36,0
15	82,6	29,9	63,8	49,9	39,6
16	67,5	24,3	64,0	43,3	35,9
17	99,4	36,7	63,1	54,5	45,2
18	94,6	37,6	60,3	51,8	45,2
19	87,9	37,3	57,6	52,1	40,7
20	78,6	36,8	53,2	53,2	32,3
21	78,1	36,3	53,5	49,7	36,4
22	80,0	39,5	50,6	54,7	31,6
23	80,3	39,7	51,8	54,7	31,9
24	77,2	40,9	47,0	50,8	34,2
MEAN	80,6	34,6	56,[illegible]	56,0	29,7
S.D.	± 11,1	±4,5		±6,1	

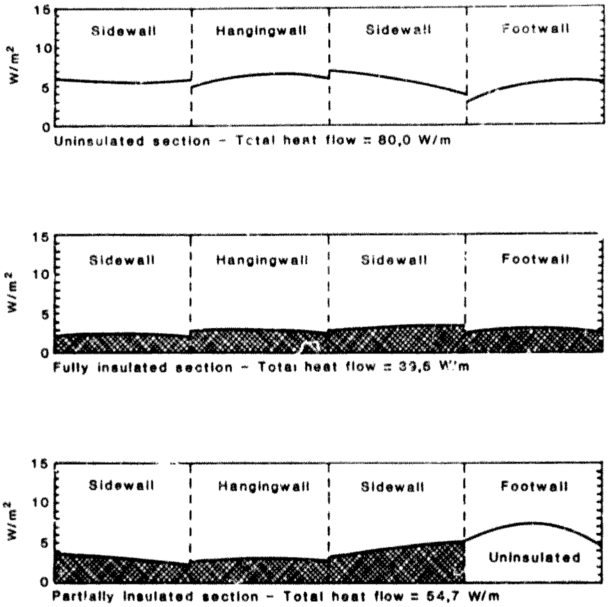

Figure 5.25 Typical heat flux variation around the tunnel perimeters during Week 22

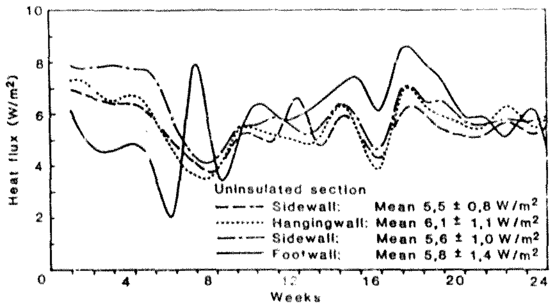

Figure 5.26 Variation in heat flux for uninsulated section (smoothed)

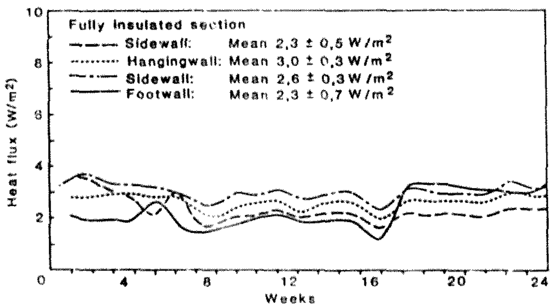

Figure 5.27 Variation in heat flux for fully insulated section (smoothed)

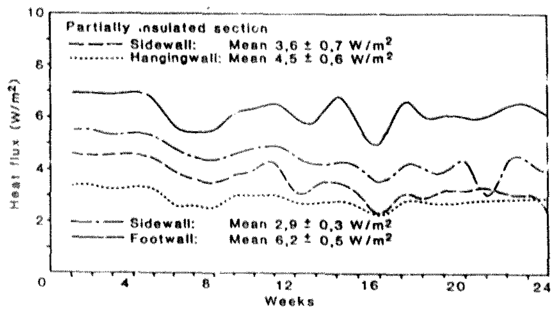

Figure 5.28 Variation in heat flux for partially insulated section (smoothed)

The variations in heat flux with time for the individual sidewalls, hangingwalls and footwalls are shown in Figures 5.26, 5.27 and 5.28. The data were smoothed using the cubic spline fitting technique. The highest average heat flux, 6,2 ± 0,5 W/m^2, of all rock surfaces was recorded from the uninsulated footwall in the partially insulated section.

This was caused by heat transfer along the path of least resistance which is away from the insulated faces and through the uninsulated footwall. This high heat flow indicates the importance of using a suitable material to insulate the footwall.

The large variation in heat flux for the uninsulated section (Figures 5.21 and 5.26) can be explained by the variation in air volume flow rate (Figure 5.7). The sharp reductions in air volume, and hence air velocity, at the 5 to 7 and 15 week periods (Figure 5.7) correspond closely to the drop in heat flux at the 6 to 8 and 16 week periods (Figure 5.21). The variation in air volume resulted in a change in air velocity passing over the rock surface and consequently a variation in the convective surface heat transfer coefficient. The fluctuations in heat flow in the insulated sections were much less because the rate of heat transfer is dominated by the thermal resistance of the insulation, and is less dependent on the surface heat transfer coefficient.

The response in heat flow to changes in air flow was investigated by stopping the air flow completely and recording temperatures daily for

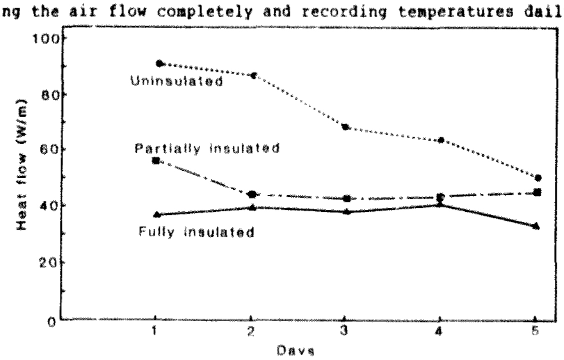

Figure 5.29 Variation in heat flow for 5 days after stopping ventilation air flow.

The variations in heat flux with time for the individual sidewalls, hangingwalls and footwalls are shown in Figures 5.26, 5.27 and 5.28. The data were smoothed using the cubic spline fitting technique. The highest average heat flux, 6,2 ± 0,5 W/m^2, of all rock surfaces was recorded from the uninsulated footwall in the partially insulated section.

This was caused by heat transfer along the path of least resistance which is away from the insulated faces and through the uninsulated footwall. This high heat flow indicates the importance of using a suitable material to insulate the footwall.

The large variation in heat flux for the uninsulated section (Figures 5.21 and 5.26) can be explained by the variation in air volume flow rate (Figure 5.7). The sharp reductions in air volume, and hence air velocity, at the 5 to 7 and 15 week periods (Figure 5.7) correspond closely to the drop in heat flux at the 6 to 8 and 16 week periods (Figure 5.21). The variation in air volume resulted in a change in air velocity passing over the rock surface and consequently a variation in the convective surface heat transfer coefficient. The fluctuations in heat flow in the insulated sections were much less because the rate of heat transfer is dominated by the thermal resistance of the insulation, and is less dependent on the surface heat transfer coefficient.

The response in heat flow to changes in air flow was investigated by stopping the air flow completely and recording temperatures daily for

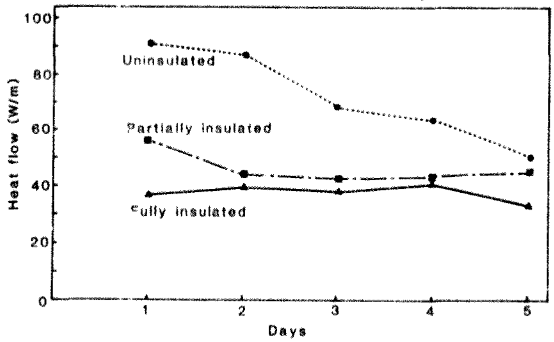

Figure 5.29 Variation in heat flow for 5 days after stopping ventilation air flow.

The variations in heat flux with time for the individual sidewalls, hangingwalls and footwalls are shown in Figures 5.26, 5.27 and 5.28. The data were smoothed using the cubic spline fitting technique. The highest average heat flux, 6,2 ± 0,5 W/m², of all rock surfaces was recorded from the uninsulated footwall in the partially insulated section.

This was caused by heat transfer along the path of least resistance which is away from the insulated faces and through the uninsulated footwall. This high heat flow indicates the importance of using a suitable material to insulate the footwall.

The large variation in heat flux for the uninsulated section (Figures 5.21 and 5.26) can be explained by the variation in air volume flow rate (Figure 5.7). The sharp reductions in air volume, and hence air velocity, at the 5 to 7 and 15 week periods (Figure 5.7) correspond closely to the drop in heat flux at the 6 to 8 and 16 week periods (Figure 5.21). The variation in air volume resulted in a change in air velocity passing over the rock surface and consequently a variation in the convective surface heat transfer coefficient. The fluctuations in heat flow in the insulated sections were much less because the rate of heat transfer is dominated by the thermal resistance of the insulation, and is less dependent on the surface heat transfer coefficient.

The response in heat flow to changes in air flow was investigated by stopping the air flow completely and recording temperatures daily for

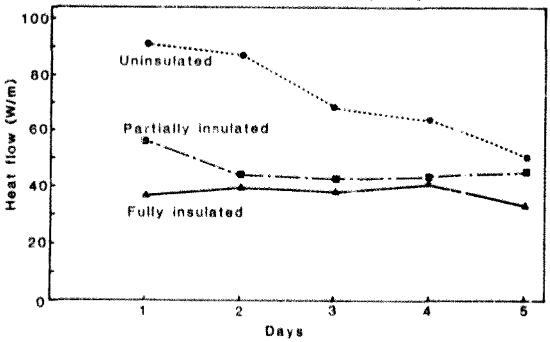

Figure 5.29 Variation in heat flow for 5 days after stopping ventilation air flow.

five days. The resulting heat flows from each section are shown in Figure 5.29. The uninsulated section showed a marked decrease in heat flow, from 91,2 to 50,5 W/m, during the five days of measurement. The insulated sections showed no definite response to stopping the air flow.

5.10.4 The effec[illegible] footwall gravel

The bulk ther[illegible] ty of packed quartz gravel has been measured as one sixth th[illegible] rock (Wiles and Maxwell, 1959). A layer of rock 300 mm thick with [illegible]hermal conductivity of 0,9 W/mK is equivalent to a 10 mm layer of good insulation. However, it is not possible to detect any reduction in heat flow due to the footwall ballast by examining the heat flux from the individual rock faces (Figures 5.26 and 5.28). The average heat fluxes from the footwalls are not lower than the heat fluxes from the other rock faces, and it would appear that the footwall ballast does not have a significant effect on rock heat flow into tunnels.

5.11 Summary

A test site at Western Deep Levels Gold Mine was divided into three sections which were

(i) uninsulated
(ii) fully insulated
(iii) partially insulated.

The specification for the insulation thickness was 50 mm. However, this was not achieved in practice, the thickness varying greatly with an average of 76,9 mm.

Temperatures within the rock body at each section were recorded for 24 weeks. From this data and a knowledge of the rock thermal conductivity the heat flux at each section was calculated. It was found that the average heat flow from the uninsulated section was 80,6 W/m, whereas for the partially and the fully insulated sections the average results were 56,0 W/m and 34,6 W/m respectively.

The average reduction in heat flow as compared with the uninsulated control section, was **56,7 per cent** in the totally insulated section and **29,7 per cent** in the partially insulated section.

In order to assess whether the ballast on the footwall had any insulating affect, the heat flows from the sidewalls, footwalls and hangingwalls were compared. The heat flow from the footwall was not found to be consistently lower than any of the other faces, as was predicted by theory.

In the next chapter a full comparison is made between results obtained at the test site and theoretical modelling.

6 COMPARISON OF EXPERIMENTAL AND THEORETICAL RESULTS

6.1 Introduction

The accurate experimental measurement of rock heat flow in mine excavations is a difficult undertaking. Acceptably accurate results are only possible if a careful experimental procedure is followed. Furthermore, the theoretical analysis of rock heat flow into tunnels is complex and it is usually necessary to accept some approximations. It is therefore appropriate to compare and to assess the results obtained by the two procedures.

In this chapter the results of the experiment are compared with results obtained firstly by finite element analysis which models the test conditions as accurately as possible and, secondly by simplified methods of predicting heat flow into tunnels.

6.2 Finite element analysis of heat flow in the experimental test sections

6.2.1 Introduction

Numerical techniques must be used to model the test site as accurately as possible. By using the finite element method it is possible to simulate all of the following: the rectangular cross-section of the tunnel, the discontinuous boundary conditions of the partially insulated section, and the temperature field which existed before the insulation was applied.

6.2.2 Finite element mesh

The knowledge acquired during the testing of the 'ADINAT' package led to the drawing up of the finite element mesh shown in Figure 6.1. The mesh consisted of 100 elements which increased in size geometrically

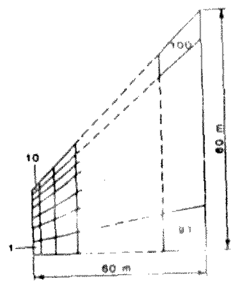

Figure 6.1 100 element mesh used for modelling the uninsulated test section.

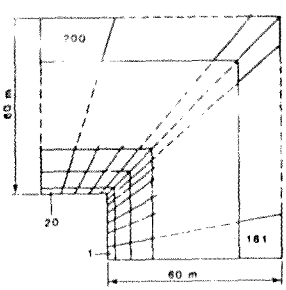

Figure 6.2 200 element mesh used for modelling the fully insulated test section.

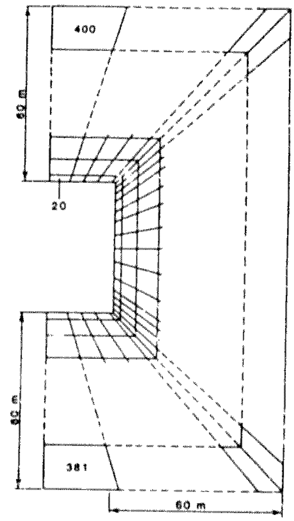

Figure 6.3 400 element mesh used for modelling the partially insulated test section.

with the distance from the tunnel perimeter. The dimensions of the tunnel cross-sections are given in Table 5.2. It was only possible to use the mesh shown in Figure 6.1 for the uninsulated section which was square and had uniform boundary conditions. The 200 element mesh shown in Figure 6.2 was used for the rectangular fully insulated section. For the partially insulated section it was necessary to use the large, 400 element mesh, shown in Figure 6.3.

6.2.3 Test conditions

Despite the use of a numerical method of modelling the conditions at the experimental test site, it was necessary to make some assumptions and approximations. The values of parameters used in the model and any approximations that were made are described below.

The values of rock thermal conductivity measured at the site, (Table 5.1,), were used in the analysis. The value used for each section was the average of 12 measurements of rock samples taken from around the perimeter of the tunnel cross-section.

The virgin rock temperature was assumed (Figure 5.6) as being 42,7 °C.

The ambient air temperature was assumed to be constant at 31 °C. This value was the average of the continuous air temperature measurements that were recorded at the site.

The ventilation air flow was assumed to be constant at 6,5 m^3/s, whereas in fact it varied considerably at the site (Figure 5.7). This assumption had the effect of giving a predicted heat flow that was smoother than that which was experimentally determined. However the overall average results are not affected and can be satisfactorily compared.

The average air volume was used to compute the heat transfer coefficients for the tunnel surfaces, which were evaluated as follows:

The surface heat transfer coefficient for smooth wall pipes can be found from a simple expression (Dittus and Boelter, 1941) given by:

$$N_u = 0{,}023\, R_e^{\,0{,}8}\, P_r^{\,0{,}4} \tag{6.1}$$

Allowance was made for the irregular surface by multiplying the right hand side of Equation 6.1 by a roughness factor (Nunner, 1956). The hydraulic diameter was used in evaluation of the Nusselt and Reynolds numbers. Substitution of the known parameters, results in surface heat transfer coefficients of 3,2 , 3,4 , and 3,7 W/m²K for the uninsulated, fully insulated and partly insulated sections prior to insulation being applied. The difference in the values of heat transfer coefficient is mainly due to the difference in hydraulic diameter at each section

The thicknesses of insulation used in the model were assumed to be constant at each section. The values were the averages of the many measurements taken at the site and were 74,9 mm for the fully insulated section, and 79,6 mm for the partially insulated section. The measured value of thermal conductivity of the insulation was 0,042 W/mK.

The procedure described in Chapter 3 was followed to allow for the effects of the thin layer of insulation on the rock surface. An equivalent surface heat transfer coefficient was computed from a combination of the actual surface heat transfer coefficient and the thermal resistance of the insulation. Following this approach yielded 0,48 and 0,47 W/m²K for the fully and partly insulated sections respectively. The uninsulated section was unchanged, with a heat transfer coefficient of 3,2 W/m²K.

The insulation was applied 87 weeks after the tunnel was holed, and the effects of insulation were analysed for 24 weeks (the duration of the experiment).

6.2.4 Results of finite element analysis

As the insulation was applied to the rock surfaces approximately 87 weeks after excavation of the tunnel, it was necessary to compute the temperature gradient within the rock body before proceeding to analyse the effects of the insulation. The heat flow from each section prior to applying the insulation is shown in Figure 6.4. There is little difference in heat flow between each section, indicating that a comparison between the insulated sections and the uninsulated control section was satisfactory both for the experiment and the theoretical prediction.

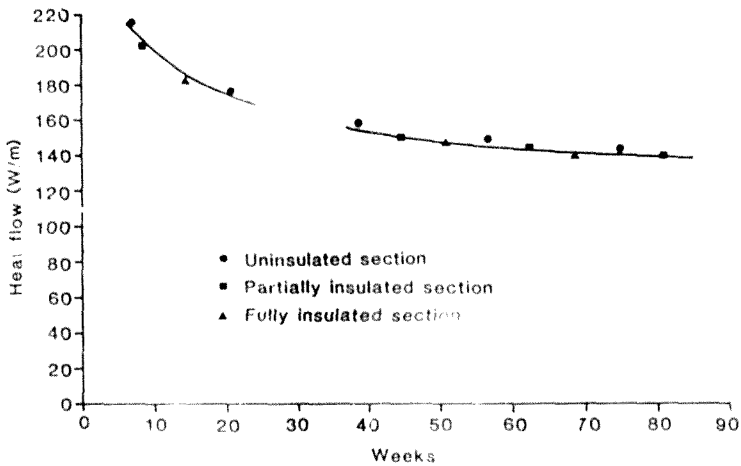

Figure 6.4 Heat flow from each test cross-section prior to insulating as predicted by finite element analysis.

The boundary conditions were then changed, where necessary, to make allowance for the insulated surfaces and finite element computations were made for a further 24 weeks. The computed heat flow for each section is shown in Figure 6.5 and the percentage reduction in heat flow in Figure 6.6.

The average heat flow was 138,8 W/m for the uninsulated section, 70,1 W/m for the partially insulated section, and 39,9 W/m for the

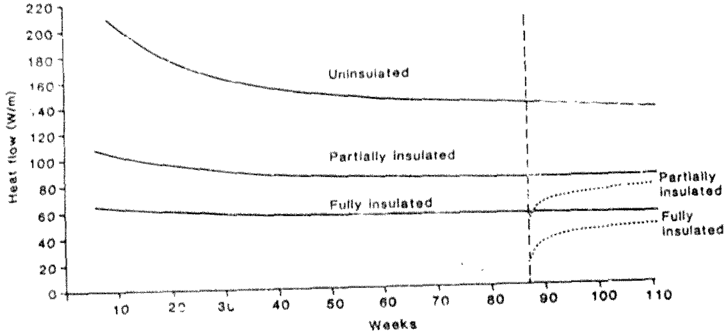

Figure 6.5 Heat flow from each test cross-section after insulating as predicted by finite element analysis

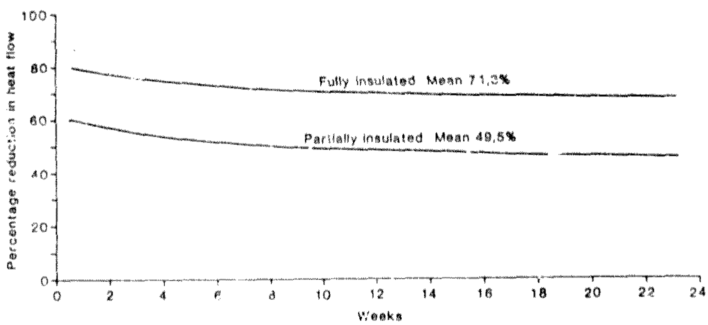

Figure 6.6 Reduction in heat flow at the fully and partially insulated cross-section as predicted by finite analysis

fully insulated section. These values are equivalent to a 49,5 per cent reduction in heat flow for the partially insulated section, and 71,3 per cent for the fully insulated section.

The results presented in Figure 6.5 can be compared directly with the measured values (Figure 5.21). The predicted heat flow of 138,8 W/m for the uninsulated section is very much higher than the measured value of 80,6 W/m. Some differences between the model and the actual test conditions are due to assuming steady air flow, average rock properties and smooth rock surfaces (except for the calculation of the surface heat transfer coefficient). However, it is unlikely that these assumptions are responsible for such a large difference. The most probable reason for the difference is that the rock was assumed to be at the virgin rock temperature on the day of excavation. It is likely that due to the position of the tunnel within the shaft pillar, the rock in the region had cooled below the virgin rock temperature. Fortunately this difference does not have significant bearing on the results of the experiment, as concern was mainly with the percentage reduction in heat flow and not the actual magnitude of the heat flow.

The percentage reduction in heat flow for the fully insulated section was on average 71,3 per cent over the 24 week period. The actual measured value was 56,7 per cent. For the partially insulated section the predicted reduction in heat flow was 49,5 per cent, which compares with the measured value of 29,7 per cent. The differences between the measured and the predicted results are most probably due to the large variation in the thickness of the insulation at the test site (see Figure 5.5). The direction of heat flow tended to follow the path of least resistance (that is through the areas of thin insulation covering), and results in a higher heat flow than that predicted by assuming a constant average thickness. As an example the effect of a varied insulation thickness was shown in Chapter 3. In the test case it was found that the heat flow through an insulated slab was increased by 20 per cent if the insulation was not of an even thickness.

6.2.5 The effects of delayed insulation application

In the analysis presented in Chapter 4, the insulation was assumed to be applied, and thus effective, from the day of holing through. In practice this would not be the case. In the case of the experiment conducted at western Deep Levels gold mine the insulation was applied 87 weeks after *holing through*. The effects can be seen in Figure 6.7 which shows the heat flow from the uninsulated section, from sections with the insulation applied after 87 weeks (a repeat of Figures 6.4 and 6.5), and from sections with the insulation effective from the day of holing through.

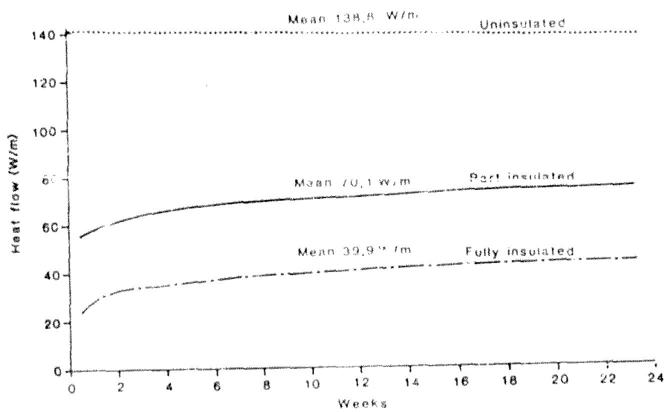

Figure 6.7 The effect on heat flow of applying insulation 87 weeks after holing the tunnel.

There is a marked reduction in heat flows immediately after the application of the insulation at week 87. The heat flows then increase to asymtotically approach the heat flows from the sections which were insulated from the day of holing through. By assuming the application of insulation to be on the day of holing through, the reduction in *heat* flow is underestimated but not by a significant amount. This result is important as it indicates that much simpler methods of predicting the reduction in *heat flow* can be used with confidence.

6.3 Simple analysis of heat flow into the experimental test sections

6.3.1 Introduction

It is impractical for the engineer wishing to predict heat flow into insulated tunnels to resort to finite element analysis. It is therefore important to assess the results of the experiment and of finite element analysis against those obtained from simplified calculation techniques.

6.3.2 Results of simplified analysis

The most suitable method of simply predicting the heat flow into a fully insulated tunnel is by means of the tables produced by Jaeger and Chamalaun (1966). This is not possible for partially insulated tunnels due to the discontinuous boundary conditions, but the quasi-steady method can be satisfactorily employed for this purpose. Both of these techniques were explained fully in Chapter 3.

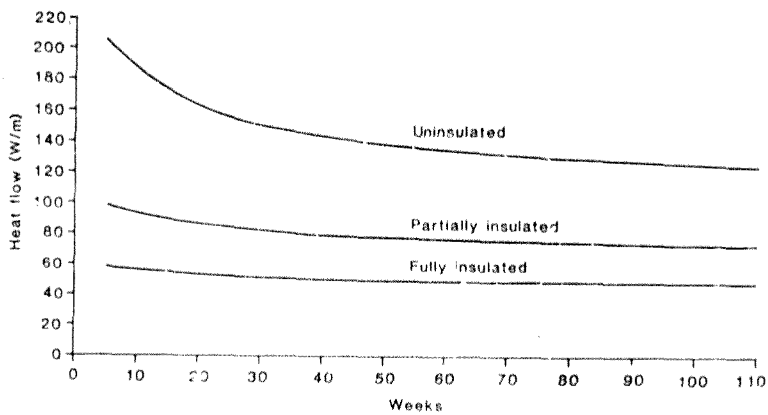

Figure 6.8 Heat flow at each test section as predicted by simple anaylsis.

Both methods have two deficiencies. Firstly, no allowance can be made for the time period prior to the application of insulation and, secondly, the methods apply only to circular tunnels. The transistion from circular to rectangular airways is made on the assumption of equal cross sectional areas. For the partially insulated section there is no foundation for this assumption other than its general acceptance (see Chapter 3).

The results of heat flow obtained using the test site conditions (Section 6.2.3) are shown in Figure 6.8. They compare well with the results obtained using finite element analysis (Figure 6.7), which are generally higher by approximately 6 W/m.

For these type of analyses it is therefore generally unnecessary to obtain finite element solutions, the simple methods being quite adequate.

6.4 Summary

The heat flow and the percentage reduction in heat flow due to insulation at the experimental test site were overestimated by theoretical methods. This was probably due to the assumption that the rock mass was at the virgin rock temperature on the day of excavating the tunnel, as well as to the large variation in insulation thickness.

After a short time no significant error resulted from the assumption that the insulation was applied immediately the tunnel was holed, and this permits the simple heat flow prediction techniques to be used.

It was found that finite element analysis was generally unnecessary. The simplified methods of analysis gave results which were slightly lower than those produced using finite element analysis, but are adequate for general engineering computations.

7 INSULATION PROPERTIES

7.1 Introduction

The main aim of this dissertation was, firstly, to analyse theoretically the effects of insulation on tunnel heat flow, and secondly, to provide some data as a check on the theoretical findings. An experiment was conducted at Western Deep Levels gold mine to obtain the empirical data. However, a suitable material for mine wide application still needs to be developed. The material needs to have the properties which are outlined in this Chapter.

It is important to note that the benefits of coating the rock surfaces are not only in the insulating effect but also in the support properties of the material. In fact, some mines are considering the complete shotcreting of all rock surfaces in the haulages and cross-cuts as they are developed (Lloyd, 1984), irrespective of any insulating benefits. A *material suitable for both support and insulation purposes* would have obvious benefits. Additionally a smooth coating on the rock surfaces would serve to reduce the resistance to airflow and this would be manifested as savings in fan power.

7.2 Insulation Material Properties

There are several factors which influence the choice of a suitable mine tunnel insulation material. For practical minewide application the insulation material needs to be reasonably priced (see Chapter 8) and easily available. The material must also possess the following properties:

Thermal Conductivity
The lower the conductivity, the less is the amount of material needed to have the same insulating effect. As a reference value it should be noted that polyurethane has a conductivity of 0,03 W/mK and it has been shown that a layer of 50 mm would be suitable for insulation purposes.

More details of choosing an optimum insulation thickness are given in chapter 8.

Toxicity

During application and curing a number of insulation foams emit harmful gases. In particular, attention will be given to formaldehyde gas which is carcinogenic and concentrations of greater than 2 ppm should be avoided.

Fire Resistance

It is extremely important that the insulation product does not support combustion, or produce noxious gases on burning.

Composition

The insulation material should not be susceptible to attack from bacteria and should be unaffected by running water or high humidity.

Structural Strength and Durability

A high structural strength would be beneficial with regard to the shoring of rock and the prevention of spalling, as well as for good durability of the insulation surface. The product should have a good adherence to the rock.

Ease and Evenness of Application

The insulation material should be simple to apply in large quantities. The hangingwall can cause difficulties as a result of the insulation falling off before setting. Product density, thermal conductivity and application thickness should be easily controlled in an underground environment. It is particulary important to be able to maintain the thickness of the insulation within reasonable limits. Optionally the material could be supplied as panels which alleviate most of these problems.

In Table 7.1 a comparison of some different insulation material is shown. Although some materials are promising, an insulation which has all the attributes required for insulating mine airways is not yet available. Many manufacturers are presently working on developing a suitable product.

Table 7.1 Comparison of some insulation materials

	CONDUCTIVITY	TOXICITY	FIRE RESISTANCE	COMPOSITION	STRENGTH AND DURABILITY	EASE OF APPLICATION
Polyurethane	GOOD	GOOD	POOR	GOOD	FAIR	GOOD
Urea Formaldehyde	GOOD	(3) FAIR	POOR	GOOD	POOR	GOOD
Phenol Formaldehyde	GOOD	(3) FAIR	FAIR	GOOD	FAIR	POOR
Cementitious Foam	FAIR	GOOD	GOOD	(2) FAIR	FAIR	FAIR
Rock Wool	FAIR	(4) GOOD	(1) GOOD	(2) FAIR	GOOD	FAIR
Fibreglass	FAIR	(4) GOOD	(1) GOOD	(2) FAIR	GOOD	FAIR

NOTES:
1. Some organic binders are combustible.
2. Can absorb large quantities of water unless treated with a finishing cement.
3. May emit toxic gases on application and for some time afterwards.
4. Can cause problems due to excess fibres in the ventilation air stream.

8 FINANCIAL ANALYSIS

8.1 Introduction

It has been shown that significant reductions in heat flow, of the order of 50 per cent, can be achieved by full insulation of mine airways. If the footwall remains uninsulated the reduction in heat load is less, being of the order of 25 per cent. However, for the engineer designing ventilation and refrigeration systems for deep level mines, the cost of insulating mine airways must be economically justified. The number of variables involved in evaluating tunnel heat flow are too numerous to permit a general analysis in this dissertation. However, presented below, by way of example, is an analysis of the cost benefits of insulation, for a particular set of underground conditions. Optimum insulation thicknesses are established for materials of various unit volume costs, and both full and partial insulation is considered.

8.2 Sample Cost Benefit Analysis and Optimisation of Insulation for Deep Level Mining

As an example of the economic benefits of insulation, the cost of insulating the airway in the following hypothetical case was examined:

A heat exchanger cools 27 kg/s of ventilation air to 20 °C saturated. The air travels along a 2 000 m long, 3x3 m intake airway, to ventilate the mine workings. The airway is dry, and the virgin rock temperature is 50 °C.

In Figure 8.1 the heat pickup from the airway is shown when the tunnel is uninsulated, and fully, or partially insulated with varying thickness of insulation at a thermal conductivity of 0,03 W/mK. A tunnel age of one year was assumed.

Figure 8.2 shows the per cent reduction in heat flow as a result of full or partial insulation of the airway with varying thicknesses of insulation.

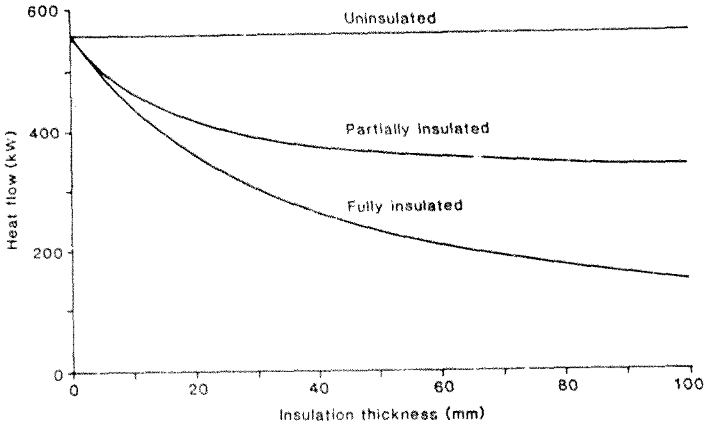

Figure 8.1 Variation in heat flow with insulation thickness

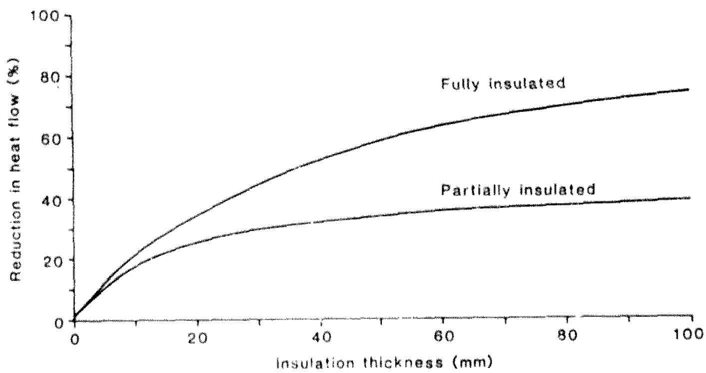

Figure 8.2 Variation of the percentage reduction in heat flow flow with insulation thickness

The capital cost of refrigeration plant was taken as R450/kW(R) and the running cost as R55/kW(R) per annum. For this example it was assumed that the associated refrigeration distribution system has a capital cost equal to the cost of the refrigeration plant.

To enable a direct comparison to be made between the cost of insulation and the running of refrigeration plants the 'annual cost' concept (Lambrechts and Howes, 1982) was employed. This is a method of expressing overall costs over the life of the system, based at an appropriate interest rate, in terms of an average in one year. An 'annual cost' multiplying factor can be found in published tables (Lambrechts and Howes, 1982). For an assumed life of 10 years and an interest rate of 15 per cent the factor is 5,02. The annual cost of supplying one kilowatt of refrigeration on a mine is thus equal to 55+(450+450)/5,02 or R234,3.

It is now possible to evaluate the cost benefits of insulating the 2 000 m length of tunnel. In Figures 8.3 and 8.4 the cost savings due to insulating the tunnel partially and fully are shown for varying thicknesses of insulation for different insulation costs. For every line representing the cost of insulation it is possible to select an optimum thickness of insulation for maximum financial return. A locus has been drawn through these points and this is termed the 'locus of maximum saving'.

For an insulation material costing R500/m^3 the optimum thickness for a fully insulated airway is 11 mm, which from Figure 8.2 results in a reduction in heat flow of only 23 per cent. The financial saving would be only R3 500 per annum and consequently it is doubtful whether the exercise would be viable. However, different (less expensive) materials present a much more positive view.

As an example, the price of urea formaldehyde insulation is R135/m^3. When fully insulating a mine airway the optimum insulation thickness is 50 mm, with a reduction in heat flow of 59 per cent and a financial saving of R45 000 per annum. For partial insulation the optimum insulation thickness is 28 mm, with a reduction in heat flow of 29 per cent and a financial saving of R26 000 p.a. The savings are now significant and it is clear that with a suitable insulation material

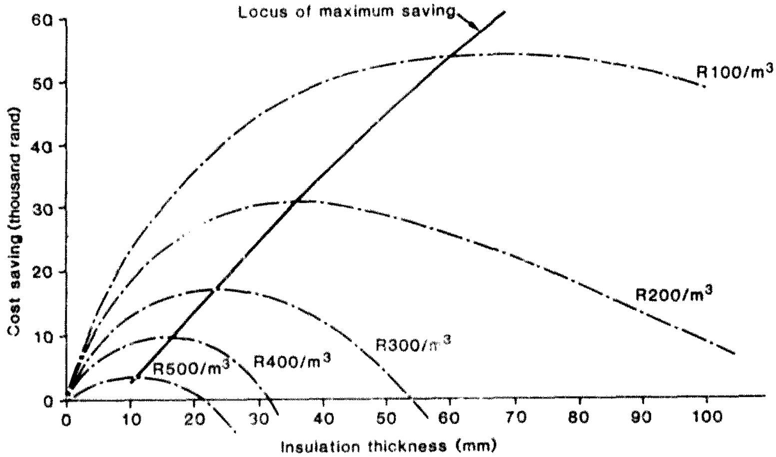

Figure 8.3 Variation in cost saving due to full insulation at different thicknesses

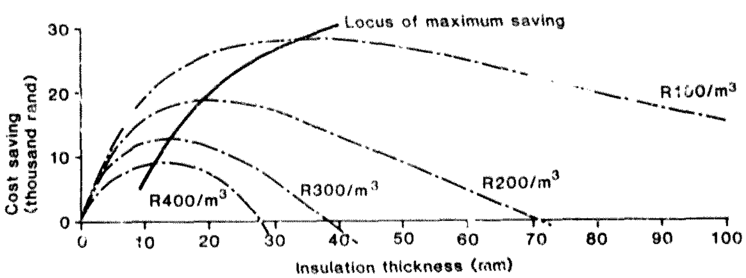

Figure 8.4 Variation in cost saving due to partial insulation at different thicknesses

and an efficient, perhaps automatic, method of application, the insulation of mine airways can be a practical proposition for both fully and partially insulated cases.

9 CONCLUSIONS AND RECOMMENDATIONS

The main conclusion that can be drawn from this work is that substantial reductions in heat flow can be realised by insulating tunnel rock surfaces.

Savings are typically between 50 and 70 per cent for fully insulated dry tunnels. Significantly, if the footwall remains uninsulated these savings are reduced to between 20 and 40 per cent. Furthermore, if the footwall is both uninsulated and damp the reductions in heat flow are marginal; less than 20 per cent.

These values are greatly affected by the rock thermal conductivity, the tunnel dimensions (radius), ventilation air flow, tunnel age, tunnel length, insulation thermal conductivity and insulation thickness. Nevertheless it has been shown that simple evaluation techniques based on solutions of heat flow into circular cross-sectional tunnels can produce adequate results. Finite element analysis was used to evaluate these methods and to investigate the effects of time delays between the excavation of the tunnel and application of the insulation, but this is not necessary for general engineering calculations.

The reduction in heat flow that can be achieved by insulating airways under a variety of condition ere computed. The results are presented as a set of nomograms in Apper D. These nomograms cover the wide range of conditions which ar in South African gold mines and serve as a useful tool for the practicing engineer.

The experiment conducted at Wes Deep Levels gold mine produced reductions in heat flow of 56,7 per cent in the fully insulated section and 29,7 per cent in the partially insulated section. These values are less than those predicted by theory and the differences are most probably due to the large variation in the thickness of the insulation at the test site. No evidence was found of an insulating effect due to the footwall ballast. Theoretically the footwall ballast should go some way to alleviating the problem of an uninsulated footwall.

It was shown that there is a clear diminishing return on increasing the thickness of the applied insulation. There is an economic optimum insulation thickness for which no global value can be given. However, it has been shown, by means of a typical example, that significant financial savings can be made by applying insulation priced between R100 and R200/m^3. Materials are available which meet this price criterion, and techniques need to be devised for effective covering of the rock surfaces economically.

If the practicing engineer is to derive benefit from this work, it is necessary to provide general recommendations as a guide to the selection and implementation of tunnel insulation. There are a number of steps that must be followed and several practical problems which must be overcome. It is recommended that the following points be considered when contemplating the insulation of tunnel surfaces.

The heat flow from the proposed network of ventilation tunnels must be evaluated. This is easily done by using one of the computer program lised in Appendix B. The heat loads from all of the airways on a mine can be computed by using a heat flow network program (Chorosz, 1986).

An estimate of the possible reductions in heat flow can be found from the nomograms in the Appendix D. If the set of nomograms do not cover the desired conditions, the reduction in heat flow can be computed from the programs in Appendix B. It can be expected that the overall reduction in heat flow will be of the order of [illegible]0 per cent for a full insulation covering. This will be halved for partial insulation and halved again for a wet footwall.

These calculations must be followed by an economic study based on the cost of insulation and the cost of applying refrigeration. A guide to the type of procedure to be followed is given in Chapter 8. The results of an economic study will give the savings in Rands that may be accrued, and the optimum thickness of insulation that is to be applied.

The selection of a suitable insulation material for mine wide application requires careful consideration. A guide to desirable properties is gives in Chapter 7. In particular fire resistance, toxicity and thermal conductivity are important parameters. A material suitable for insulating the footwall should be sought since approximately 60 per cent of the total heat flow passes through the footwall in a partially insulated tunnel. Finally a material which can be evenly applied must be used.

APPENDIX A

A1 The Quasi-Steady Method

The published version of the quasi-steady method needs some modification before it is possible to allow for the effects of an insulated surface. In order to account for insulation on the tunnel surface the thermal capacity is ignored and an 'equivalent' surface heat transfer coefficient is calculated. This 'equivalent' surface heat transfer coefficient, h_e, includes the effect of insulation and the convective heat transfer coefficient, h :

$$h_e = \frac{\text{insulation thickness}}{\text{insulation conductivity}} + \frac{1}{h}].$$

The geometry of the partially insulated airway is shown in Figure A 1. The cross-section is assumed to be circular. The uninsulated portion subtends an angle 2β at the centre of the circle.

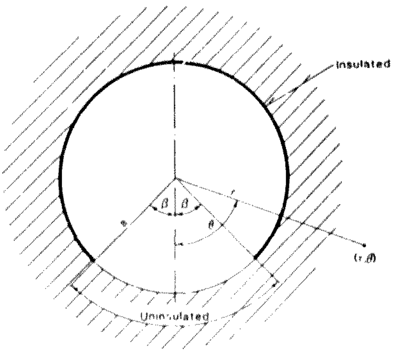

Figure A1 Geometry of airway cross-section.

The heat transfer at the surfaces is by a combination of convection and radiation. At the bare surface the heat flux is given by:

$$\frac{k\partial T}{\partial r} = h(T_S - T_{DB}) + K(T_S - T_{INS}) + f\lambda E[P_{SAT}(T_S) - P] \text{ ,} \qquad \text{(A1)}$$

while at the insulated surface:

$$\frac{k\partial T}{\partial r} = h_e(T_s - T_{DB}) + K'(T_S - T_{UNINS}) \quad \text{(A2)}$$

where

$K' = K(\pi-\beta)/\beta$

If we introduce a function $g(\theta)$, which has a value one on the insulated portion and zero on the bare surface, i.e.

$$g(\theta) = 1 \quad \text{for} \quad |\theta| <= \beta$$
$$= 0 \quad \text{for} \quad |\theta| > \beta$$

it is possible to combine equations (A1) and A2).

Thus:

$$\frac{k\partial T}{\partial r} = g(\theta)[h(T_S - T_{DB}) + K(T_S - T_{INS}) + f\lambda E(P_{SAT}(T_S) - P)]$$

$$+ [1-g(\theta)] [h_e(T_S - T_{DB}) + K'(T_S - T_{UNINS})] \quad \text{(A3)}$$

which holds on $r = a$ for all θ.

Now

$$P_{SAT}(T_S) = P_{SAT}(T_{UNINS}) + (T_S - T_{UNINS}) P'_{SAT}(T_{UNINS})$$

where P'_{SAT} is the slope of the curve for saturated vapour pressure.

By re-arranging we obtain:

$$\frac{(\partial T)}{(\partial r)_{r=a}} = q_1 + q_2T_S + q_3g(\theta) + q_4T_Sg(\theta) \quad \text{(A4)}$$

where

$q_1 = -(h_eT_{DB} + K'T_{UNINS})/k,$

$$q_2 = (h_e + K')/k,$$

$$q_3 = ((-hT_{DB} - KT_{INS} + h_e T_{DB} + K'T_{UNINS}) + f\lambda E\,(P_{SAT}(T_{UNINS})$$

$$- T_{UNINS}\,P'_{SAT}(T_{UNINS}) - P))/k,$$

and

$$q_4 = ((h + K - h_e - K') + f\lambda E\,P'_{SAT}(T_{UNINS})/k.$$

Instead of solving the heat diffusion equation, we are to solve Laplace's equation given by:

$$\frac{\partial^2 T}{\partial r^2} + \frac{1}{r}\frac{\partial T}{\partial r} + \frac{1}{r^2}\frac{\partial^2 T}{\partial \theta^2} = 0$$

The general solution can be derived by the method of separation of variables and is given by:

$$T(r,\theta) = A_0 + A_0' \ln r + \sum_{n=1}^{\infty} (A_n r^n + A_n' r^{-n}) \sin n\theta$$

$$+ \sum_{n=1}^{\infty} (B_n r^n + B_n' r^{-n}) \cos n\theta$$

If the condition imposed by the quasi-steady approach that at $r = R$, $T = T_R$ for all θ is applied, then it can be easily shown that:

$$T(r,\theta) = T_R + C_0 \ln(r/R) + \sum_{n=1}^{\infty} C_n[(r/R)^n - (R/r)^n] \cos n\theta \qquad \textbf{(A5)}$$

It only remains to satisfy the condition given by equation **(A4)**.

By differentiating equation (A5) at $r = a$ we obtain

$$\frac{(\partial T)}{(\partial r)_{r=a}} = C_0/a + \sum_{n=1}^{\infty} C_n[(n/R)(a/R)^{n-1} + (nR/a^2)(R/a)^{n-2}] \cos n\theta \qquad \textbf{(A6)}$$

We are only concerned with temperatures on the surface $r = a$.

If we write:

$$T_S = T(a,\theta) = T_R + A_o + \sum_{n=1}^{\infty} A_n \, \text{Cos } n\theta \qquad \text{(A7)}$$

and

$$\frac{(\partial T)}{(\partial r)_{r=a}} = A_o \gamma_o + \sum_{n=1}^{\infty} A_n \, \gamma_n \, \text{Cos } n\theta \qquad \text{(A8)}$$

then by comparison with equation (A5) and (A6) it can be shown that:

$$\gamma_o = 1/[a \ln(a/R)]$$

and

$$\gamma_n = (n/a)[(a/R)^{2n} + 1]/[(a/R)^{2n} - 1] \qquad \text{(A9)}$$

for

$n = 1, 2, \ldots\ldots$

It is then sufficient to find values of $A_0, A_1, \ldots\ldots$ without evaluating $C_0, C_1, \ldots\ldots$

By expanding the function $g(\theta)$ in a Fourier series from $-\pi$ to π we can write:

$$g(\theta) = B_o + \sum_{n=1}^{\infty} B_n \, \text{Cos} n\theta \qquad \text{(A10)}$$

where $B_o = \beta/\pi$

and $B_n = (2/n\pi) \text{ Sin } n\beta$

substituting A(7), A(8), and A(10) into A(4) gives

$$A_o\gamma_o + \Sigma A_n\gamma_n \operatorname{Cos} n\theta = q_1 + q_2 (T_R + A_o + \Sigma A_n \operatorname{Cos} n\theta)$$

$$+ q_3 (B_o + \Sigma B_n \operatorname{Cos} n\theta)$$

$$+ q_4 (B_o + \Sigma B_n \operatorname{Cos} n\theta)(T_R + A_o$$

$$+ \Sigma A_n \operatorname{Cos} n\theta)$$

Which, by comparing like terms in Cos $n\theta$ for $n=0,1,2....N$ leads to a set of linear equations. These equations can be expressed as:

$$\sum_{n=0}^{N} G_{mn} A_n = C_m \qquad m = 0,1,2....N \qquad \text{(A11)}$$

where

$$C_o = q_1 + q_2 T_R + B_o (q_3 + q_4 T_R)$$

$$G_{oo} = \gamma_o - q_2 - q_4 B_o$$

if $n <> 0$

$$C_m = B_m (q_3 + q_4 T_R)$$

$$G_{mo} = -q_4 B_m$$

$$G_{mm} = \gamma_m - q_2 - q_4 B_o - q_4 B_{2n}/2$$

if $m <> 0$

$$G_{on} = q_4 B_n/2$$

and if both $n <> 0$ and $m <> 0$

$$G_{mn} = - q_4(B_{n+m} + B_{n-m})/2$$

By solving this system of equations the A coefficients can be found and hence the rock surface temperature from equation (A7). An iterative algorithm, presenting a method of solution is shown in Figure . Improved values of average temperature for the uninsulated and insulated surfaces are given by:

$$T_{UNINS} = T_R + A_O - \sum_{n=1}^{N} [A_n/n(\pi-\beta)] \text{ Sin } n\beta \tag{A12}$$

and

$$T_{INS} = T_R + A_O + \sum_{n=1}^{N} (A_n/n\beta) \text{ Sin } n\beta \tag{A13}$$

respectively.

The heat transfer can then be found by summing the results from equations (A1) and (A2).

A2 An Integration Algorithm

To find the total heat transfer from the rock to the ventilation air over a finite length of tunnel a stepping method is used. The total length of airway is divided into short sections over which conditions are assumed to be constant. Changes in air temperature can then be incrementally evaluated, the condition of outlet air from one section being used as the inlet condition for the subsequent section.

A complete listing of a computer program which implements both the quasi-steady method and the above stepping procedure is given in Appendix B.

APPENDIX B

Computer Programs

The full listings of two computer programs used for the calculation of heat flow into insulated tunnels are presented in this appendix.

The first program was used for calculating heat flow into uninsulated or fully insulated tunnels, and is based on the published tables of Jaeger and Chamalaun. The second program was used for calculating heat flow into partially insulated airways and is based on the quasi-steady method.

```
10    ! *****************************************************
20    ! ROUTINE TO CALCULATE HEAT FLOW FROM UINSULATED & FULLY INSULATED
30    ! AIRWAYS.
40    ! SEE:JAEGER,J.C. & CHAMALAUN,T. HEAT FLOW IN AN INFINITE REGION
50    !     BOUNDED EXTERNALLY BY A CIRCULAR CYLINDER WITH FORCED
60    !     CONVECTION AT THE SURFACE..MET.NOV/DEC 1983.
70    !     AUST.J.PHYS.,1966
80    ! AUTHOR:P.BOTTOMLEY
90    !         CHAMBER OF MINES RESEARCH LABORATORIES
100   !         P.O.BOX 91230
110   !         AUKLAND PARK 2006
120   ! *****************************************************
130   PRINTER IS 16
140   ! *****************************************************
150   ! I/O Routine ........Input Parameters.
160   ! *****************************************************
170   PRINT PAGE
180   PRINT "ROCK CONDUCTIVITY (W/M DEG.C)?"
190   INPUT Cond
200   PRINT "ROCK DIFFUSIVITY (M**2/S)?"
210   INPUT Diffus
220   PRINT "INSULATION CONDUCTIVITY (W/M DEG.C)?"
230   INPUT Ki
240   PRINT "INSULATION THICKNESS (mm)?"
250   INPUT Thick
260   PRINT "DRY-BULB TEMPERATURE (DEG.C)?"
270   INPUT Air
280   PRINT "BAROMETRIC PRESSURE (KPa)?"
290   INPUT Pressure
300   PRINT "AIR QUANTITY (M**3/S)?"
310   INPUT Volume
320   PRINT "VIRGIN ROCK TEMPERATURE (DEG.C)?"
330   INPUT Vrt
340   PRINT "AIRWAY AGE (YEARS)?"
350   INPUT Yrs
360   PRINT "AIRWAY RADIUS (M)?"
370   INPUT Aa
380   PRINT "LENGTH OF AIRWAY (M)?"
390   INPUT Km
400   PRINT "NUMBER OF STEPS?"
410   INPUT Steps
```

```
420   ! ****************************************************
430   !  Print Input Parameters
440   ! ****************************************************
450   PRINTER IS 0
460   PRINT " INPUT PARAMETERS  :"
470   PRINT "Rock Conductivity                      :";Cond;"W/m.degC  "
480   PRINT "Rock Difusivity                        :";Diffus;"M^2/S"
490   PRINT "Insulation Conductivity                :";Ki;"W/m degC"
500   PRINT "Insulation Thickness                   :";Thick;"mm"
510   PRINT "Dry-bulb Temperature                   :";Air;"degC"
520   PRINT "Wet-bulb Temperature                   :";Wet;"degC"
530   PRINT "Barometric Pressure                    :";Pressure;"Kpa"
540   PRINT "Air Quantity                           :";Volume;"M^3/S"
550   PRINT "Virgin Rock Temperature                :";Vrt;"degC"
560   PRINT "Age of Airway                          :";Yrs;"years"
570   PRINT "Airway Radius                          :";Aa;"m"
580   PRINT "Length Of Airway                       :";Km;"M"
590   PRINT "Number Of Steps                        :";Steps;
600   PRINT
610   PRINT
620   PRINT
630   PRINT "    DISTANCE       DRY-BULB      kW       TOTAL kW"
640   PRINT
650   ! ****************************************************
660   !  Main Routine
670   ! ****************************************************
680   Velocity=Volume/(PI*Aa*Aa)                  !Air velocity
690   Fourier=Diffus*Yrs*365*24*3600/(Aa*Aa)      !FOURIER Number
700   Dx=Km/Steps                                 !Step length
710   Senst=0
720   ! --------------------------------------------------
730   ! Step Along Airway.
740   ! --------------------------------------------------
750   FOR Istep=1 TO Steps
760   Dens=Pressure/(.287045*(273.15+Air))        !Air Density
770   Mass=Dens*PI*Aa*Aa*Velocity                 !Air Mass Flow
780   Re=67000*Velocity*Aa*Dens/.6                !REYNOLDS Number
790   Hc=.00028/Aa
800   Hc=Hc*Re^.8
810   Hc=1/(1/Hc+Thick/(Ki*1000))                 !Equivalent Surface H.T.C
820   Bi=Hc*Aa/Cond                               !BIOT Number
830   ! --------------------------------------------------
840   ! Compute Tabulated Function By Approximation
850   ! SEE:GIBSON,K.THE COMPUTER SIMULATION OF CLIMATIC CONDITIONS IN
860   !      UNDERGROUND MINES.Ph.D.THESIS UNIVERSITY OF NOTTINGHAM 1976.
870   ! --------------------------------------------------
880   X2=LGT(Fourier)
890   X22=X2*X2
900   X23=X22*X2
910   X24=X23*X2
920   X25=X24*X2
930   Ca=-.016218*X23+.163336*X22+.558742*X2+.622702
940   Cb=.012454*X23-.120683*X22-.398410*X2-.255263
950   Cc=-.009933*X23+.103367*X22+.762691*X2+1.041458
960   Cd=.000007*X23-.000250*X22+.001292*X2-.001661
970   Ct=1/(.001073*X25-.004525*X24-.01572*X23+.1459*X22+.7288*X2+1.017)
980   Cy=1/(1/Bi+Ca)
990   Gib=Ct*(Cy*Cy*Cb+Cy*Cc+Cd)
1000  Gib=Gib/Bi
1010  ! --------------------------------------------------
1020  ! Compute Heat Transfer For This Section & Sum
1030  ! --------------------------------------------------
1040  Sens=2*PI*Aa*Hc*(Vrt-Air)*Gib*Dx/1000
1050  Senst=Senst+Sens
1060  Air=Air+Sens/(Mass*1.005)            !Air Temp.To Next Section
1070  Dist=Istep*Dx
1080  PRINT USING 1090;Dist,Air,Sens,Senst
1090  IMAGE 5X,4D,7X,3D.2D,5X,3D.3D,5X,5D.2D
1100  NEXT Istep
1110  END
```

```
10      ! ************************************************
20      ! QUASI-STEADY METHOD FOR HEAT FLUX CALCULATION ALONG AN INSULATED AIRWAY
30      ! SEE:STARFIELD,A.M. & BLELOCH,A.L. A NEW METHOD FOR THE COMPUTATION
40      !     OF HEAT AND MOISTURE TRANSFER IN PARTLY WET AIRWAYS.
50      !     JOURNAL OF S.A.INST.OF MIN.MET.NOV/DEC 1983.
60      ! AUTHOR:P.BOTTOMLEY
70      !         CHAMBER OF MINES OF S.A.
80      !         P.O.BOX 91230
90      !         AUKLAND PARK 2006
100     ! ************************************************
110     DIM A(40),B(40),C(3),D(3),G(20,21),Gam(40)
120     PRINTER IS 16
130     ! ************************************************
140 Begin:! I/O Routine ........Input Parameters.
150     ! ************************************************
160     PRINT PAGE
170     PRINT "ROCK CONDUCTIVITY (W/M DEG.C)?"
180     INPUT Cond
190     PRINT "ROCK DIFFUSIVITY (M**2/S)?"
200     INPUT Diffus
210     PRINT "INSULATION CONDUCTIVITY (W/M DEG.C)?"
220     INPUT Ki
230     PRINT "INSULATION THICKNESS (mm)?"
240     INPUT Thick
250     PRINT "RADIATION CONSTANT (W/M**2 DEG.C)?"
260     INPUT Hrad
270     PRINT "DRY-BULB TEMPERATURE (DEG.C)?"
280     INPUT Air
290     PRINT "WET-BULB TEMPERATURE (DEG.C)?"
300     INPUT Wet
310     PRINT "WETNESS FACTOR?"
320     INPUT Wetf
330     PRINT "BAROMETRIC PRESSURE (KPa)?"
340     INPUT Pressure
350     PRINT "AIR QUANTITY (M**3/S)?"
360     INPUT Volume
370     PRINT "VIRGIN ROCK TEMPERATURE (DEG.C)?"
380     INPUT Vrt
390     PRINT "AIRWAY AGE (YEARS)?"
400     INPUT Yrs
410     PRINT "AIRWAY RADIUS (M)?"
420     INPUT Ra
430     PRINT "PROPORTION INSULATED (PERCENT)?"
440     INPUT Alfa
450     Alfa=Alfa/100
460     PRINT "LENGTH OF AIRWAY (M)?"
470     INPUT Km
480     PRINT "NUMBER OF STEPS?"
490     INPUT Steps
```

```
500     ! ******************************************************
510     !  Print Input Parameters
520     ! ******************************************************
530     PRINTER IS 0
540     PRINT " INPUT PARAMETERS  :"
550     PRINT "Rock Conductivity                          :";Cond;"W/m.degC  "
560     PRINT "Rock Diffusivity                           :";Diffus;"M^2/S"
570     PRINT "Insulation Conductivity                    :";Ki;"W/m degC"
580     PRINT "Insulation Thickness                       :";Thick;"mm"
590     PRINT "Radiation Coefficient                      :";Hrad;"W/m^2.degC"
600     PRINT "Dry-bulb Temperature                       :";Air;"degC"
610     PRINT "Wet-bulb Temperature                       :";Wet;"degC"
620     PRINT "Wetness Factor                             :";Wetf
630     PRINT "Barometric Pressure                        :";Pressure;"Kpa"
640     PRINT "Air Quantity                               :";Volume;"M^3/S"
650     PRINT "Virgin Rock Temperature                    :";Vrt;"degC"
660     PRINT "Age of Airway                              :";Yrs;"years"
670     PRINT "Airway Radius                              :";Ra;"m"
680     PRINT "Proportion of Tunnel that is Insulated :";Alfa*100;"Percent"
690     PRINT "Length Of Airway                           :";Km;"M"
700     PRINT "Number Of Steps                            :";Steps;
710     PRINT
720     PRINT
730     PRINT
740     PRINT "   DISTANCE      DRY-BULB      WET-BULB      kW      TOTAL kW"
750     PRINT
760     PRINTER IS 16
```

```
770    ! ******************************************************
780    !  Main Routine
790    ! ******************************************************
800    Maxiter=100
810    Bb=FNGoch(Diffus*24*365*3600*Yrs/(Aa*Aa))    !Thermal Gradient
820    Bb=Aa*EXP(1/Bb)
830    N=15                                         !No Of Summation Steps
840    Alfa=(1-Alfa)*PI
850    GOSUB Bcalc                                  !B Coefficients
860    Hrad=Hrad/Cond
870    Hrad2=Hrad*(PI-Alfa)/Alfa
880    Velocity=Volume/(PI*Aa*Aa)                   !Air velocity
890    Hci=Ki*1000/Thick                            !Insulation Equivalent h.t.c
900    Dx=Km/Steps                                  !Step length
910    Senst=0
920    ! ------------------------------------------------------
930    ! Compute Airflow In Kg/s
940    ! ------------------------------------------------------
950    Ashi=622*FNP(Wet,Air,Pressure)/(Pressure-FNP(Wet,Air,Pressure))
960    Density=(Pressure-FNP(Wet,Air,Pressure))/(.287045*(273.15+Air))
970    Mass=Density*PI*Aa*Aa*Velocity
980    GOSUB Gamcalc                               !Compute Gamma Coefficients.
990    ! ------------------------------------------------------
1000   ! Step Along Airway.
1010   ! ------------------------------------------------------
1020   FOR Istep=1 TO Steps
1030   ! ------------------------------------------------------
1040   ! Compute Surface h.t.c.
1050   ! ------------------------------------------------------
1060   Density=(Pressure-FNP(Wet,Air,Pressure))/(.287045*(273.15+Air))
1070   Ka=(24.2+.075*Air)*1E-3
1080   Kw=(16.2+.084*Air)*1E-3
1090   Ep=FNP(Wet,Air,Pressure)/Pressure
1100   Aircond=(3.07*(1-Ep)*Ka+2.62*Ep*Kw)/(3.07-.45*Ep)
1110   Cpair=1005+1884*.662*FNP(Wet,Air,Pressure)/(Pressure-FNP(Wet,Air,Pressure
))
1120   Diffusion=1.192E-7*(Air+273.15)^1.75/Pressure
1130   Viscosity=4.74E-8*Air+1.716E-5
1140   Re=2*Velocity*Aa*(Density/1.2)/Viscosity
1150   Hc1=.02*Re^.8*Aircond/(Aa*2)
1160   Evap=Hc1/Cpair*(Cpair*Density*Diffusion/Aircond)^(2/3)*622/P    sure
1170   ! ------------------------------------------------------
1180   ! Compute Equivalent h.t.c.
1190   ! ------------------------------------------------------
1200   Hc2=1/(1/Hc1+1/Hci)
1210   Hc1=Hc1/Cond
1220   Hc2=Hc2/Cond
1230   Q2=Hc2+Hrad
1240   Vbotn=Air                                  !1st Guess Average Surface Temp
1250   Vtopn=Air
1260   Lat=2501-2.387*Wet
1270   Cc=Lat*Evap/Cond
1280   C=Wetf*Cc
```

```
1290    ! --------------------------------------------------------
1300    ! Iteration Loop For Surface Temp.
1310    ! --------------------------------------------------------
1320    Ind=1
1330 Iter:Vtop=Vtopn
1340    Vbot=Vbotn
1350    Psatd=FNPsat(Vbat)*17.27*237.3/(237.3+Vbot)^2
1360    Q1=-Hc2*Air-Hrad*Vbot
1370    Q4=Hc1-Hc2-Hrad+Hrad2+C*Psatd
1380    Q3=-Hc1*Air-Hrad2*Vtop+Hc2*Air+Hrad*Vbot+C*(FNPsat(Vbot)-Vbot*Psatd-FNP(W
et,Air,Pressure))
1390                GOSUB Coeffcalc                   !Compute C AND G Coefficients.
1400                GOSUB Linsolve                    !Solve Equations.
1410                GOSUB Avetemp                     !Compute Average Temp.
1420    IF (ABS(Vtopn-Vtop)<.1) AND (ABS(Vbotn-Vbot)<.1) THEN Ind=0
1430    IF Ind=0 THEN Heatsum
1440    Ind=Ind+1
1450    IF Ind=Maxiter THEN Fail
1460    GOTO Iter
1470    ! --------------------------------------------------------
1480    ! No Convergence
1490    ! --------------------------------------------------------
1500 Fail:PRINTER IS 0
1510     PRINT "Maximum number of iterations exceeded - no convergence"
1520     PRINTER IS 16
1530     GOTO End
1540    ! ********************************************************
1550 Heatsum:! Calculate Heat Transfer For This Section And Sum.
1560    ! ********************************************************
1570     PRINTER IS 0
1580     Sens=2*Cond*Aa*(Hc1*Alfa*(Vbotn-Air)+Hc2*(PI-Alfa)*(Vtopn-Air))/1000*Dx
1590     Dmoist=Dx*Alfa*2*Aa*Evap*Wetf*(FNPsat(Vbot)-FNP(Wet,Air,Pressure))
1600     Asho=Ashi+Dmoist/Mass
1610     Air=Air+Sens/(Mass*Cpair/1000)
1620     Lath=Dmoist*(2501-2.387*Wet)/1000
1630     Senst=Senst+Sens+Lath
1640     Dist=Istep*Dx
1650     PRINT USING 1660;Dist,Air,Wet,Sens,Senst
1660     IMAGE 5X,4D.D,2(7X,DD.D),7X,5D.DD,6X,6D.DD
1670    ! --------------------------------------------------------
1680    ! Compute Inlet W.B.To Next Section Using NEWTON-RAPHSON Iteration
1690    ! --------------------------------------------------------
1700    Twbg=Wet+.5
1710    Ft=FNPsat(Twbg)-.000644*Pressure*(Air-Twbg)-Pressure*Asho/(622+Asho)
1720    Ftd=FNPsat(Twbg)*(17.27/(237.3+Twbg)-17.27*Twbg/(237.3+Twbg)^2)+.000644*P
ressure
1730    Wet=Twbg-Ft/Ftd
1740    IF ABS(Ft/Ftd)<.01 THEN 1770
1750    Twbg=Wet
1760    GOTO 1710
1770    Ashi=Asho
1780     NEXT Istep
1790     PRINT LIN(2)
1800 End: STOP
1810     ! ********************************************************
1820 Avetemp:! Calculates The Average Temperatures Of The Two Surfaces.
1830     ! ********************************************************
1840     Term=0
1850        FOR I=1 TO N
1860            Term=Term+A(I)*SIN(I*Alfa)/I
1870        NEXT I
1880     Vbotn=Vrt+A(0)+Term/Alfa
1890     Vtopn=Vbotn
1900     IF Alfa<PI THEN Vtopn=Vrt+A(0)-Term/(PI-Alfa)
1910    RETURN
```

```
1920    ! ****************************************************
1930 Coeffcalc:! Sets Up The Coefficients For The Set Of Linear Equations That L
ead To The Fourier Series Coefficients Of The Final Solution For Temperature
1940    ! ****************************************************
1950     G(0,N+1)=Q1+Q2*Vrt+B(0)*(Q3+Q4*Vrt)
1960     G(0,0)=Gam(0)-Q2-Q4*B(0)
1970        FOR I=1 TO N
1980            G(I,N+1)=B(I)*(Q3+Q4*Vrt)
1990            G(I,0)=-Q4*B(I)
2000            G(0,I)=-.5*Q4*B(I)
2010               FOR J=1 TO N
2020                   Term=-.5*Q4*B(ABS(I-J))
2030                   IF I=J THEN Term=Gam(J)-Q2-Q4*B(0)
2040                   G(I,J)=Term-.5*B(I+J)*Q4
2050               NEXT J
2060        NEXT I
2070     RETURN
2080    ! ****************************************************
2090 Gamcalc:! Calculates Gamma Terms.
2100    ! ****************************************************
2110      Ratio=Bb/Aa*(Bb/Aa)
2120      Term=Ratio
2130      Gam(0)=1/(Aa*LOG(Aa/Bb))
2140         FOR I=1 TO N
2150             Gam(I)=I/Aa*(1+Term)/(1-Term)
2160             Term=Term*Ratio
2170         NEXT I
2180     RETURN
2190    ! ****************************************************
2200 Bcalc:! Calculates The B Coefficients For The Funtion G(Theta).
2210    ! ****************************************************
2220      B(0)=Alfa/PI
2230         FOR I=1 TO 2*N
2240             B(I)=2*SIN(I*Alfa)/(I*PI)
2250         NEXT I
2260     RETURN
```

```
2270   ! *****************************************************
2280 Linsolve:! Solves The Set Of Linear Equations For The Fourier Coefficients
Of The Solution Temperature Using Gaussian Elimination.
2290   ! *****************************************************
2300      Nplus=N+1
2310        FOR K=0 TO N-1
2320           Store=K
2330           Max=ABS(G(K,K))
2340             FOR I=K+1 TO N
2350                IF ABS(G(I,K))<=Max THEN 2380
2360                Max=ABS(G(I,K))
2370                Store=I
2380             NEXT I
2390           IF Store=K THEN 2450
2400             FOR I=K TO Nplus
2410                Max=G(K,I)
2420                G(K,I)=G(Store,I)
2430                G(Store,I)=Max
2440             NEXT I
2450             FOR I=K+1 TO N
2460                FOR J=K+1 TO Nplus
2470                  G(I,J)=G(I,J)-G(I,K)*G(K,J)/G(K,K)
2480                NEXT J
2490             NEXT I
2500        NEXT K
2510      A(N)=G(N,Nplus)/G(N,N)
2520        FOR I=1 TO N
2530           Ni=N-I
2540           Sum=G(Ni,Nplus)
2550             FOR J=1 TO I
2560                Nj=N-J+1
2570                Sum=Sum-G(Ni,Nj)*A(Nj)
2580                A(Ni)=Sum/G(Ni,Ni)
2590             NEXT J
2600        NEXT I
2610     RETURN
```

```
2620    ! **************************************************
2630    ! Compute Goch Patterson Thermal Gradient Using A Polynomial Approx.
2640    ! **************************************************
2650    DEF FNGoch(Alpha)
2660    Z=LGT(Alpha)
2670    Goch=1.017+.7288*Z+.1459*Z*Z-.01572*Z^3-.004525*Z^4+.001073*Z^5
2680    Goch=1/Goch
2690    IF Alpha<1.5 THEN Time
2700    RETURN Goch
2710    ! --------------------------------------------------
2720    ! Time Period Too Short.
2730    ! --------------------------------------------------
2740 Time:PRINTER IS 0
2750    PRINT "TIME TOO SMALL - THESE RESULTS ARE TOTALLY UNRELIABLE"
2760    PRINTER IS 16
2770    RETURN Goch
2780    FNEND
2790    END
2800    ! **************************************************
2810    ! SATURATED VAPOUR PRESSURE
2820    ! **************************************************
2830    DEF FNPsat(X)
2840    Psat=.6105*EXP(17.27*X/(237.3+X))
2850    RETURN Psat
2860    FNEND
2870    ! **************************************************
2880    ! Vapour Pressure
2890    ! **************************************************
2900    DEF FNP(W,D,P)
2910    Pvair=(FNPsat(W)*(371.4+.24*D-.6*W)-.24*(D-W)*P)/(371.4+.04*D-.4*W)
2920    RETURN Pvair
2930    FNEND
2940    END
```

APPENDIX C

C1 Detailed Analysis of Radiation Heat Exchange in a Tunnel Cross-section

In a ventilation airway heat transfer due to radiation takes place between the rock surfaces and the ventilation air, and also between rock surfaces which are at different temperatures, for example in airways with partially wet surfaces or with partially insulated surfaces. The overall radiation heat exchange process is shown in Figure 4.7. In order to analyse the radiation heat exchange the 'radiation equivalent network method' is used (Oppenheim, 1956). The basis of the method is that an analogy is drawn between the radiation heat transfer process and an electrical equivalent. The heat flow is considered as the current, the difference in radiosity as the potential difference and other terms are expressed as an electrical resistance. A full explanation can be found in many texts (Kolman, 1981).

Referring to Figure 4.7, the energy leaving surface 1 which is transmitted through the air and arrives at surface 2 is given by

$$J_1 A_1 F_{12} \tau_a \qquad \text{(C1)}$$

and similarly that which leaves surface 2 and arrives at surface 1 is:

$$J_2 A_2 F_{21} \tau_a \qquad \text{(C2)}$$

J_i is the radiosity or the total radiation leaving surface i per unit time per unit area,

A_i is the area of surface i,

F_{ij} is the geometric view factor or the fraction of energy leaving surface i that reaches surface j,

τ_a is the fraction of radiation leaving the surface which is transmitted by the air stream.

Therefore the net heat exchange between the two radiating surfaces is given by

$$q_{12} = J_1A_1F_{12}\tau_a - J_1A_2F_{21}\tau_a \tag{C3}$$

By Kirchoff's identity for a non-reflecting medium the emissivity is equal to the absorptivity.

$$\epsilon_a = \alpha_a \tag{C4}$$

so that

$$\epsilon_a + \tau_a = 1 \tag{C5}$$

where ϵ_a is the emissivity of the air,
and α_a is the absorptivity of the air.

The radiative reciprocity relation states that

$$A_1F_{12} = A_2F_{21} \tag{C6}$$

and therefore by substiteting Equations C5 and C6 in Equation C3 we obtain

$$q_{12} = A_1F_{12}(1-\epsilon_a)(J_1-J_2) \tag{C7}$$

Using the electrical analogy Equation C7 can be represented by the network element shown in Figure C1.

Considering the energy exchange between surface 1 and the ventilation air, the energy emission from the ventilation air (other than that which is transmitted, and has already been considered) is given by the Stefan-Boltzmann law as

$$J_a = \epsilon_a \sigma T_a^4 \tag{C8}$$

where σ is the Stefan-Boltzmann constant ($5{,}699 \times 10^{-8}$ W/m^2 K^4),
and T_a is the absolute bulk air temperature.

The fraction of this energy which reaches surface 1 is given by

$$A_a F_{a1} \epsilon_a \sigma T_a^4 \qquad \text{(C9)}$$

At the same time the energy absorbed by the ventilation air from surface 1 is given by

$$J_1 A_1 F_{1a} \alpha_a \qquad \text{(C10)}$$

or

$$J_1 A_1 F_{1a} \epsilon_a \qquad \text{(C11)}$$

The net energy interchange between the air and surface 1 is given by

$$q_{a1} = A_a F_{a1} \epsilon_a \sigma T_a^4 - J_1 A_1 F_{1a} \epsilon_a \qquad \text{(C12)}$$

Again using the reciprocity relation to simplify Equation C12 we obtain

$$q_{a1} = A_1 F_{1a} \epsilon_a (\sigma T_a^4 - J_1) \qquad \text{(C13)}$$

The similar relationship for the interchange between surface 2 and the air is given by

$$q_{a2} = A_2 F_{2a} \epsilon_a (\sigma T_a^4 - J_2) \qquad \text{(C14)}$$

This radiation exchange can also be represented by an electrical equivalent and is shown in Figure C2.

For a reflecting solid which does not transmit energy

$$\rho + \epsilon = 1 \qquad \text{(C15)}$$

where ρ is the reflectivity,

and further the radiosity is the sum of the energy emitted and the energy reflected, that is

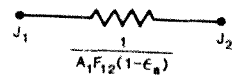

Figure C1 Network element for the radiation transmitted through the air.

Figure C2 Network element for the radiation exchange between air and the surface.

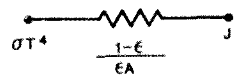

Figure C3 Network element for the surface resistance.

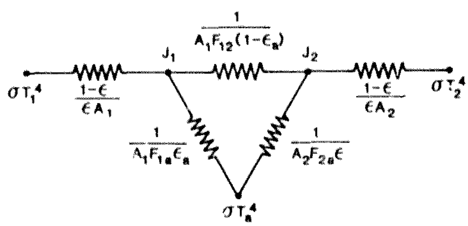

Figure C4 Total network for the radiation heat exchange process in a tunnel containing an absorbing gas.

$$J = \epsilon\sigma T^4 + \rho G \tag{C16}$$

where G is the *irradiation*, or the total radiation incident upon a surface, per unit time, per unit area.

By substituting Equation 15 into Equation 16 we obtain

$$J = \epsilon\sigma T^4 + (1-\epsilon)G \tag{C17}$$

Now the net radiation leaving a surface is the difference between the radiosity and the irradiation:

$$q = A(J-G) \tag{C18}$$

by eliminating the irradiation, by subsitution of Equation C17 in equation C18, the net radiation *heat transfer is given by*

$$q = \frac{\epsilon A}{1-\epsilon}(\sigma T^4 - J), \tag{C19}$$

which is *represented* by the network shown in Figure C3.

It is possible to combine the networks represented in Figures C1, C2 and C3, to produce the network for the whole energy exchange as shown in Figure C4. The components of radiation heat flow in ventilation tunnels can be simply found by obtaining the solution for this network.

The net heat transfer between surfaces 1 and 2 is given by

$$q = \sigma(T_1^4 - T_2^4)/\Sigma R \tag{C20}$$

where the equivalent network resistance, R_T, is

$$R_T = (1-\epsilon)/\epsilon A_1 + 1/(A_1F_{12}(1-\epsilon_a) + A_1A_2F_{1a}F_{2a}\epsilon_a/(A_1F_{1a}+A_2F_{2a})) + (1-\epsilon)/\epsilon A_2 \tag{C21}$$

An example will now be solved to investigate the magnitude of radiation heat transfer in mine airways.

EXAMPLE

It was assumed that a 3x3 m airway was ventilated with air at a temperature of 30 °C dry-bulb, 25 °C wet-bulb and a barometric pressure of 100 kPa. The mean footwall rock surface was 35 °C and the remaining rock surfaces were 32 °C.

The evaluation of view factors can be complicated and lead to errors. In fact it is not necessary to evaluate the view factors for this type of problem, rather the 'crossed-string' method of determining exchange areas (AF) is used (Hottel and Sarofim, 1967). It should be noted that by the reciprocity relation the exchange area holds for each energy exchange. The 'crossed-string' method is suitable when surfaces have (Gray and Müller, 1960):

(a) lengths much greater than their widths,
(b) constant cross-sections normal to their lengths, and
(c) constant separation along their lengths.

These rules are all true of the idealized ventilation tunnel. In Figure C5, representing the tunnel cross-section, the exchange area between the two surfaces A and B given by the 'crossed-string' method is:

$AF = (L_1+L_2-L_3-L_4)/2$

For the tunnel cross-section L_3 and L_4 are equal to zero and hence L_1 equals L_2. For unit length of tunnel the exchange area is therefore equivalent to the distance between the two end points of one of the surfaces. In this case

$AF = 3\ m^2$

The emissivity of the gases in ventilation air depend upon their partial pressure and mean beam length, and can be found from charts. Most gases are transparent to radiation, the only ones in normal air which are of concern are carbon dioxide and water vapour. The percentage volume of carbon dioxide in normal air is typically very low, 0,03 per cent (Mayhew and Rodgers, 1968), and thus has a very low partial pressure so that the radiation effects can be neglected for all

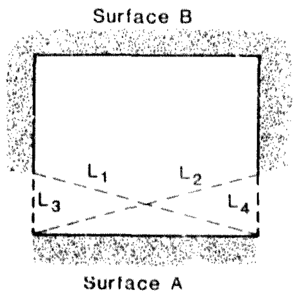

Figure C5 'Crossed-strings' for evaluation of the radiation exchange areas in a square tunnel

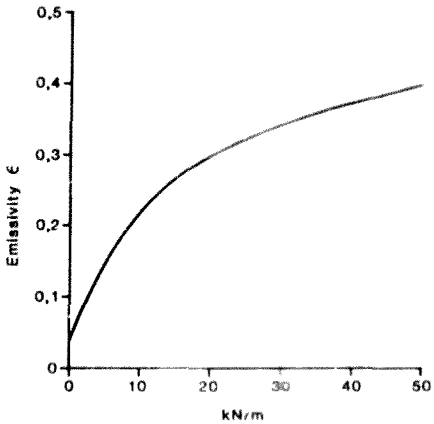

Figure C6 Emissivity of water vapour practical purposes The partial pressure of water vapour at 25 °C wb, 30 °C db and 100 kPa was derived from psychrometric charts as 2,8 kPa (Barenbrug).

The mean beam length is given by (Holman, 1981):

$$L_e = 3{,}6\ V/A$$

where V is the total volume of gas and A is the total surface area. Therefore, in this case the mean beam length is 2,7 m.

The relation between mean beam length, partial pressure and emissivity for water vapour at 30 °C and 100 kPa is shown in Figure C6. This chart was derived from previously published data (Hottel and Sarofim, 1967). For a value of 7,6 kN/m the emissivity of water vapour is 0,18. It is interesting to note that an emissivity of 0,4 was quoted in the literature (Starfield and Dickson, 1967). This value corresponds to 56 kN/m and cannot be justified in normal mining conditions.

The emissivity of rock surfaces was assumed to be 0,95 (Whillier, 1982).

The resistances shown in Figure C4 were evaluated as follows:

$$\frac{1-\varepsilon}{\varepsilon A_1} = 0{,}006 \qquad \frac{1-\varepsilon}{\varepsilon A_2} = 0{,}018$$

$$\frac{1}{A_1F_{12}(1-\varepsilon_a)} = 0{,}407 \qquad \frac{1}{A_1F_{1a}\varepsilon_a} = \frac{1}{A_2F_{2a}\varepsilon_a} = 1{,}852$$

The equivalent resistance of the networks in parallel is equal to 0,367 and thus the total resistance is 0,391.

Figure C7 Network for the radiation heat exchange process in a tunnel containing a transport medium.

The total heat transfer between surfaces 1 and 2 is found from equation 20, and in equal to 50,2 W. This quantity of heat radiation is surprisingly high when considering that the heat flow due to convection in a similar tunnel would be of the order of 100 W/m. If it is assumed that the ventilation air is transparent to radiation, the equivalent network is that shown in Figure C7, the total resistance ,ΣR, is given by

$$\Sigma R = (1-\epsilon)/\epsilon A_1 + 1/A_1F_{12} + (1-\epsilon)/\epsilon A_2 \tag{C22}$$

and the heat transfer between the two surfaces is given by

$$q = \sigma(T_1^4 - T_2^4)/\Sigma R \tag{C23}$$

which is equivalent, in this case, to 55,1 W.

It is now clear that although a large amount of heat is transferred between the two surfaces the effect upon the ventilation air is only 4,9 W.

C2 Simplified Analysis

In the preceeding analysis it has been shown that the effect of radiation on the ventilation air is small, and it is doubtful whether the complex approach described is necessary for day to day engineering calculations. This is doubtful when it is considered that the analysis is based on a highly idealized set of conditions. It is convenient for most computations to use the Stefan-Boltzmann relation (Whillier, 1982)

$$q = A_1F_{ev}(T_1^4 - T_2^4) \tag{C24}$$

where F_{ev} is a combined emissivity and view factor.

By comparing Equations (20) and (24) it can be seen that

$$F_{ev} = 1/A_1R_T \tag{C25}$$

with a value for the example of 0,55.

A linearized form of the Stefan-Boltzmann equation is often used:

$$q = h_R A F_{ev} (t_1 - t_2) \qquad \text{(C26)}$$

where h_R is the radiative heat transfer coefficient. Values of h_R can be computed from

$$h_R = 4,62(1+(t_1+t_2)/545,3)^3 \qquad \text{(C27)}$$

The linearized form of the equation is as accurate as the Stefan-Boltzmann equation and often greatly simplifies the calculation of heat flow into tunnels. This form of the equation has been used by several authors when proposing methods for the solution of tunnel heat flow (Hemp, 1985; Starfield and Bleloch, 1983).

When calculating the heat load on the ventilation air stream due to radiation some care needs to be exercised in evaluating F_{ev} when applying Equations C25 or C26. We have seen that a value of 0,85 is typical for the radiation between the two rock surfaces. However, the value for energy interchange between the rock surfaces and the air stream is quiet different, and is given by

$$F_{ev} = 1/A_1 \Sigma R - 1/A_1 R_T$$

For the example described the effective view factor between the rock surfaces and the ventilation air has a value of 0,08. The effective view factor has been incorrectly evaluated in the past, with values of the order of unity being assumed (Hemp, 1985).

C3 Conclusions

It has been shown that it is unnecessary to employ a more rigorous treatment of the effects of radiation heat transfer than that normally used when evaluating heat flow into mine workings. The contribution of radiation heat transfer to the overall heat load is a small portion of the total, and errors incurred by applying a simple method of analysis are not significant.

APPENDIX D

Nomograms showing reduction in heat flow due to insulation

In this Appendix the theoretically predicted reduction in heat flow due to insulation is presented in the form of nomograms. The nomograms are for fully insulated, partially insulated and partially uninsulated with a damp footwall. Each nomogram includes the effects of variations in ventilation air velocity, tunnel age and tunnel length. In addition different nomograms are presented for variations in tunnel size, rock thermal conductivity, insulation thermal resistance, footwall wetness and ventilation air humidity.

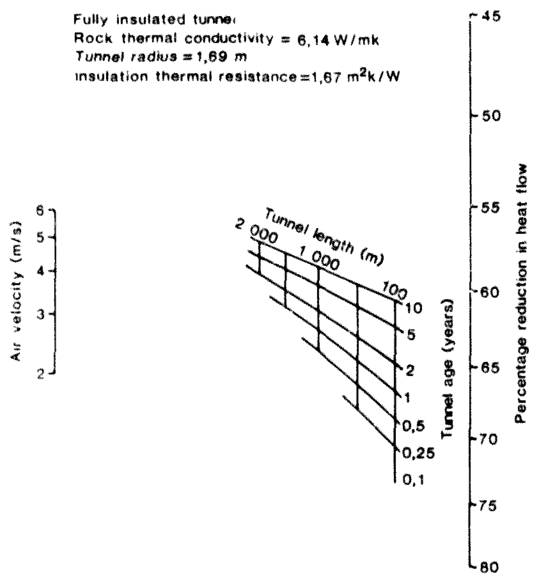

Figure D1 Reduction in heat flow for fully insulated tunnels - average conditions.

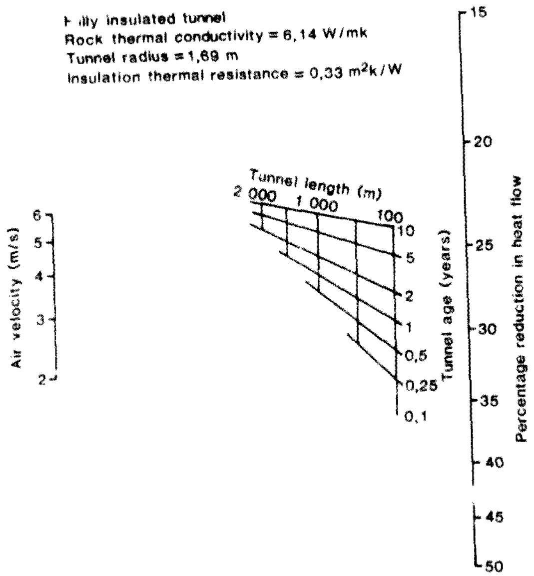

Figure D2 Reduction in heat flow for fully insulated tunnels - insulation thermal resistance 0,33 m^2K/W

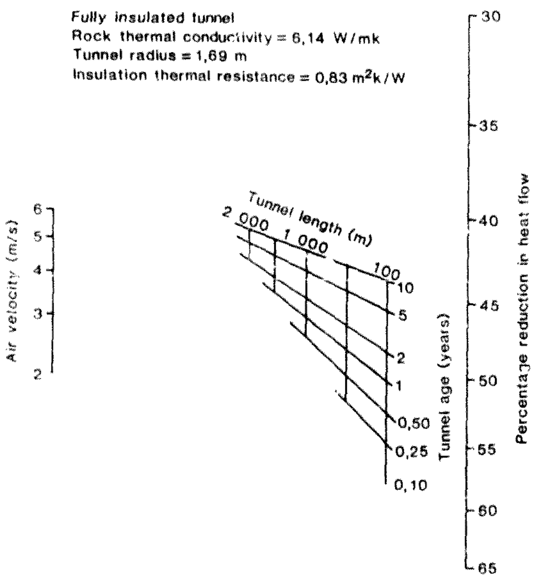

Figure D3 Reduction in heat flow for fully insulated tunnels - insulation thermal resistance 0,83 m^2k/W.

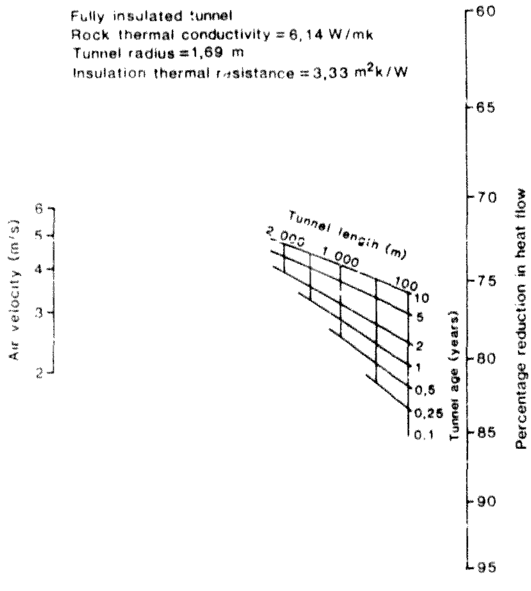

Figure D4 Reduction in heat flow for fully insulated tunnels - insulation thermal resistance 3,33 m^2K/W

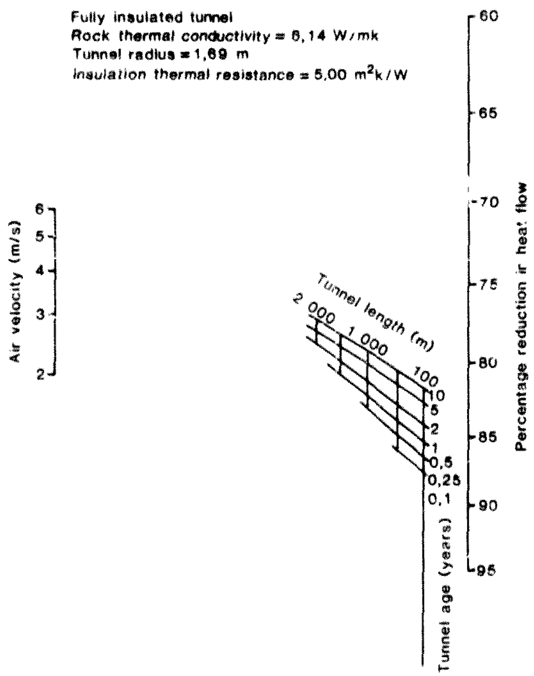

Figure D5 Reduction in heat flow for fully insulated tunnels - insulation thermal resistance 5,00 m^2K/W

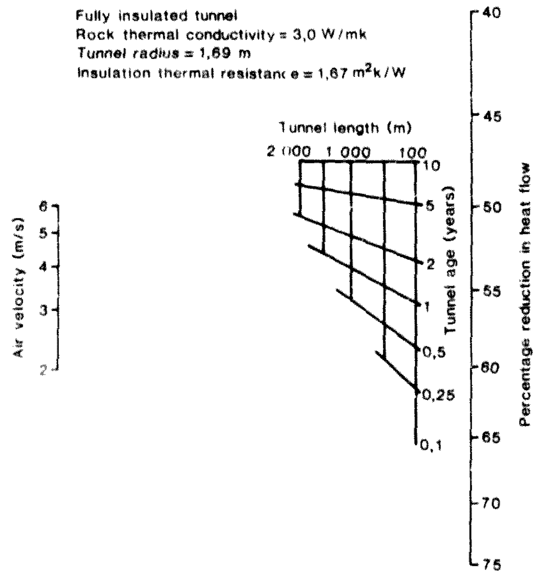

Figure D6 Reduction in heat flow for fully insulated tunnels - rock thermal conductivity 3,0 W/mK.

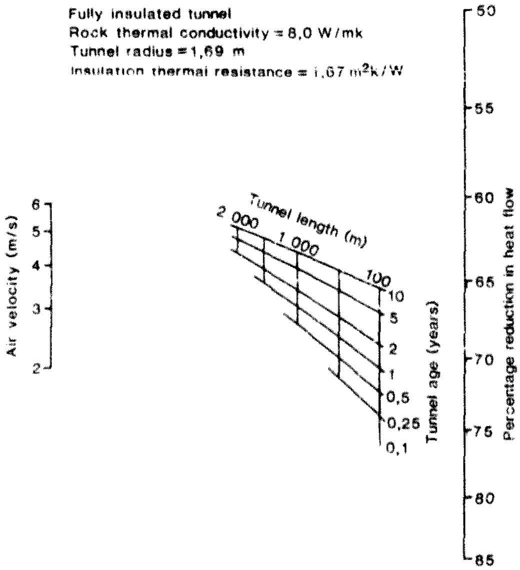

Figure D7 Reduction in heat flow for fully insulated tunnels - rock thermal conductivity 8,0 W/mK.

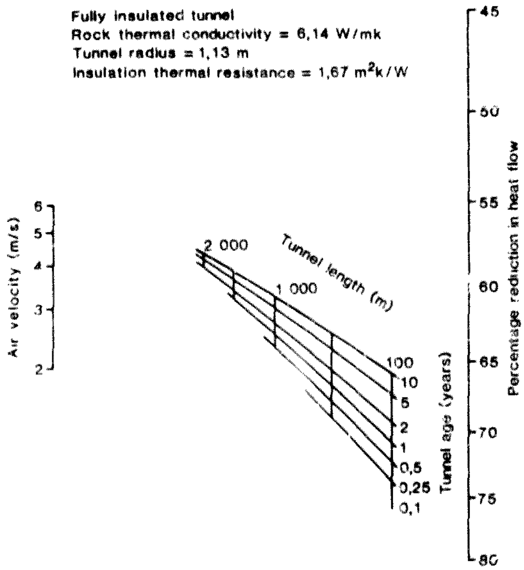

Figure 08 Reduction in heat flow for fully insulated tunnels - tunnel radius 1,13 m.

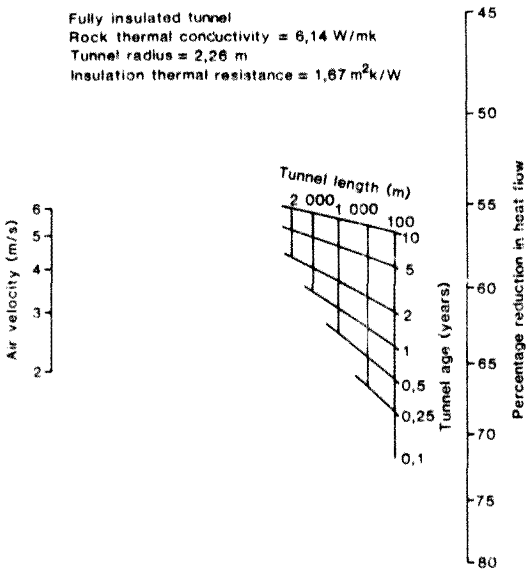

Figure D9 Reduction in heat flow for fully insulated tunnels - tunnel radius 2,26m.

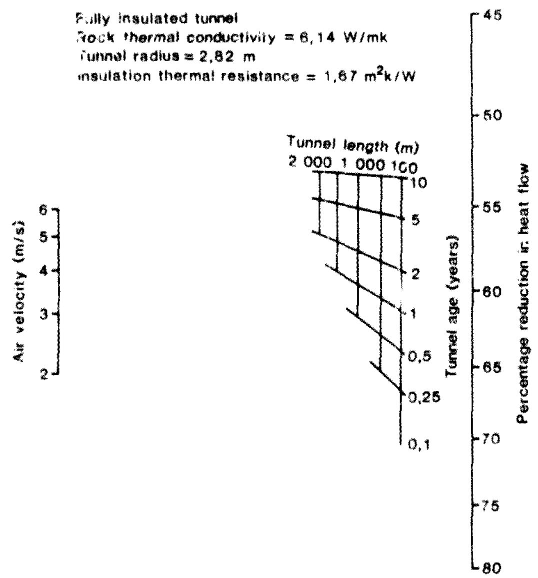

Figure D10 Reduction in heat flow for fully insulated tunnels - tunnel radius 2,82 m.

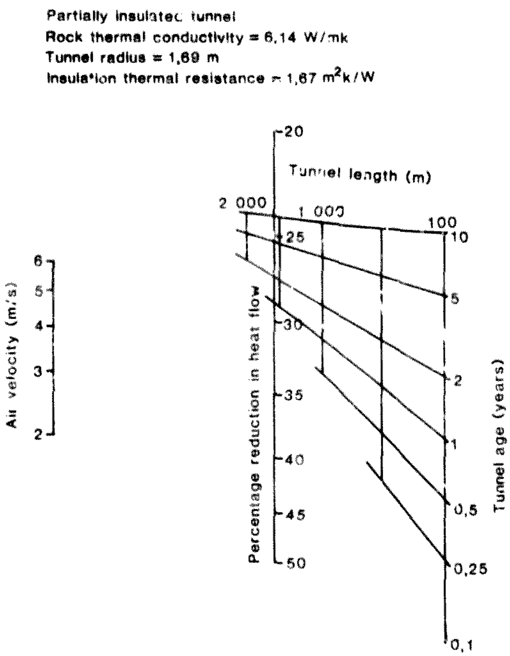

Figure D11 Reduction in heat flow for partially insulated tunnels - average conditions.

Partially insulated tunnel
Rock thermal conductivity=6,14 W/mk
Tunnel radius = 1,69 m
Insulation thermal resistance = 0,33 m²k/W

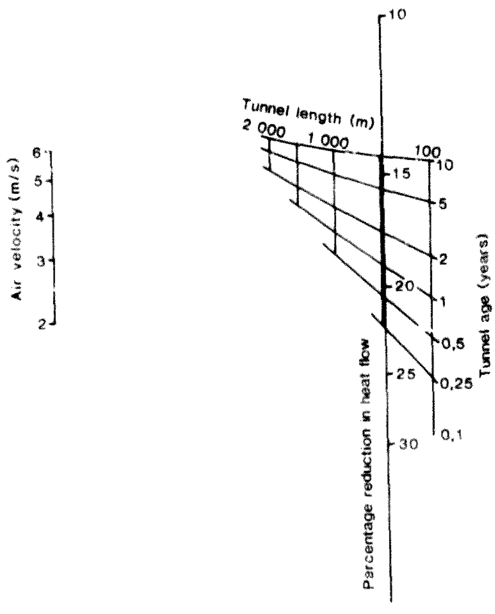

Figure D12 Reduction in heat flow for partially insulated tunnels - insulation thermal resistance 0,33 m^2K/W

Partially insulated tunnel
Rock thermal conductivity = 6,14 W/mk
Tunnel radius = 1,69 m
Insulation thermal resistance = 0,83 m^2k/W

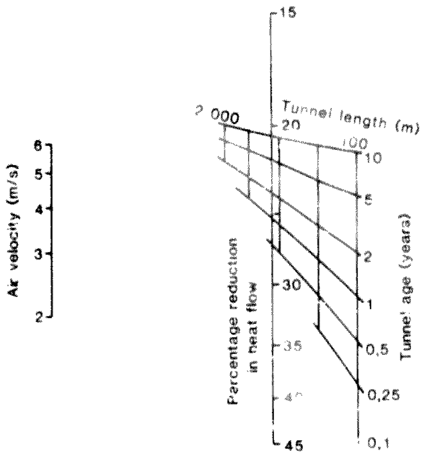

Figure D13 Reduction in heat flow for partially insulated tunnels - insulation thermal resistance 0,83 m^2K/W

Partially insulated tunnel
Rock thermal conductivity = 6,14 W/mk
Tunnel radius = 1,69 m
Insulation thermal resistance = 3,33 m²k/W

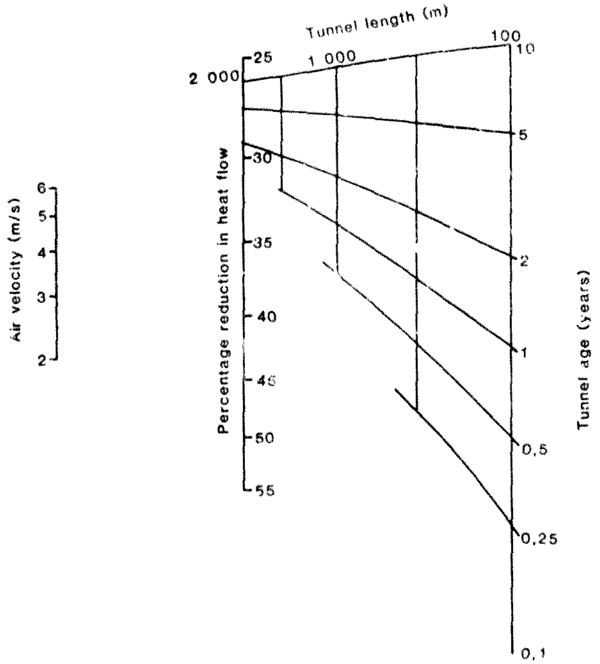

Figure D14 **Reduction in heat flow for partially insulated tunnels - insulation thermal resistance 3,33 m²/KW**

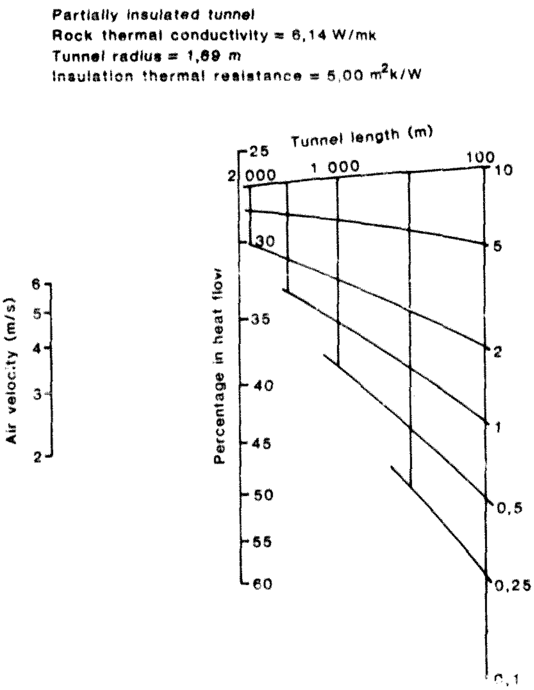

Figure D15 Reduction in heat flow for partially insulated tunnels - insulation thermal resistance 5,00 m^2K/W

Partially insulated tunnel
Rock thermal conductivit, = 3,0 W/mk
Tunnel radius = 1,69 m
Insulation thermal resistance = 1,67 m²k/W

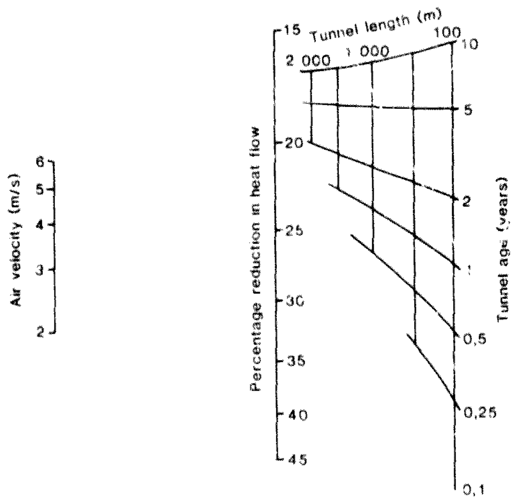

Figure D16 Reduction in heat flow for partially insulated tunnels - rock thermal conductivity 3,0 W/mK.

Partially insulated tunnel
Rock thermal conductivity = 8,0 W/mk
Tunnel radius = 1,69 m
Insulation thermal resistance = 1,67 m^2k/W

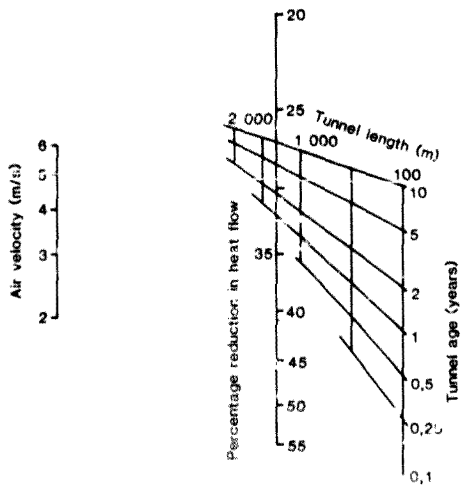

Figure D17 Reduction in heat flow for partially insulated tunnels - rock thermal conductivity 3,0 W/mK.

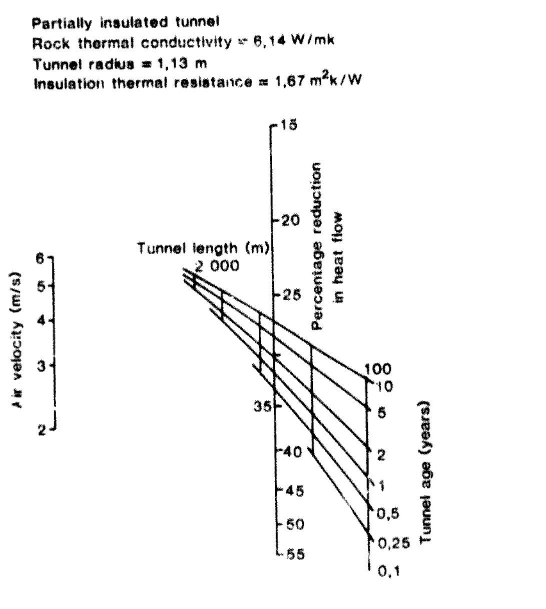

Figure D18 Reduction in heat flow for partially insulated tunnels - tunnel radius 1,13 m.

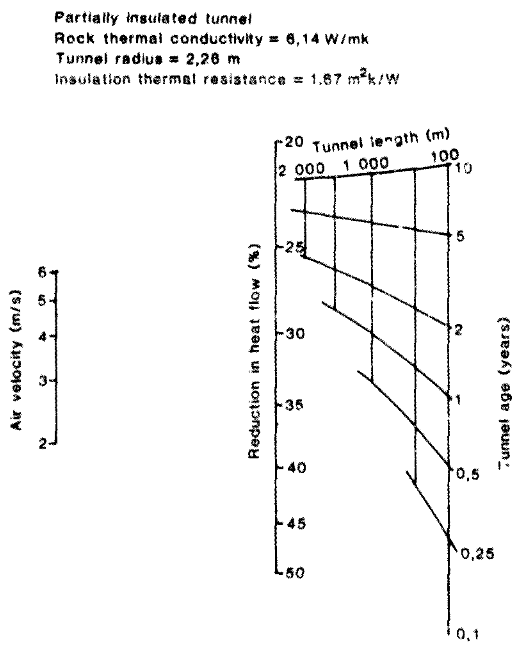

Figure D19 Reduction in heat flow for partially insulated tunnels - tunnel radius 2,26 m.

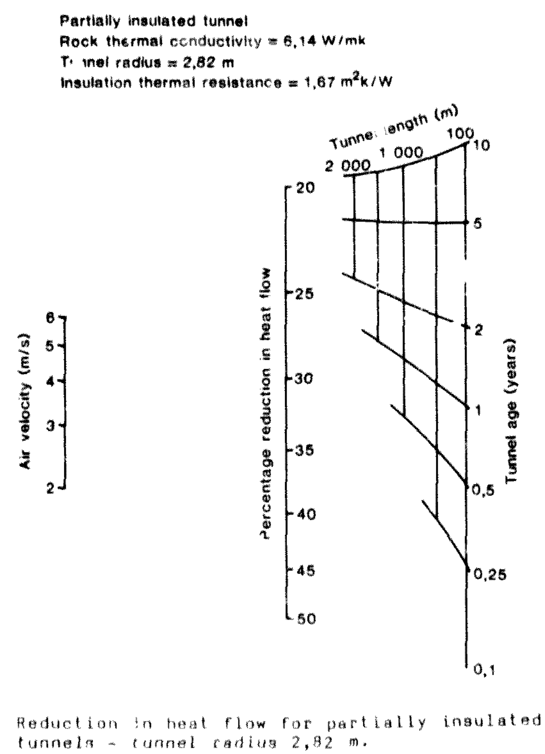

Figure D20 Reduction in heat flow for partially insulated tunnels - tunnel radius 2,82 m.

Partially insulated tunnel
Wetness factor = 0,2
Relative humidity = 50%
Rock thermal conductivity = 6,14 W/mk
Tunnel radius = 1,69 m
Insulation thermal resistance = 1,67 m^2k/W

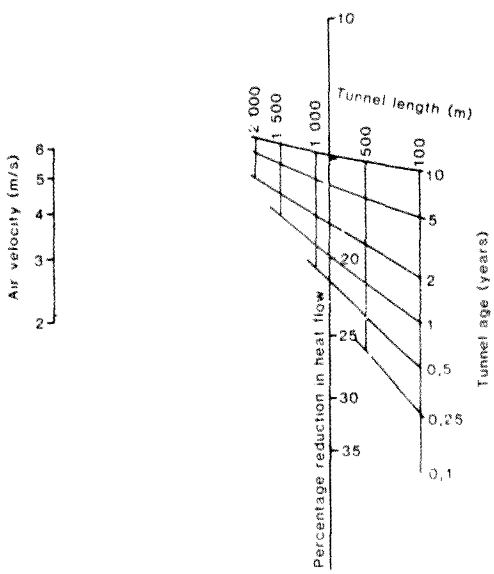

Figure D21 Reduction in heat flow for partially insulated tunnels - wetness 0,2 - humidity 50 %.

Partially insulated tunnel
Wetness factor = 0,2
Relative humidity = 75%
Rock thermal conductivity = 6,14 W/mk
Tunnel radius = 1,69 m
Insulation thermal resistance = 1,67 m^{2}k/W

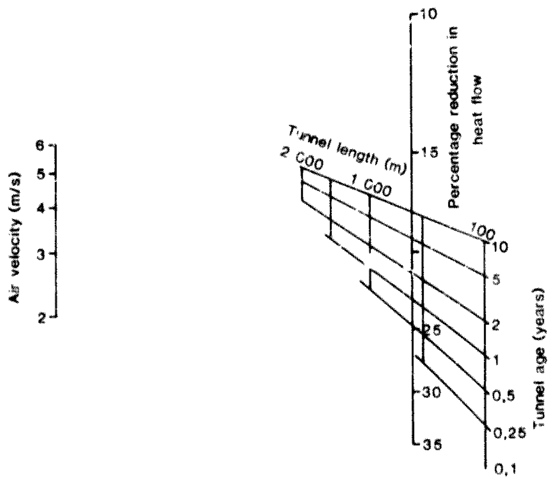

Figure D24 Reduction in heat flow for partially insulated tunnels - wetness 0,2 - humidity 75 %.

Partially insulated tunnel
Wetness factor = 0,5
Relative humidity = 75%
Rock thermal conductivity = 6,14 W/mk
Tunnel radius = 1,69 m
Insulation thermal resistance = 1,67 m^2k/W

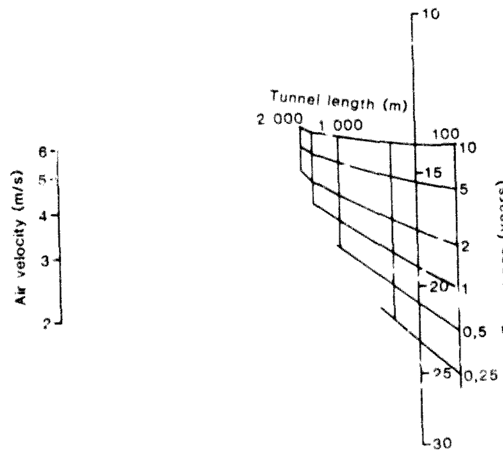

Figure D25 Reduction in heat flow for partially insulated tunnels - wetness 0,5 - humidity 75 %.

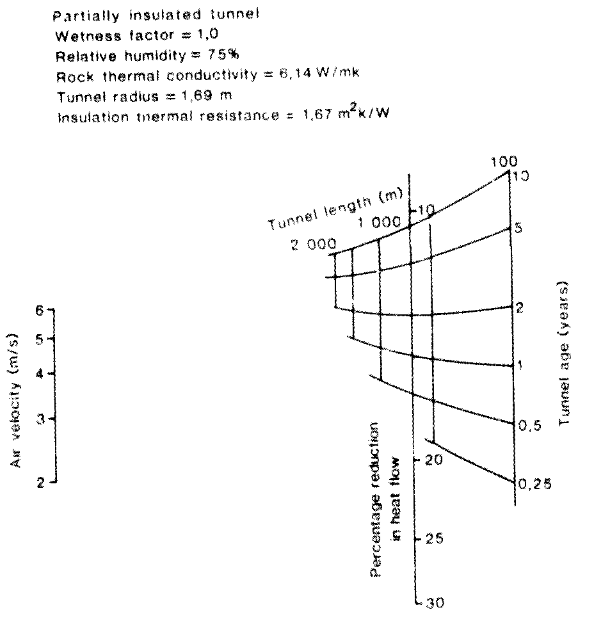

Figure 26 Reduction in heat flow for partially insulated tunnels - wetness 1,0 - humidity 75 %.

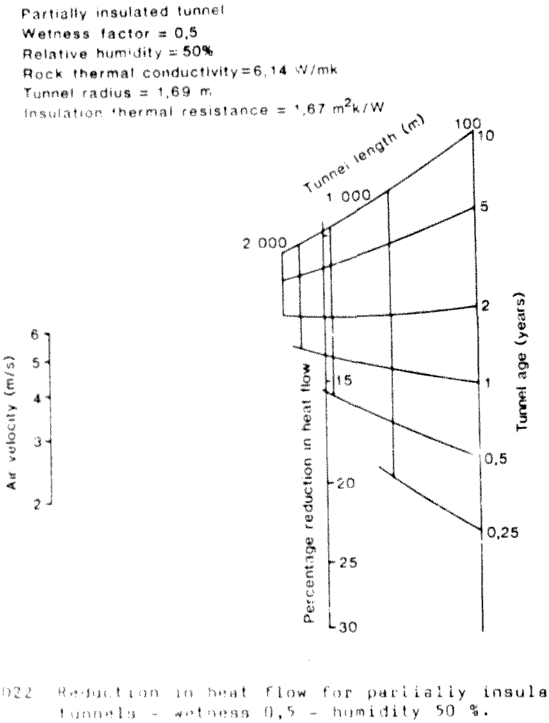

Figure D22 Reduction in heat flow for partially insulated tunnels - wetness 0,5 - humidity 50 %.

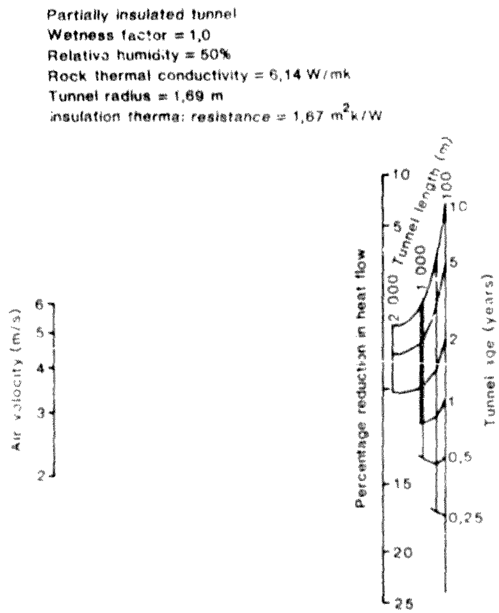

Figure [illegible] Reduction in heat flow for partially insulated tunnels - wetness 1,0 - humidity 50 %.

REFERENCES

ADINAT USERS MANUAL Adina Engineering, Inc, 71 Elton Ave, Watertown, Mass, 02172, USA.

ALBERTSON, M.L., BARTON, J.R. and SIMONS, D.B. (1966) **Fluid Mechanics For Engineers**. 1st ed. Prentice Hall, 1966.

BARENBRUG, A.W.T. (1974), **Psychrometry and Psychrometric Charts**. 3rd ed. Cape Town: Cape and Transvaal Printers (Pty) Limited, 1974.

BAYLEY, F.J., OWEN, J.M., and TURNER, A.B. (1972), **Heat Transfer**, 1st ed. Thomas Nelson and Sons, Ltd, 1972.

BLUHM, S.J., ALEXANDER, N.A., MARCH, T.W., BOTTOMLEY, P. and VON GLEHN, F. (1986), **The measurement of heat loads in a deep level stope in the Klerksdorp Goldfields**. Journal of the Mine Ventilation Society of South Africa, vol.39, no.10, Oct. 1986, pp 129-140.

CARSLAW, H.S. and JAEGER, J.C. (1959), **Conduction of Heat in Solids**, 2nd ed. Oxford University Press, 1959.

CHOROSZ, G. (1986), **HEATFLOW: An Interactive Computer Program for the Analysis of Heat Production in Gold Mines**. M.Sc. Dissertation, University of the Witwatersrand, Johannesburg, RSA.

DESAI, C.S., and ABEL, J.F. (1972), **Introduction to the Finite Element Method**, 1st ed. Van Nostrand Reinhold Co, 1972.

DITTUS, F.W. and BOELTER L.M.K. (1930), *University of California*, Publications in Engineering, 1930.

GIBSON, K. (1976), The Computer Simulation of Climatic Conditions in Underground Mines. PhD Thesis University of Nottingham, U.K.

GOCH, D.C. and PATTERSON, H.S (1940), **The Heat Flow into tunnels**, Journal of The Chemical, Metallurgical and Mining Society of SA, vol.49, Sept. 1940, pp 117-127.

GOLDSTEIN, S. (1932), **Some diffusional two dimensional problems with circular symmetry,** Proceedings of the London Mathematical Society, vol.34, series 2, 1932, pp 51-88.

GOULD, M.J. (1968), **The Determination of Parameters Concerned with Heat Flow into Underground Excavations.** M.Sc. dissertation, University of the Witwatersrand, Johannesburg, RSA.

GRAY, W.A. and MULLER, R. (1974), **Engineering Calculations in Heat Transfer,** (international series on materials science and technology, vol 13). Pergrammon Press, 1974.

HEMP, R. (1966), **Temperature Increases in 53 Haulage East, Crown Mines, Ltd.** *Rand Mines Ltd. Report No. 15. May 1966.*

HEMP, R. (1967), **Heat Flow in Drives - Measurements at Six Sites at Harmony Gold Mining Company Ltd.** Rand Mines Ltd. Report No. 21. Oct 1967.

HEMP, R. (1969), **Heat Flow Measurements at Libanon Gold Mining Company Ltd.** Rand Mines Ltd. Report No. 22. Sept. 1969.

HEMP, R. (1970), **Heat Flow in Drives - A Short Summary of Previous Reports.** Rand Mines Ltd. Report No 23 Jan. 1970.

HEMP, R. (1982), **Environmental Engineering In South African Mines,** 1st ed. Cape Town. Cape and Transvaal Printers (Pty) Ltd, 1982, pp 569-612.

HOLMAN, J.P. (1981), **Heat Transfer,** 5th ed. McGraw-Hill 1981, pp 305-406.

HUEBNER, K.H. (1975), **The Finite Element Method For Engineers,** 1st ed. John Wiley and Sons Inc, 1975.

HUGHES, R.O. (1978), **A Few Thoughts on Heat Loads in Intake Haulages,** Journal of Mine ventilation Society of South Africa, vol.78, no.3, March 1978, pp 50-53.

HURLBURT H.Z. (1980), **Curve Fitting By Computer,** Hydrocarbon Processing, August 1980, pp 107-110.

JAEGER, J.C. and CHAMALAUN, T. (1966), **Heat Flow in and infinite region bounded internally by a circular cylinder with forced convection at the surface,** Australian Journal of Physics, vol.19, 1966, pp 475-488.

LAMBRECHTS, J de V. (1967), **Prediction of Wet-Bulb temperature gradients in mine airways,** Journal of the South African Institute of Mining and Metallurgy, vol.20, no.6, June 1967, pp 595-610.

LAMBRECHTS, J de V. and HOWES, M.J. (1982), **Environmental Engineering in South African Mines,** 1st ed. Cape Town: Cape and Transvaal Printers (Pty) Ltd, 1982, pp 847-875.

LLOYD, F. (1984), Western Deep Levels Gold Mine. Private Communication.

MAYHEW, W.H. and ROGERS, G.F.C. (1967), **Thermodynamic and Transport Properties of Fluids - SI Units,** 3rd ed. Basil Blackwell, 1967.

McADAMS, W.H. (1954), **Heat Transmission,** 3rd ed. McGraw-Hill, 1954.

MYERS, G.R. (1971), **Analytical Methods in Conduction Heat Transfer,** 1st ed. McGraw-Hill, 1971.

NICHOLSON, J.W. (1921), **A problem in the theory of heat conduction,** Proceedings of the Royal Society, vol 100, no. A704, Sept. 1921.

NUNNER, W. (1956) **Wärmeübergang und Druckabfall in rauhen Rohren,** Z. Ver. Deut. Ing. Forschungsheft, vol.455, 1956, pp 5-32.

OPPENHEIM, A.K. (1956), **Radiation Analysis by the Network Method,** Transactions of the American Society of Mechanical Engineers, vol.78, 1956.

OWEN, D.R.J., and HINTON, E. (1980), **A Simple Guide To Finite Elements,** 1st ed. Pineridge Press Ltd., 1980.

ROHSENOW, W.M. and CHOI, H.Y. (1963), **Heat mass and momentum transfer.** 1st ed. Prentice Hall, 1963.

SCOTT, D.R. (1959), **The Cooling of Underground Galleries,** Journal of the Mine Ventilation Society of South Africa, vol.12, no.4, April 1959, pp 77-103.

SHEER, J., BURTON, R.C. and BLUHM, S. (1984), **Recent Developments in the Cooling of deep mines,** The South African Mechanical Engineering, vol 34, no 1, Jan. 1984, pp 2-8.

SPIEGEL, R.M. (1971), **Theory and Problems of Advanced Mathematics,** 1st ed. Schaum's Outline Series, McGraw-Hill, 1971.

STARFIELD, A.M (1966), **The Computation of Air Temperature Increases In Wet and Dry Airways,** *Journal of Mine Ventilation Society of South* Africa, vol.59, no.12, Dec. 1966, pp 189-199

STARFIELD, A.M. (1969), **A Rapid Method of Calculating Temperature Increases Along Mine Airways,** Journal of S.A. Institute of Mining and Metallurgy, vol 70, no.11, Nov. 1969, pp 77-83.

STARFIELD, A.M and BLELOCH, A.C (1983), **A New Method For the Computation of Heat and Moisture Transfer In Partly Wet Airways,** Journal of S.A. Institute of Mining and Metallurgy, vol.84, no.11, Nov/Dec. 1983, pp 263-269.

STARFIELD, A.M. and DICK, A.J. (1967), **A Study of Heat Transfer and Moisture Pick-up in Mine Airways,** Journal of S.A. Institute of Mining and Metallurgy, vol.68, no.12, Dec. 1967, pp 115-122.

VOST, K.R. (1982), **The Prediction of Air Temperature in Intake Haulages in Mines,** Journal of S.A. Institute of Mining and Metallurgy, vol 83, no.11, Nov. 1982, pp 316-328

WHILLIER, A. (1982), Env **Engineering in South African Mines,** 1st ed. Cape Town: Ca aal Printers (Pty) Ltd, 1982, pp 465-494.

WILES, G.G. and GRAVE, D.F.H. (1954), **Heat Flow Studies Using an Electrolytic Tank,** Journal of the Chemical, Metallurgical and Mining Society of South Africa, vol.55, no.12, Dec. 1954, pp 149-153.

WILES, G.G. AND MAXWELL, A.D. (1959), **The Thermal Conductivity of Footwall Gravel,** *Journal of the Mine Ventilation Society of South Africa*, vol.12, no.3, March 1959, pp 64-66.